EFFECTS OF SOY PROTEIN ISOLATE ON THE DIELECTRIC POLARIZATION OF POLY(ETHYLENE OXIDE)

A Thesis by

Soheil Rashidi

Bachelor of Science, Shiraz University, 2012

Submitted to the Department of Mechanical Engineering
and the faculty of the Graduate School of
Wichita State University
in partial fulfillment of
the requirements for the degree of
Master of Science

December 2016

EFFECTS OF SOY PROTEIN ISOLATE ON THE DIELECTRICAL POLARIZATION OF POLY(ETHYLENE OXIDE)

The following faculty members have examined the final copy of this thesis for form and content, and recommend that it be accepted in partial fulfillment of the requirement for the degree of Master of Science with a major in Mechanical Engineering.

Bin Li, Committee Chair

Hamid Lankarani, Committee Member

Ramazan Asmatulu, Committee Member

Pingfeng Wang, Committee Member

DEDICATION

To my parents, my brother, my sister,
and my dear friends

ACKNOWLEDGEMENTS

I would like to use this opportunity to express my sincere gratitude to everyone who supported me throughout my graduate studies at Wichita State University. I am grateful for their inspiring guidance and invaluable advice during my thesis work.

I would like to thank my advisor, Bin Li, for his patient guidance and support. I also would like to extend my gratitude to members of my committee, Hamid Lankarani, Ramazan Asmatulu, and Pingfeng Wang for their helpful comments and suggestions.

I am deeply indebted to my parents. Words cannot express how grateful I am to my father, my mother, my sister, and my brother for their constant love and support.

ABSTRACT

With increasing demands for renewable materials applications, biomaterials originated from natural resources have obtained great attention. Among them, plant proteins have been extensively studied for composites, packaging as well as biomedical applications. Despite the diverse and complex polar structures, plant proteins have rarely been studied for energy related applications. In this study, soy protein isolate (SPI), a high protein content product extracted from soy flour, was used to modify energy storage performances of poly (ethylene oxide) (PEO). PEO is a type of soluble and biodegradable thermoplastic polymer with good biocompabitlity and low toxicity, and it is usually considered as an ideal candidate for environment friendly applications. The pure PEO membranes are highly polarizable, but they also have extremely high energy loss during charging/discharging cycles. The high loss is not only responsible for the unsatisfactory energy storage performance, but also responsible for high dielectric heating. The addition of SPI to PEO leads to greatly reduced polarization and stored energy density determined by monopolar hysteresis analysis. However, it also largely reduces the current leakage and energy loss of the resulting membranes, leading to significantly enhanced discharged energy density and energy efficiency. The strong interactions between PEO and SPI should be the primary reason for the improve energy storage properties. Meanwhile, such interactions also result in a more brittle fracture behavior and reduced crystallinity of the PEO/SPI membranes. The enhanced discharged energy density and low energy loss suggest that PEO/SPI membranes are promising dielectric materials in high efficiency capacitor applications.

TABLE OF CONTENTS

Chapter Page

1. INTRODUCTION 1

1.1 Theoretical Background of Dielectric Capacitor 1
1.2 Applications of Capacitors 4
1.2.1 Energy Storage 5
1.2.2 Filtering and DC Blocking 5
1.2.3 RF Coupling 6
1.2.4 Power Conditioning 6
1.3 Classification of Capacitors 7
1.3.1 Ceramic Capacitors 8
1.3.2 Glass Capacitors 12
1.3.3 Paper Capacitors 14
1.3.4 Plastic Capacitors 15
1.4 Polymeric Dielectric Materials 18
1.5 Strategies to Improve Polymer Dielectrics 19
1.6 Soy Protein and Its Applications 21
1.6.1 Denaturation and Modification of Soy Protein 22
1.6.2 Non-Food Functional Properties of Soy Protein 26
1.7 Proposed Research and Objectives 28

2. METHODOLOGY 30

2.1. Materials 30
2.1.1 Poly(ethylene oxide) 30
2.1.2 Deionized Water 30
2.1.3 Soy Protein Isolate 30
2.2 Sample Preparation 31
2.3 Characterizations 33
2.3.1 Contact Angle Measurement 33
2.3.2 Fourier Transform Infrared Spectrum 33
2.3.3 X-ray Diffraction 34
2.3.4 Scanning Electron Microscopy 34
2.3.5 Current-Voltage Characteristics 34
2.3.6 Hysteresis Measurement 34

3. RESULTS AND DISCUSSION 36

3.1 Contact Angle Measurement 36
3.2 Fourier Transform Infrared Spectrum 38
3.3 X-ray Diffraction 43
3.4 Scanning Electron Microscopy 46
3.5 Current-Voltage Characteristics 55

TABLE OF CONTENTS (continued)

Chapter Page

3.6 Hysteresis Behaviors of PEO/SPI Membranes 58
3.6.1 Effects of SPI Content on Energy Performances of HPEO/SPI Membranes 63
3.6.2 Effects of SPI Content on Energy Performances of LPEO/SPI Membranes 66
3.6.3 Effects of Polymer Molecular Weight on Energy Performances 66

4. CONCLUSION 70

5. FUTURE RESEARCH 75

6. REFERENCES 76

LIST OF TABLES

Table Page

1.1. COMPARISON BETWEEN CLASS I AND CLASS II DIELECTRICS 9

1.2. LOW VOLTAGE AND HIGH VOLTAGE PORCELAINS PROPERTIES....................11

1.3. VARIOUS PROPERTIES OF COMMERCIAL GLASSES...13

2.1. DIFFERENT COMPOSITIONS AND CONDITIONS USED AS SAMPLE PREPARATION 31

3.1. THE CONTACT ANGLE OF DIFFERENT SOLUTIONS ON A HYDROPHOBIC SURFACE...37

3.2. FTIR PEAK ASSIGNMENT OF PURE PEO...39

3.3. FTIR PEAK ASSIGNMENT OF SPI POWDER..40

3.4. FTIR PEAK ASSIGNMENT OF HEAT TREATED SPI...41

3.5. ASSIGNMENT OF XRD DIFFRACTION PEAKS IN PEO 45

3.6. CRYSTALLINITY OF PEO/SPI MEMBRANES 45

3.7. ELECTRICAL RESISTIVITY OF THE MEMBRANES...57

3.8. MAXIMUM POLARIZATION OF HPEO MEMBRANES...60

3.9. MAXIMUM POLARIZATION OF LPEO MEMBRANES 62

LIST OF FIGURES

Figure Page

1.1. Parallel-plate capacitor connected to a DC source 2

1.2. The roles of capacitors in power conditioning..6

1.3. Different types of capacitors...7

1.4. Monolithic ceramic capacitor 8

1.5. Cubic perovskite structure 10

1.6. Glass capacitor (Leyden jar) 13

1.7. Paper capacitor..14

1.8. Construction of a foil capacitor...16

1.9. Construction of an extended single metallization capacitor 16

1.10. Construction of a mixed dielectric capacitor 17

1.11. Construction of a mixed dielectric capacitor by using a double metallized 17

1.12. Protein structures 23

2.1. Soy protein isolate powder...30

2.2. Hot plate with magnetic stirring 31

2.3. Branson ultrasonic cleaner...32

2.4. Film applicator with the range of thicknesses from 5 to 50 mils......................................32

3.1. Effect of contact angle on hydrophobicity...36

3.2. FTIR spectrum of of pure PEO..39

3.3. FTIR spectrum of as received SPI powder 40

3.4. FTIR spectrum of heat treated SPI...41

3.5. FTIR spectra of HPEO and HPEO/SPI membranes 42

3.6. FTIR spectra of LPEO and LPEO/SPI membranes 43

LIST OF FIGURES (continued)

Figure Page

3.7. XRD spectra of HPEO and HPEO/SPI membranes 44

3.8. XRD spectra of LPEO and LPEO/SPI membranes 44

3.9. Free surface of HPEO/10wt% SPI membrane 46

3.10. Fracture surface of HPEO/10wt% SPI membrane 47

3.11. Free surface of HPEO/30wt% SPI membrane 48

3.12. Fracture surface of HPEO/30wt% SPI membrane 48

3.13. Free surface of HPEO/50wt% SPI membrane 49

3.14. Fracture surface of HPEO/50wt% SPI membrane 50

3.15. Free surface of LPEO/10wt% SPI membrane 51

3.16. Fracture surface of LPEO/10wt% SPI membrane 51

3.17. Free surface of LPEO/30wt% SPI membrane 52

3.18. Fracture surface of LPEO/30wt% SPI membrane 53

3.19. Free surface of LPEO/50wt% SPI membrane 54

3.20. Fracture surface of LPEO/50wt% SPI membrane 54

3.21. Different electrical properties determined by current-voltage curve 55

3.22. Effects of SPI content on I-V characteristics of HPEO/SPI membranes 56

3.23. Effects of SPI content on I-V characteristics of LPEO/SPI membranes 57

3.24. Example of a bipolar hysteresis loop 58

3.25. Monopolar hysteresis loops of HPEO and HPEO/SPI membranes 60

3.26. Effects of SPI content on hysteresis behaviors of HPEO/SPI membranes 61

3.27. Effects of SPI content on hysteresis behaviors of LPEO and LPEO/SPI membranes.......61

3.28. Effects of SPI content on hysteresis behaviors of LPEO and LPEO/SPI membranes.......62

LIST OF FIGURES (continued)

Figure | Page

3.29. Effects of SPI on HPEO/SPI membranes:
(a) Consumed energy, and (b) Stored energy 64

3.30. Effects of SPI on HPEO/SPI membranes:
(a) Released energy, and (b) Efficiency..65

3.31. Effects of SPI on LPEO/SPI membranes:
(a) Consumed energy, and (b) Stored energy 67

3.32. Effects of SPI on LPEO/SPI membranes:
(a) Released energy, and (b) Efficiency..68

LIST OF ABBREVIATIONS

ADM	Archer Daniels Midland
BHT	Butylated Hydroxytoluene
CPB	Cross-linked Polymer Blend
DC	Direct Current
DKL	Demethylated Kraft Lignin
DMSO	Dimethyl Sulfoxide
EES	Electrical Energy Storage
FTIR	Fourier Transform Infrared Spectroscopy
HPEO	High Molecular Poly(ethylene oxide)
I-V	Current-Voltage
LPEO	Low Molecular Poly(ethylene oxide)
PE	Polyethylene
PEI	Polyethylenimine
PEO	Poly(ethylene oxide)
PET	Poly(ethylene terephthalate)
PMMA	Polymethylmethacrylate
PPM	Parts Per Million
PTFE	Polytetrafluoroethylene
PVA	Poly(vinyl alcohol)
PVC	Poly(vinyl chloride)
PVDF	Poly(vinylidene fluoride)
PVP	Poly(4-vinyl)phenol

LIST OF ABBREVIATIONS (continued)

SC	Sedimentation Coefficients
SEM	Scanning Electron Microscope
SI	Systeme Internationale
SPI	Soy Protein Isolate
TEFLON	Polytetrafluoroethylene
XRD	X-ray Diffraction

CHAPTER ONE

INTRODUCTION

Pieter van Musschenbroek was a Dutch professor who discovered that the electric energy could be stored and he invented Leyden jar in 1746 to store the energy. Just after that, it transpired the first capacitor had been designated by Ewald Georg von Kliest before Musschenbroek with the same structure [1, 2].

Capacitors (also known as condensers) are devices used in electrical circuits to store electrical energy. Their configuration includes two conducting surfaces carrying equal amount of opposite charges and a dielectric material in between. When a capacitor is connected to a circuit, the current flows through the capacitor and charges it where the dielectric material performs a prominent role. When the capacitor is discharged, the charge on both electrodes will be drained. While a voltage is applied, new electrons enter one side and repels electrons on the other side to achieve energy storage (charge Q is moved from one conductor to the other one, one has a positive charge +Q, and another has a negative charge –Q). This stored energy can be used when the circuit is off [3].

1.1 Theoretical Background of Dielectric Capacitor

The two conducting surfaces, known as electrodes, are separated by a dielectric material which is a poor conductor or an insulator. The most common capacitor is a parallel-plate capacitor, shown in Figure 1.1. The capacitance of a capacitor is proportional to the area of the electrodes and the distance between the electrodes. When a capacitor is connected to a battery, the charges transfer from X to Y, instantaneously. As a consequence, there is an aggregation of negative charges on Y and positive charges on X. As a result, there will be a voltage difference between the two electrodes. The movement of the electrons makes a current flow. This current is maximum when the plates have no charge. Once the voltage between the electrodes is equal to the battery voltage, this current flow will be zero [1, 2].

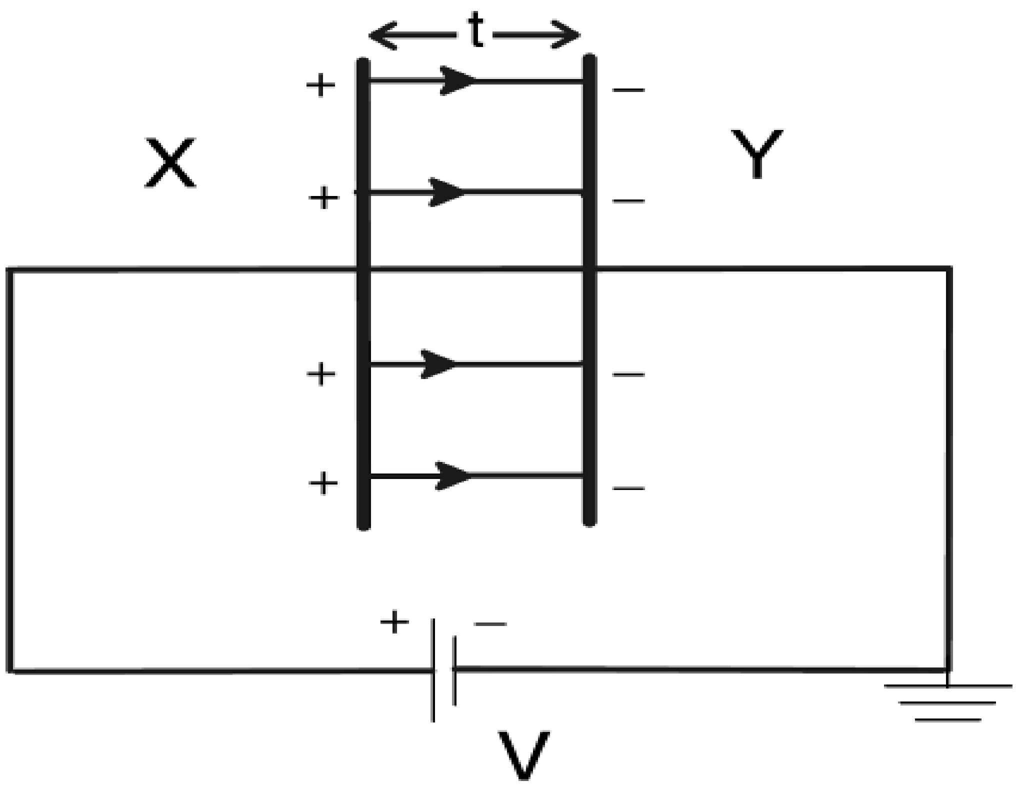

Figure 1.1. Parallel-plate capacitor connected to a DC source [1].

Each capacitor has two important ratings:

- The capacitor's ability to store electrical charge at a given voltage, i.e. capacitance (C, SI unit is Farad, F)
- The maximum voltage that capacitor can handle before it is shorted (electrical breakdown).

If the charge held on the electrodes is q at an applied voltage V, the capacitance can be measured by equation 1.1:

$$C = \frac{q}{V} \tag{1.1}$$

1 Farad is the capacitance of a capacitor which needs one coulomb charge to make a potential difference with the magnitude of one volt. Since one farad is a big unit, some lower units are using

for the measurement of capacitance, such as microfarad (µF), nanofarad (nF), and picofarad (pF) [1].

In order to charge a capacitor and store energy, a work is required to push the charges from battery to the capacitor. The amount of work (dW) required to transfer an element of charge (dq) from one electrode of the capacitor to the another electrode can be found by equation 1.2:

$$dW = \frac{Q}{C}\,dq \tag{1.2}$$

Where the SI unit of work (dW) is in Joules, for the charge (Q) is in Coulombs, and for the capacitance (C) is in farads.

The stored energy in a capacitor can be measured by integrating the equation 1.2:

$$W_{charging} = \int_0^Q \frac{q}{C} dq = \frac{1}{2}\frac{Q^2}{C} = \frac{1}{2}\,QV = \frac{1}{2}\,CV^2 = W_{stored} \tag{1.3}$$

The amount of electrical charges on the electrodes is related to the induced charge separation (formation of dipoles) within the insulator between the electrodes. The induced charge separations determine dielectric permittivity (ε) which measures the ability of a material to store electrical energy in presence of an electric field. Relative permittivity (ε_r), which is more frequently used, is the ratio of the permittivity of the dielectric in use to permittivity of the free space (a vacuum). Each material has its specific value for relative permittivity. The relative permittivity for vacuum is 1 (ε_r=1), and for the other dielectric materials it has a value greater than 1. The higher value of ε_r indicates the more capacitance of the material. The capacitance can also be calculated by equation 1.4:

$$C = \varepsilon_r \varepsilon_0 \frac{A}{d} = (8.85 \times 10^{-12})\varepsilon_r \frac{A}{d} \tag{1.4}$$

Where C is the capacitance (F), ε_r is the relative permittivity of the insulator, ε_0 is the permittivity of the vacuum (8.85×10^{-12} F.m), A is the area (m^2) of the electrodes, and d is the distance between two electrodes (m) [4].

By combining equation 1.3 and equation 1.4, the stored energy can be calculated by equation 1.5:

$$W_{charging} = \frac{1}{2}\,CV^2 = \frac{1}{2}\,\varepsilon_r\varepsilon_0\frac{A}{d}\,V^2 \tag{1.5}$$

According to the equation 1.2, the capacitance of a capacitor is a function of area of the electrodes and the distance between them. There is more to be considered than that. For instance, the charge storage can increase by enhancing the voltage. But if that voltage is higher than the dielectric insulating ability, a breakdown will occur [5]. The insulator breakdown voltage (also known as striking voltage [6]) is the minimum voltage that leads a portion of the material to become conductive. Alternatively, the breakdown electric field is used to evaluate the insulating ability. There are different breakdown electric field ranges for different dielectric materials, for example mica has a range from 100 MV/m to 300 MV/m. Since the breakdown voltage can be affected by some factors like electrode geometry, there is a possibility to have local breakdowns. Hence, for higher voltages a thicker dielectric material is required in compare to lower voltages. The breakdown leaves carbon behind and can make an explosion in capacitors at high voltages [7].

1.2 Applications of Capacitors

Capacitors have enormous uses in electrical devices. There are a large variety of capacitors and insulator materials, and each application takes the advantage of a specific type of capacitor more than others. The costs, voltage sensitivity, energy capacitance, breakdown voltage, voltage frequency, and more other factors have effects on the selection process. As a result, one type of capacitor could not be suitable for all applications. In order to provide an electrical system with the best capacitor related to the application, these applications should be known and categorized.

1.2.1 Energy Storage

Electrical Energy Storage (EES) for capacitors refers to a process of saving electrical energy from a circuit into a capacitor and discharging back to the circuit when needed. In this application, the capacitors can be used as both a charge unit and a discharge unit. In other words, this application, which is the main usage of capacitors, enables to store energy at times of low cost generation demand and be used at times of high cost generation demand [8]. However, for traditional capacitors the main issue is the low energy density. In order to improve the energy storage, the bigger dielectric surface is one effective approach, which leads to have uneconomical large capacitors. As a result, nowadays among many different capacitors with good energy storage capability, those capacitors with higher energy densities and compact designs are better options for EES application. Today, a vast variety of companies and capacitors developers are working on the improvement of this application like PowerSystem Co. [8].

1.2.2 Filtering and DC Blocking

There is a definition for electronic filter that blocks a range of signals and passes other signals. Typically, there are two types of filters based on the frequency range: high-pass filter and low-pass filter. In high-pass filters, there is a minimum (certain) frequency, and the signals with lower frequencies are not able to pass this filter, and only those signals, which have higher frequencies, can pass it. There are a large number of utilities for high-pass filters like DC blocking, in which the AC signals can pass through the capacitors but the DC signal is unable to pass. In contrast, the low-pass filter is used to remove high frequency signals, such as in audio applications. The combination of a low-pass and high-pass filters makes another type of filters called band-pass filters. In a band-pass filter, there are a range of signals within both minimum and maximum frequency limits are allowed to pass the filter [9].

1.2.3 RF Coupling

In electronics, coupling and decoupling of frequencies could be done by using capacitors. An AC coupling capacitor is used to link a number of circuits, in which the DC signal is isolated and just the AC signals pass. This application causes the fact that the capacitor works as an amplifier by making continuous amplification. For this application, the capacitor should be small with low loss and high capacitance per volume, so that the ceramic capacitors and the polystyrene capacitors are more reliable than other types. The capacitors is also used for decoupling in a power supply in order to protect the circuit from signals [10].

1.2.4 Power Conditioning

Capacitors can be used for the protection against power impulses as power conditioners in which the output wave of an AC rectifier is flattened. In a large number of electrical devices, the capacitors have been set parallel to the DC power circuit in order to smooth the fluctuations of signals. The car audio equipment is a crystal clear example, in which a number of capacitors are used to improve the voice quality by reducing the harmonic distortion from AC to DC power circuits [9, 11]. Figure 1.2 illustrates the unsmoothed and smoothed DC signals by capacitor charging and discharging. The dotted line refers to unsmoothed DC singles, while the solid line shows the smoothed DC signals [12, 13].

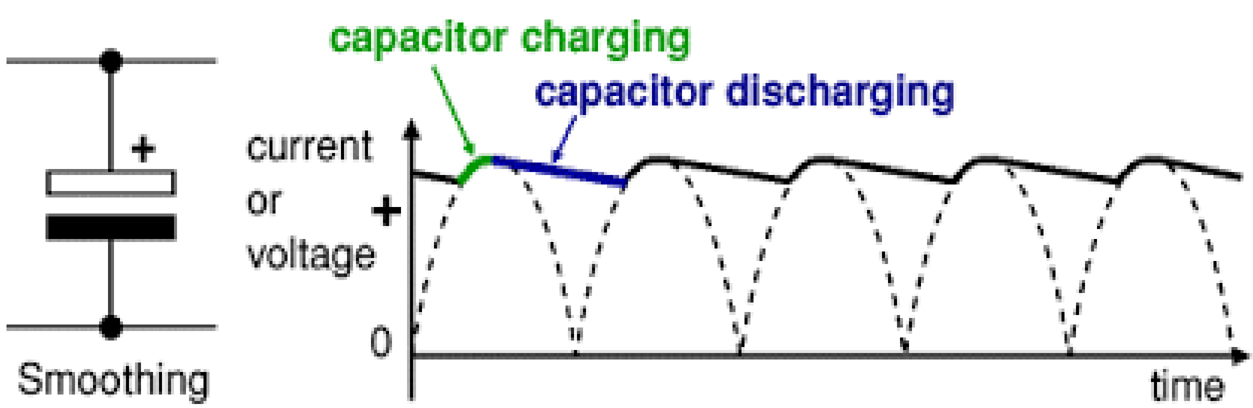

Figure 1.2. The roles of capacitors in power conditioning [12].

1.3 Classification of Capacitors

Capacitors, as given in Figure 1.3, can be classified based on the dielectric material used, electrode structure, polarization nature, and device packaging. On the basis of the capacitance, there are two different types: fixed type with constant capacitance value and variable type with changeable capacitance [14]. For some low capacitance applications, there is vacuum between electrodes to have high voltage operation and low loss. This vacuum will be replaced by a dielectric material for high capacitance applications. Insulators are the most common dielectric materials which have high permittivity and breakdown voltage. Glass, ceramic, paper, air, mica and polymer materials are some types of dielectrics used in capacitors [15]. In this section we will introduce some of these capacitors, their constructions and applications.

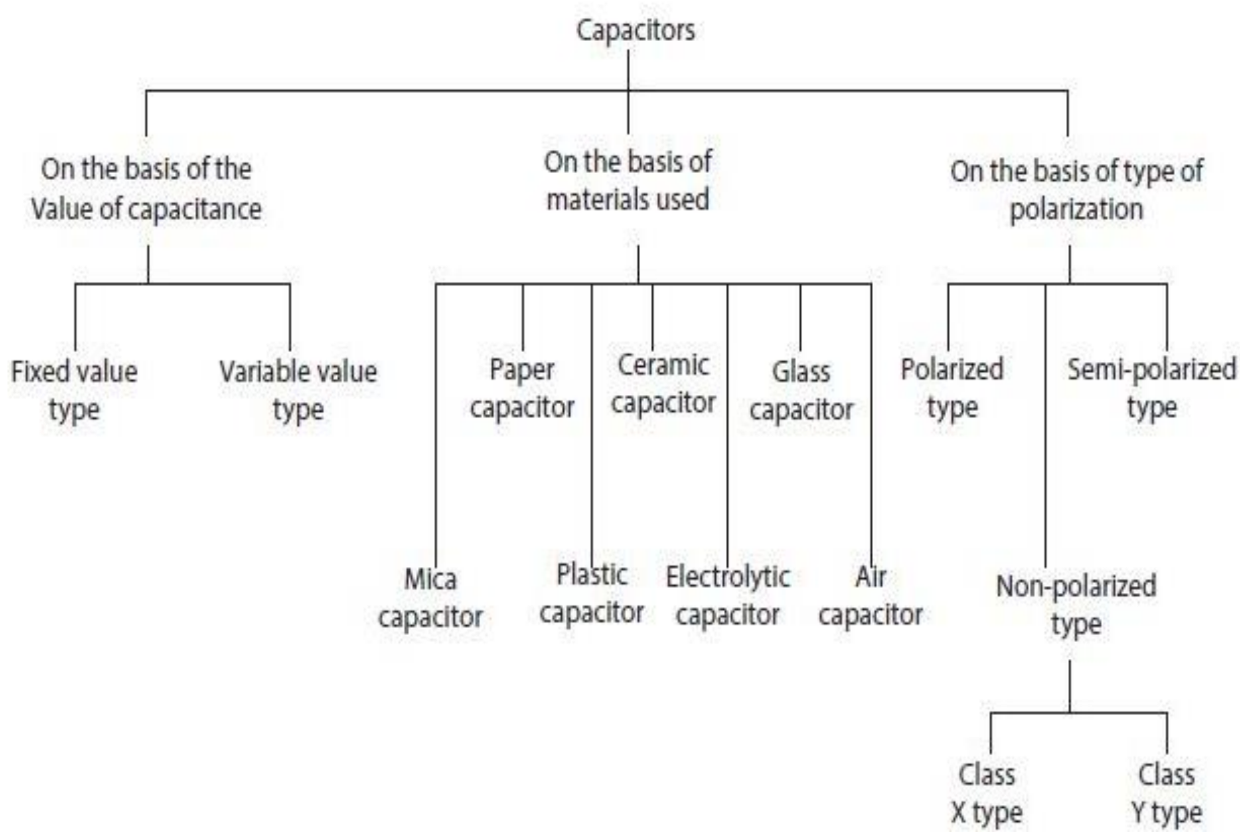

Figure 1.3. Different types of capacitors [14].

1.3.1 Ceramic Capacitors

Ceramic capacitors are designed to be used when a small physical size with large capacitance and high insulation resistance is required. These capacitors are not intended for precision applications but are suitable to use as bypass, filter and noncritical coupling elements in high frequency circuits where appreciable changes in capacitance (caused by temperature variations) can be tolerated [4]. Ceramic capacitors are also used in aerospace, telecommunication and semiconductor industries [16]. There are a vast variety of ceramic capacitors with different constructions based on the capacitance values required [14]. Different types of classifications for ceramic capacitors exist, regarding to the temperature stability, accuracy, and size [3]. One form of ceramic capacitor with the classical model of a parallel plate capacitor is called ceramic disc capacitor. There is another type offering much higher capacitance per unit volume than the ceramic disc capacitor, which is called monolithic ceramic capacitor as shown in Figure 1.4.

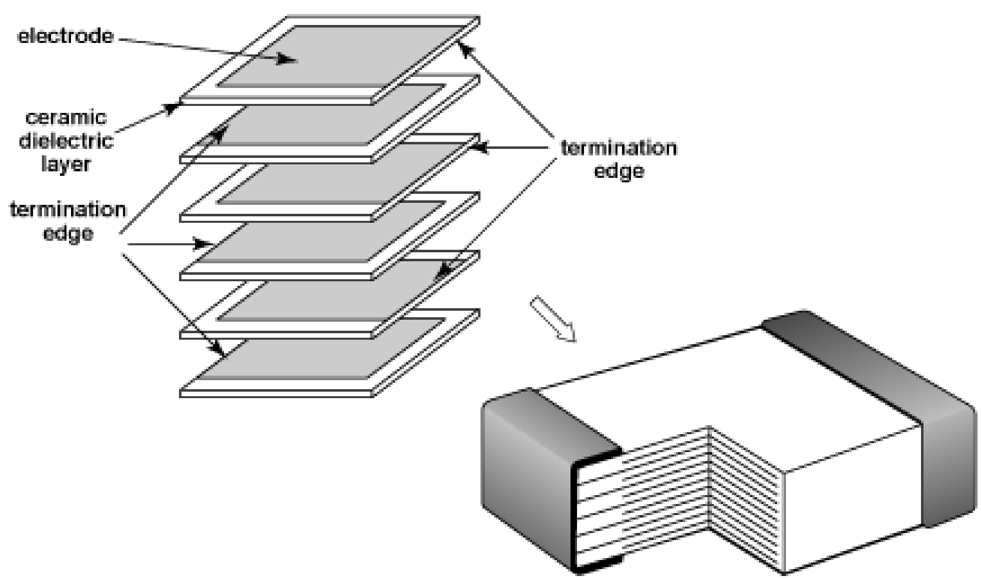

Figure 1.4. Monolithic ceramic capacitor [17].

Ceramic insulators have high permittivity that make it compatible with high frequency applications. These capacitors have capacitance value between 1 pF and 0.1 μF [14]. Ceramic dielectric materials are good for propagation of electrostatic charge, which is necessary for taking place the electrostatic attraction and repulsion [16].

Class I Dielectrics. The main material in this class is TiO_2, BaO, La_2O_3, and Nd_2O_5 also belong to this class. The class I dielectrics have low constant and low temperature coefficients. Moreover, these dielectric materials have low dielectric constant leading to limited capacitance values.

Class II Dielectrics. This class of dielectrics consists of ferroelectric dielectrics, such as $BaTiO_3$, which have high dielectric constant leading to high energy density. However, this class has some drawbacks in comparison with class I dielectrics, such as being less stable and having higher losses. Table 1.1 illustrates some differences between these two classes.

TABLE 1.1. COMPARISON BETWEEN CLASS I AND CLASS II DIELECTRICS [14]

S. No.	Class I	Class II
1.	Almost linear capacitance/temperature function	Non-linear capacitance temperature function
2.	No voltage dependency of capacitance and loss angle	-
3.	No ageing	Slight ageing of capacitance
4.	High insulation resistance	High insulation resistance, extremely high capacitance value per unit volume
5.	Very small dielectric loss	-
6.	High dielectric strength	-
7.	Normal capacitance tolerance ±1% to ±10%	Normal capacitance tolerance ±5% to ±20%

Since the interatomic bonds in ceramics are primarily ionic bonding and covalent bonding, they have high thermal stability and high melting points, meanwhile ceramic dielectric materials are hard and brittle materials with low toughness and tensile strength. These properties also play important roles in the applications of ceramic dielectric materials.

There are an enormous groups of ceramics used as dielectrics. Ceramic dielectric materials are widely utilized because of their high dielectric constant and energy density. Popular ceramic dielectric materials are Barium Titanate ($BaTiO_3$), porcelain, silicon, alumina (Al_2O_3), magnesia (MgO), and boron nitride (BN), etc. Some representative ceramics are introduced below.

Barium Titanate: Barium Titanate ($BaTiO_3$) is the first dielectric material used in dielectric ceramics capacitors, and it is the most commonly used ferroelectric ceramic. It has been used a large number of applications because of its brilliant ferroelectric and dielectric properties [18]. These properties are very dependent on the crystal structures of $BaTiO_3$ (cubic and tetragonal crystals). $BaTiO_3$ is a type of perovskite ceramics with an ABO_3 structure. This name comes from $CaTiO_3$, the mineral perovskite [19]. The ABO_3 structure is shown in Figure 1.5. The barium (A), titanium (B) and oxygen atoms are represented as blue, red, and green spheres, respectively.

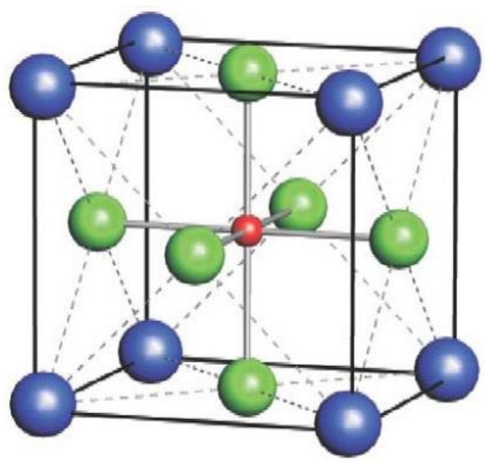

Figure 1.5. Cubic perovskite structure [20].

Some of the excellent $BaTiO_3$ characteristics are moderate dielectric loss and high dielectric constant. As a result, it has been studied for a number of applications aiming at energy storage, such as capacitors. However, it should be mentioned that its dielectric properties are also highly dependent on the ceramic processing [21]. Like other ceramic materials, a difficult processing is regarded as the disadvantage of using $BaTiO_3$ in capacitors. For instance, as a conventional solid-state reaction, calcination is a required step in $BaTiO_3$ preparation. This calcination process is a high temperature process usually between 1000 °C and 1300 °C [22-24].

Calcium Titanate: Calcium titanate ($CaTiO_3$) is one of the alkaline earth titanates also known as Calcium titanate oxide. It can be synthesized by a combination of calcium oxide and titanium oxide. $CaTiO_3$ has a perovskite structure (ABO_3) which contributes to good dielectric properties and is considered as a ferroelectric material [25, 26]. The reported dielectric constant for $CaTiO_3$ has a value of 167 at room temperature [25]. $CaTiO_3$ has also been observed as an illustrative of the low loss dielectric material [26].

Porcelain: The porcelain which is regarded as a ceramic material is a compound consisting of finely grinded clay, quartz and feldspar (for low frequency) or barium carbonate ($BACO_3$) (for high frequency). Porcelain has been used in different applications as fuse holders, line insulators, disconnecting switches, transformer bushing pins, etc. Additionally, porcelain can be used for both low and high voltage services. Table 1.2 illustrates some properties of these two types of porcelains at 298 K.

TABLE 1.2. LOW VOLTAGE AND HIGH VOLTAGE PORCELAINS PROPERTIES [27].

S. No.	Description	Low voltage porcelain	High voltage porcelain
1.	Power factor (at 50 Hz)	0.007-0.020	0.008-0.025
2.	Dielectric constant (at 50 Hz)	5.5	5.7
3.	Dielectric strength (MV/m)	5	5.5
4.	Volume resistivity (Ω-m)	10^9-10^{12}	10^{10}-10^{12}
5.	Specify gravity	2.4	2.7
6.	Water absorptivity	0.5-2.5%	0.0-0.5%
7.	Softening temperature	1300-1270°C	1400-1450°C

Ceramic materials, in the meantime, have a number of drawbacks that lead to the exploration of other insulating materials in capacitor applications. For instance, ceramics need a high processing temperature that makes it highly energy consuming and costly. These materials are known for their brittleness and high mass density. As a consequence, the life time of ceramic materials can be very short when a crack appears and the crack propagation occurs at a high speed rate. Also, the high mass density and rigidity limit the applications of ceramic capacitors.

Today, there is a huge demand for flexible electronic devices. For instance, manufactories of mobile phones, tablets, and laptops are trying to make their products as flexible, small and light as possible. As a result, ceramic materials with high mass density and rigidity are not useful materials to meet these the requirements. The answer is laid behind another category of materials known as polymer dielectric materials which take the advantages of having light weight and great flexibility compared with ceramics. In addition, polymer materials can also be used in applications when a very high breakdown strength is a necessity.

1.3.2 Glass Capacitors

Glass has an amorphous structure with high melting point. The corrosion and chemical resistivity of the glasses are very high, and based on different applications, there are a number of commercial glass products including Lead glass, Pyrex (Borosilicate) glass, Soda lime (window) glass, and Vycor (high silica) glass. These glass materials have found applications in capacitors, bulbs, bushings and some other applications due to their high dielectric strength and low dielectric loss. The insulating properties of these glasses are shown in Table 1.3.

Glass capacitors are very expensive and have important applications for highly accurate and reliable operations, in particular for high performance radiofrequency applications, and they offer the highest performance and reliability features in capacitor industry [4, 28]. However, Glass capacitors have a relatively low capacitance value.

There are three basic elements in a glass capacitor; glass dielectric, aluminum foil electrodes, and wire leads [28, 29]. The construction of a glass capacitor is shown in Figure 1.6. The electrodes have been welded by lead [4].

TABLE 1.3. VARIOUS PROPERTIES OF COMMERCIAL GLASSES [27].

S. No.	Description	Sodalime glass	Lead glass	Borosilicate glass	High silica glass
1.	Dielectric constant	7.0	6.6	4.7	3.4
2.	Power factor (at 1 MHz, 293 K)	0.004	0.0016	0.0046	0.0002
3.	Coefficient of thermal expansion (/°C)	85×10^{-7}	91×10^{-7}	32×10^{-7}	5.5×10^{-7}
4.	Resistivity (Ω-m at 298 K)	0.065	0.089	0.081	0.12
5.	Specific heat (cal/gm K at 298 K)	0.20	0.19	0.18	0.17
6.	Density (kg/m^3)	1450	2850	2130	2200
7.	Softening Point (°C)	730	630	820	1665

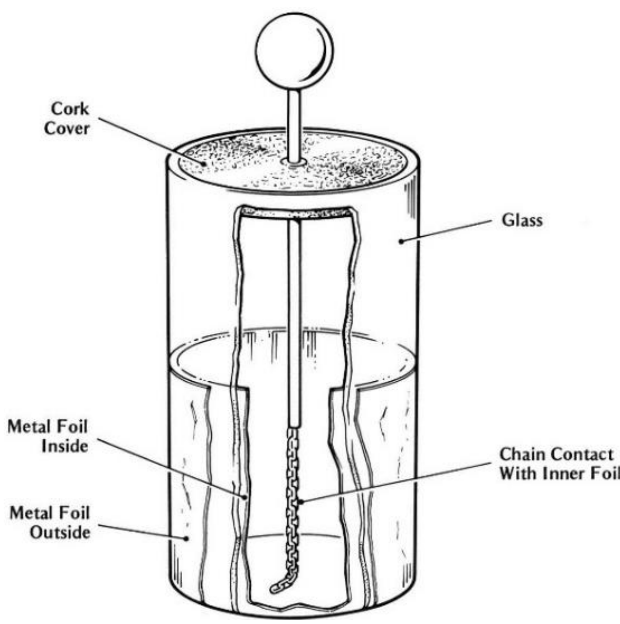

Figure 1.6. Glass capacitor (Leyden jar) [30].

Glass capacitors are highly resistant against high temperatures, voltage breakdown, and nuclear radiation. These capacitors can find applications in many areas where high power amplifiers, high tolerance areas, and high Q circuits are required [28]. In addition, glass capacitor is used in applications in which failure is not acceptable, and replacement of the failed part is not possible.

1.3.3 Paper Capacitors

Paper capacitor is regarded as one of the simplest capacitors with a paper dielectric material used in high DC and AC applications where the losses are not too important [14]. This type of capacitor shown in Figure 1.7 is made by wrapping and placing a waxed or impregnated tissue paper between two aluminum foils [31]. The waxing and impregnation is to prevent moisture absorption. Moreover, the impregnation enhances the dielectric strength of the paper capacitor. In the last step, the wrapped paper and foils are encapsulated in a metal can.

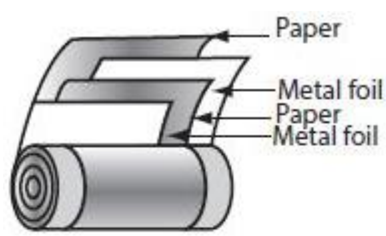

Figure 1.7. Paper capacitor [14].

These capacitors have large dimensions, and tend to absorb moisture without proper impregnation, which increases the dielectric losses and decreases the insulation resistance [32]. In case of capacitance stability, they have medium accuracy and their capacitance change dramatically with the temperature having values between 500 pF and 10 mF.

Paper capacitors have a short working life (shorter than any other capacitors), but excellent high voltage characteristics. They are also more expensive than ceramic capacitors. Since paper capacitors have higher leakage resistance, they are used in single phase motors and power factor correction devices [14, 33].

1.3.4 Plastic Capacitors

Plastic capacitors contain some plastic film layers between the metal foils, which is the same construction as paper capacitors. Polymeric materials are widely used as dielectrics in capacitors due to the uniformity they have and the ability of being thin and nonporous. There is a vast variety of plastic films to be selected as dielectric materials in capacitors such as Polypropylene, Polyester or Polyethylene terephthalate (PET), Polystyrene, Polytetrafluoroethylene (TEFLON or PTFE), Poly(vinylidene fluoride) (PVDF), etc. [14]. There are two main methods to manufacture capacitors with plastic materials: metal foil capacitors and metalized film capacitors.

There are some differences between these two types of plastic capacitors. In metal foil capacitors, metal foils are placed in between the plastic thin films, while in metalized film capacitors metallic electrodes are deposited onto plastic films. However, the encapsulation process is same for both. The capacitance tolerance and voltage ranges for plastic film capacitors are often between 1 to 20% and 50V to 400V, respectively, depends on its type and materials [14].

Foil capacitors

This type of capacitors is composed of metal foil electrodes and a flexible biaxially aligned dielectric plastic film. The foil electrodes are extended from two ends, called *as extended foil* technique that facilitates electrical contact. This ohmic contact leads to low loss and low impedance in a capacitor. The construction of a foil capacitor is shown in Figure 1.8.

Polyester is the most well-known polymer insulator for this type of capacitors. Regarding to the DC applications, polyester film based capacitors take the place of paper capacitors, due to the fact that polyester capacitors are much smaller than paper capacitors besides having lower moisture absorption. However, the temperature stability of PET is inferior to paper capacitor. As a result, the polyester capacitor with high dielectric heating is not appropriate for radio frequency applications [32].

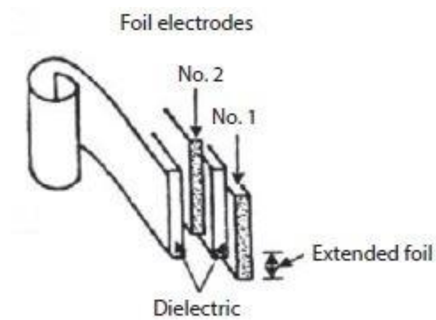

Figure 1.8. Construction of a foil capacitor [14].

Metalized plastic film capacitors

The metallized plastic film capacitor consists of a plastic dielectric film on which thin metal layers are vacuum deposited. The structure of a metalized plastic film capacitor is shown in Figure 1.9. However, the construction can be either a rolled cylinder or a stacked pack. As can be seen in Figure 1.9, this construction, called as *extended metallization*, is the same as the extended foil structure, and it makes a good connection with the electrodes.

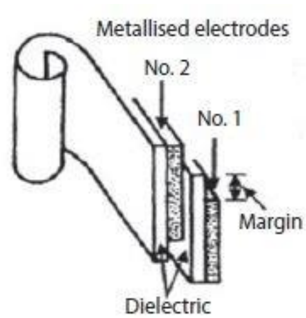

Figure 1.9. Construction of an extended single metallization capacitor [14].

The most common dielectric materials used in metallized plastic film capacitors are polypropylene, polyester, and their metallized types. Polypropylene has a lower dielectric loss and dissipation factor. Moreover, it has higher insulation resistance and higher dielectric strength than polyester. As a result, polypropylene is usually used at higher AC voltages, and it has also found good applications in high frequency range. However, polyester can be used where a thinner film is required and it has a higher dielectric constant than polypropylene [14, 32].

<u>Mixed dielectric capacitors</u>

One of the most common methods to gain better properties for a capacitor is to combine different dielectric materials such as metalized plastics, metalized paper, separate foil and plastic films, and so on. The structure of a type of mixed dielectric capacitor is shown in Figure 1.10, consisting of a mixed dielectric paper and polypropylene. This construction is made by the combination of a metalized paper and a polypropylene dielectric film, and it has high dielectric strength, low inductance and low loss at high voltages.

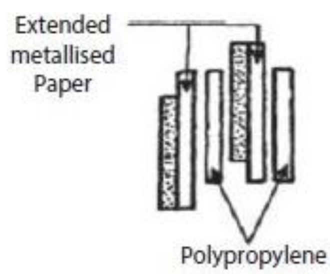

Figure 1.10. Construction of a mixed dielectric capacitor [14].

There is another construction of the mixed dielectric capacitor in Figure 1.11. This structure consists of a polypropylene film and a double metalized poly(ethylene terephthalate) film.

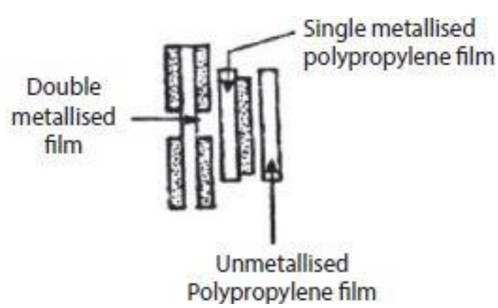

Figure 1.11. Construction of a mixed dielectric capacitor by using a double metallized polymer [14].

1.4 Polymeric Dielectric Materials

Today, polymers are known as a class of flexible and light weight dielectric materials in a number of capacitor applications [34-37]. Although polymer dielectric materials have low dielectric permittivity compared to ceramics, the breakdown strength is much higher for this group dielectric materials than ceramics. Low dielectric loss is another important attractive property for polymeric dielectric materials. In addition, they have much better chemical resistance than ceramics [38]. The advantages of polymer dielectric materials also include the fact that they are more flexible and lighter weight than traditional ceramic dielectric materials. In case of processing, polymers are much easier to be produced than ceramics, which also contributes to the increasing popularity of polymer dielectric materials. Moreover, polymer based capacitors are famed for the ability of self-healing. This phenomenon makes polymer dielectric materials much reliable for high electric field applications [39]. In contrast, ceramic dielectric materials not only do not show the self-healing ability, but also they have some size limitation. They cannot be produced as large as polymer dielectric materials can.

Polymer dielectric materials can be made into a vast variety of products with different shapes and sizes, due to their outstanding processibility and adjustable flexibility. Furthermore, there are different types of polymer materials intended for different capacitor applications, and one of the basic classification is based on the chemical structures and related behaviors in response to applied heat: thermoplastics and thermosetting plastics [27].

Thermoplastics

Thermoplastics are those polymers which show a solid-liquid transition when they are heated up, which is reversible by decreasing the temperature. Typically, thermoplastics have long linear or branched chain structures, which are connected by physical chain entanglement and secondary bonding. They are soluble and fusible. There are a large number of thermoplastics such as poly(vinyl chloride) (PVC), polytetrafluoroethylene (PTFE), polyethylene (PE), nylon, cellulose acetate, polypropylene (PP) and polystyrene (PP), etc [40].

Thermosetting plastics

Thermosetting plastics become hardened by heating up the resins, which is not a reversible process. In fact, instead of melting or softening, the thermosetting plastics will decompose due to intense heating. Thermosetting plastics have 3-dimensional network structures resulted from crosslinking of resin monomers, which contributes to the hardening upon heating as well as high strength and modulus. The increasing temperature will eventually break down the covalent bonds in the 3-D network, leading to thermal decomposition. Thermosetting plastics include Epoxy, Polyester, and Phenolic, etc [41].

1.5 Strategies to Improve Polymer Dielectrics

Polymers used for dielectric applications are required to have a large band gap, high dielectric constant and breakdown strength, applicable glass transition temperature, and low dielectric loss [42]. While a polymer may not have all these features simultaneously, there are different strategies to improve the dielectric properties.

Some parameters that can serve integral roles in improvement of polymer dielectrics include crosslinking, chain polarity, polarizability and free volume. For example, aromatic rings and sulphur have high polarizability, and presenting them to a polymer leads to a growth in dielectric constant. In the meanwhile, using fluorine that has small atomic radius and electron cloud brings a lower dielectric constant due to a low polarizability [43]. Free volume is regarded as another important parameter which is defined to the not occupied volume of the polymeric material. The higher the free volume is, the lower the dielectric constant would be. In other words, the unoccupied volume (such as microvoids) will act just like air with the relative permittivity of one. As a result, this free volume should be replaced by some new polymer structures in order to increase the dielectric constant [44, 45].

It is obvious that synthesizing new polymers contributes to new dielectric properties, and it can be regarded as an effective strategy to improve polymer dielectric materials. However, the majority of the studies are based on modification of present polymeric dielectric materials. One of the strategies comes from the attitude to take the advantages of both dielectric ceramics and polymer dielectrics. Dielectric ceramics which are brittle and energy consuming in case of processing can be introduced to the flexible polymeric dielectrics to achieve both high dielectric constant and more improvements in ease of processing and material flexibility [43]. A number of studies have been done on polymer/ceramic composites, such as adding Al_2O_3, $BaTiO_3$ and ZrO_2 to polyimide, and enhanced dielectric properties were reported [46-48]. Meanwhile, adding carbon black particles and fibers to a polymeric matrix could also lead to a large dielectric constant [49].

The high dielectric constant of polymer composites is typically from both high dielectric constant of the dielectric ceramics and interfacial polarization between the polymer matrix and ceramic materials. Polymer blends is another strategy using muti-phase polymeric materials to achieve excellent insulting properties and tunable capacitance values.

The space charge formation in a polymer blend made of polypropylene and polyethylene have been studied by Katsunami et al, and they proved that this polymer blend had a higher dielectric strength than two homopolymers at room temperature [50]. It should be mentioned that for polymer blends, the structures of each polymer play an integral role on the dielectric properties of the blends. For instance, in the blends of amorphous polar polymers and liquid crystalline side-chain polymers, the former had a very low loss and high energy density below the glass transition temperature while the latter had a good dipole mobility contributes to a limitation of electrical energy after dipole saturation [34].

There are some other methods to improve the dielectric properties of polymeric materials such as introducing some structural defects like bulky comonomers, so that the lateral unit cell will be expanded through crystalline lattice [34]. It should be realized that each method has some benefits and a number of drawbacks, and the selection of these methods for enhancing the dielectric properties mainly depends on the required applications.

1.6 Soy Protein and Its Applications

Soybean is a low cost crop with great add-on values. There are three different commercial categories for soy products: soybean flour, concentrate soybean, and soy protein isolate (SPI) with the protein content of 50%, 70% and 90%, respectively. The major consumption procedures of the soybean are in the form of traditional soy foods, such as soy milk, soy sauce, kori-tofu, etc. [51]. Due to the physiological properties of soybean, the consumption of soy protein has started to boost in United States in 1997 as a turning point [52]. Today, soy protein is being used in a number of foods like cheeses, breads, cereals, pastas and etc., since soy protein is rich in nutrition in case of essential amino acids.

Soy protein is regarded as an economical and high-quality vegetable protein source found in soybeans that does not contain cholesterol or high saturated fat [51, 53]. The commercial soy protein products mentioned above are getting more attention due to their non-food functional properties. Binding, water absorption, gelation, foaming, fat absorption, and emulsification are regarded as some of these functional properties [51]. Due to the unique chemical and physical structures of soy protein, a great number of scientists have been researching on soy protein based materials, basically on two most popular research areas: one is to make some bio-plastics from those soy protein structures and another one is to produce some bio-based adhesives used for laminated composite structures.

In the case of chemical structures, there are eight essential amino acids provided by soy protein and all the amino acids form covalent chemical linkages called peptide bonds which make linear unbranched polymeric structures [54, 55]. According to the classification based on sedimentation properties, four protein fractions can be found in soy protein: 2S, 7S, 11S and 15S fractions which contain 8%, 35%, 52% and 5% of total protein content, respectively [56]. The highest protein content of soybean is stored in β-conglycinin and glycinin, the former has the sedimentation coefficients (SC) of 7S while the latter has 11S [51, 56]. The SC of 7S can also be found in γ-conglycinin. The SC of 7S and 11S are regarded as two major components of soy proteins. Both 7S and 11S fractions belong to the family of globulin shwoing some differences in point of view of physicochemical properties and structures. For instance, the minimum solubility of 11S protein happens at pH 6.4, while the 7S is insoluble at pH 4.8 [56].

1.6.1 Denaturation and Modification of Soy Protein

SPI has poor processability and brittleness. When the soybean flakes are defatted and washed in oil or water, the sugar and other fibers can be removed by washing in alcohol or water. This process is one of the soy protein modification methods that will be discussed in continue. Protein has four structure levels as shown in Figure 1.12: primary, secondary, tertiary, and more complicated quaternary structures.

The primary structure is the linear sequence of amino acids, and the combination of this chain with the string describes the secondary structure. When the string folds to its final shape, it makes a three dimensional structure known as tertiary structure. This is where protein shows its biological function. A number of tertiary structures construct the quaternary structure of the protein [57, 58].

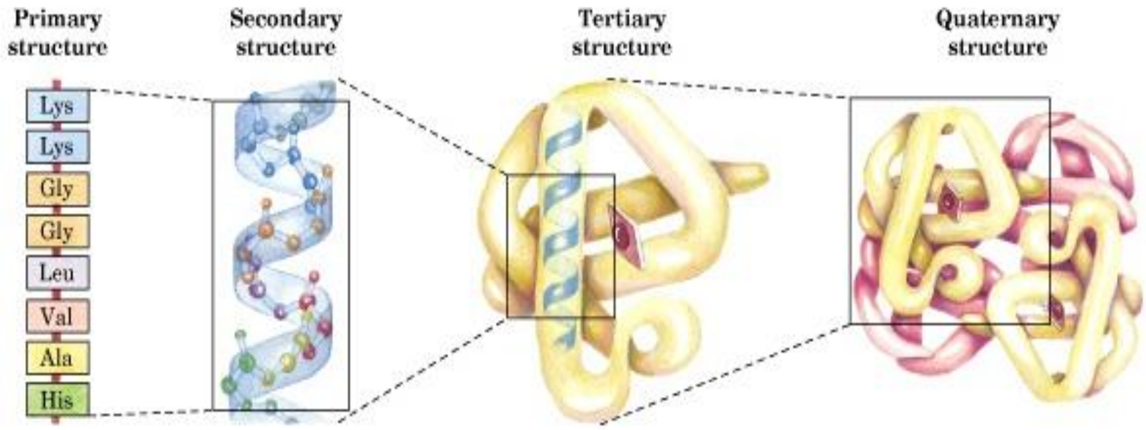

Figure 1.12. Protein structures [59].

The stable condition of the protein is to be folded, so that the Gibb’s free energy would be minimum. The denaturation of protein is linked to the protein structure disorder. In other words, denaturation happens in order to uncoil the protein structure randomly. As a result, the protein loses its biological function and other functional properties are achievable [60].

The denaturation process contributes to a better processibility and desired product properties for the soy protein isolate like strength, water resistance, adhesion, etc. However, from a dielectric perspective, the soy protein denaturation can induce the changes in the polar structures of soy protein. In fact, one of the important characteristics of soy protein is that it has really polar structure in each level. This polar structure is related to internal interactions and chemical bonds such as hydrogen bonds, ionic interactions, disulfide bonds, hydrophobic interactions, etc. This polar structure indicates the potential of a strong and adjustable polarization of soy protein based functional materials. Consequently, this polarizability helps to develop all protein based materials and also use them in some dielectric polymers to modify those existing dielectric polymers.

Soybean protein modification can be done by physical, chemical and enzymatic treatments [56]. The main reason of the treatment is to gain different functional properties. The functional properties of soy protein can be changed by heating, hydrolysis, pH adjustment (alkalis and acids), and detergents [51, 56].

Thermal Modification

Thermal treatment is the oldest and most common method for soy protein denaturation where better functional properties are provided and the proteins digestibility is increased. Studies proved that heating the soy protein to temperatures above 70°C contributed to some major changes in structures and the formation of protein aggregates. The structural changes happen via some electrostatic forces, along with hydrophobic and disulfide interchange mechanisms [51]. Thermal treatment not only increases the solubility of the protein, but also enhances the emulsifying properties. In addition, heating does not add any other chemicals to the protein and has not any effect on its purity. Thermal modification is a really controllable method in comparison with other modification methods. Moreover, it is a cheap process that provides good enough efficiency.

Thermal susceptibility of glycinin and β-conglycinin as two main protein stores are different. The thermal transition of 7S globulin is about 71°C, while it is 92°C for the 11S globulin due to its more stable and compact structures [61]. The protein aggregation does not take place during heating process where both 11S and 7S basic subunits are presented [62]. During last two decades, the effect of different conditions such as protein concentration, pH, temperature and ionic strength on functional properties of SPI have been studied and demonstrated the functionality highly depends on the degree of denaturation, dissociation and aggregation of 11S and 7S globulins [63-68]. The SPI has both soluble and insoluble proteins and the functionality of the SPI can be recognized by studying the types and contents of soluble and insoluble proteins. There are different methods for heat treatment but studies show that dry heating does not have an impressive effect on the denaturation of soy protein isolate. Heating could be more effective on denaturation process of the SPI when it is accompanied by moisture [69-71].

<u>High Pressure Modification</u>

This is another method used for denaturation of the soy protein isolate by affecting on the structure and the protein-protein connections. By applying pressure on the SPI, the electrostatic and hydrophobic interactions are disrupted and the hydrophobicity and solubility of the protein would be changed [72, 73]. However, there are not many studies working on the dynamic pressure modification of soy protein because it is a high cost process.

<u>Chemical Modification</u>

Chemical modification of soy protein has become one of the most common research areas during three last decades. As a result, different methods of chemical modification have been recognized. Based on the required applications, the purposes of chemical modification could vary, such as changing the protein solubility and decreasing protease activity, etc. Protein denaturation involves the breaking of covalent bonds and some destructions in structure caused by various secondary bonding, leading to the exposure of more hydrophobic structures on the outside of the protein structures. Consequently, the changes in the protein properties will take place.

The most important issue in using chemicals for modification is the chemical reactions. Since those changes coming from chemical reactions are often not desirable, the nondestructive chemical modification should be more ideal. There are some nondestructive chemical reactions such as acylation, alkylation and esterification, oxidation and reduction, and treatment with alkalies and acids which we will discuss the last one in pH modification [74].

There are different chemicals like urea, dimethyl sulfoxide (DMSO), etc. that can be added to soy protein in order to change protein structure as desired for a specific application. For instance, maleic anhydride, polyethylenimine (PEI), demethylated kraft lignin (DKL), etc. are some of chemical materials used for chemical denaturation of soy protein for adhesive applications. They have some functional groups such as the catechol moiety, primary amino group, and a mercapto group that can modify the structures of soy protein [75].

pH Modification

Acid-alkali denaturation is a popular modification method which can change the solubility of glycinin and β-conglycinin in different pH ranges [76]. For example, pH 4.0-5.0 is reported as the range of the minimum solubility of 7S and 11S globulins [77]. Soy protein has very low solubility in acidic media, in contrast with the basic media where a number of studies proved that the soy protein solubility would be increased at pH 11-12 [78]. The pH adjustment is regarded as an efficient method to modify the functional properties of SPI. However, it should be noted that in the most cases, adjustment of pH has been accompanyed by the heat treatment to achieve more effective modification.

1.6.2 Non-Food Functional Properties of Soy Protein

Soy protein isolate is one of the biological materials that can have the ability of storing electrical energy as well as dissipating it. SPI is a mixture of complex random copolymers of amino acids, and comprise a mixture of neutral, polar, and charged side chains. Soy protein has been increasingly studied in recent years as next-generation biopolymer materials for composites and packaging applications [79-81], and hydrogels for biomedical applications [82, 83]. As early as the 1930s, studies on the dielectric properties of protein-containing materials systems have been proposed [84, 85]. As of today, the studies are generally classified into the following categories:

protein solutions [84-87], hydrated proteins [88, 89], and amino acids/peptides [90, 91] for biological or food applications. Meanwhile, protein materials as dielectric components in electronic devices have been reported, such as transistors [92, 93] and switching devices [94].

However, the application of materials derived from proteins in dielectric energy storage applications have rarely been explored, although proteins have great potential in storing electrical energy due to its diverse polar structures [95]. Few studies have attempted to use soy protein for this application. For example, in a study of Polymethylmethacrylate (PMMA)-g-Soy composites, the soy protein was used to initiate the surface polymerization of PMMA[96]. Denatured soy protein was employed to disperse carbon nanotubes, leading to nanocomposites with enhanced dielectric constant [97].

Zhu et al. proved that using SPI for gel polymer electrolyte contributes to a remarkable electrochemical performance. That means high ionic conductivity and good electrochemical permanency. In another recent study, Zhong et al. found the molecular structures in SPI and having various functional groups lead to ion transporting through protein macromolecules [98]. Bazinet et al. did a research work on the effects of soy protein concentration on the performance of bipolar membrane electro-acidification by using an electric field as the driving force. Their procedure was to dissociate water molecules and produce protons by using a bipolar membrane. The main purpose of this study was to improve the method of purifying food productions. However, the results showed that the high concentration of soy protein could contribute to a resistance change. Based on this paper, there could be an idea to use soy protein to increase the number of charges in solution [99]. In 2011, Liu et al. studied the effects of pulsed electric field on the secondary structure and thermal properties of SPI. They observed a change in secondary structure of SPI after applying pulsed electric field which led to polarizing some bonds through the SPI as well as unfolding molecules and dissociation of its subunits [100]. This change in polarizability of SPI alongside being a renewable and environment friendly food product contributes to the idea of using SPI for energy storing and in electrical researches.

1.7 Proposed Research and Objectives

Poly(ethylene oxide) (PEO) is a type of highly polar semi-crystalline polymer with great solubility in a variety of solvents. It has been a popular polymer material studied for various electrochemical devices [101-103]. PEO has been frequently blended with SPI to fabricate new functional polymer materials [104, 105], such as electro-spun mats for wound healing [106, 107], air filtering applications [108, 109] and polymer electrolyte for lithium battery applications [110]. In recent years, with the increasing demand for transient and disposable electronic devices, the soluble polymers such as polyvinyl alcohol (PVA) [111] have been gaining increasing attention as the candidates. PEO, as a type of soluble and biodegradable thermoplastic polymer with good biocompabitlity and low toxicity [112], has great potential in such applications. The pure PEO membranes were highly polarizable, but it also has extremely high energy loss during charging/discharging cycles. The high loss is not only responsible for the unsatisfactory energy storage performance, but also leads to high dielectric heating.

This study focused on the dielectric energy storage applications of PEO, and SPI was used to modify energy storage performances of two types of PEO with different molecular weights. The electrical properties and energy storage performances of the resulting membranes were studied by current-voltage tests and hysteresis analysis. The microstructures including fracture surfaces and crystallinity were studied by scanning electron microscope (SEM) and X-ray diffraction (XRD). In addition, Fourier transform infrared spectroscopy (FTIR) and contact angle analysis were used to study the SPI-PEO interactions. The objectives of this research include (a) study of the effects of SPI on the microstructures of PEO/SPI membranes; (b) investigate the roles of SPI in the dielectric polarization of PEO/SPI membranes and (c) explore the potential of PEO/SPI membranes as dielectric energy storage materials. The success of this work will help us explore non-food functional applications of plant proteins and increase add-on values of renewable natural resources. Meanwhile, it will lead to new sustainable transient electronic materials and devices with high performances.

CHAPTER TWO

METHODOLOGY

2.1. Materials

2.1.1 Poly(ethylene oxide)

Poly(ethylene oxide) powder was purchased from Sigma-Aldrich and used as received. Two average molecular weights of PEO is used in this study, M_w = 1,000,000 g/mol (denoted as high molecular PEO (HPEO)) and M_w = 100,000 g/mol (denoted as low molecular PEO (LPEO)). They contain 200-500 ppm butylated hydroxytoluene (BHT) as inhibitor. The melting and glass transition temperatures are 65 °C and 67°C, respectively.

2.1.2 Deionized Water

Deionized water was purchased from Sigma-Aldrich. The molecular weight of the deionized water is 18.02g/mol and has the boiling point at 100°C. It also has a density of 1.000g/mL at 3.98°C.

2.1.3 Soy Protein Isolate

PRO-FAM 891 isolated soy protein was generously donated by Archer Daniels Midland (ADM) and contains 90% protein. The shelf life is eighteen months while the storage temperature should not exceed 25°C for an extended period of time. The soy protein isolate powder is shown in Figure 2.1.

Figure 2.1. Soy protein isolate powder.

2.2 Sample Preparation

The PEO/SPI membranes were made via slide-casting and drying aqueous solutions of PEO/SPI at 45°C temperature. The amount of water has been used for the all samples is 15ml. Table 2.1 shows the composition and preparation conditions of different samples.

TABLE 2.1. DIFFERENT COMPOSITIONS AND CONDITIONS USED AS SAMPLE PREPARATION.

NO.	SPI (wt%)	Water(ml)	Mixing Temperature (°C)	Heat Treatment Temperature (°C)	Dry Temperature (°C)
1	0	15	60	60	45
2	10	15	60	60	45
3	30	15	60	60	45
4	50	15	60	60	45
5	70	15	60	60	45

Heat Treatment of SPI

The first stage of the process is heat treatment of SPI in deionized water. Soy protein isolate was added to the water after being weighted. The bottle was put in an oil bath on a hot plate shown in Figure 2.2 and the solution was mixed by a distributor with the rotational speed of 350 rpm. In order to have a completely heat treated SPI solution, the solution should be mixed for 4 hours at the same condition. It should be noted that for the pure PEO samples, the process starts from the next step directly.

Figure 2.2. Hot plate with magnetic stirring.

Fabrication of PEO/SPI Membranes

The weighted PEO was added after the heat treatment of SPI in deionized water, and the mixing process was up to 10 hours to have a homogenous solution. During this step, a large number of air bubbles are diffused to the solution and a sonication process is needed before casting. The sonication for 30-45 minutes can remove the air bubbles through the samples. The ultrasonic cleaner is shown in Figure 2.3.

Figure 2.3. Branson ultrasonic cleaner.

The solution should be casted with required thicknesses. For this purpose, an applicator shown in Figure 2.4 is used to cast the films on a non-polar and hydrophobic polyethylene surface for the convenience of the membrane separation. Different samples have various wettability, undoubtedly. As a result, the shrinkage happens for the samples with high polarity and hydrophilicity.

Figure 2.4. Film applicator with the range of thicknesses from 5 to 50 mils.

The last step of the preparation process is drying the wet membranes in the oven at required temperature for 48 hours. The wet membranes should be placed on a flat surface in the oven in order to prevent any non-uniformity.

2.3 Characterizations

It is necessary to figure out the structure of the samples in order to track the property changes. Three different tests have been do ne on the samples to study the structure of membranes including Fourier Transform Infrared Spectrum (FTIR), X-ray diffraction (XRD), and Scanning Electron Microscopy (SEM). Moreover, the electric and dielectric properties of the membranes have been studied by current-voltage (I-V) tests and hysteresis analysis.

It must be noted that the film samples were cut to square pieces with the thickness of ~55μm for all tests. In addition, all tests have been done at room temperature. For each case, each test has been performed at the same condition at least three times, in order to make sure that the results are reliable and repetitive. The average values were used for analysis and discussion

2.3.1 Contact Angle Measurement

The droplets of PEO/SPI aqueous solutions were injected onto a hydrophobic surface by a hypodermic needle. In this study, all the contact angle measurements have been collected 75 second after dropping on the surface when the droplets were stabilized on the surface. The contact angles were measured and the averages data are provided in chapter 3.

2.3.2 Fourier Transform Infrared Spectrum

In order to do the FTIR test on samples, the equipment should be calibrated and a reference was used for testing membranes. The data collected on 32 steps by the FTIR software. Once the sample is tested, the data are ready to be gathered and a list of peaks could be extracted from the software. The results would be plotted by transmitted intensity versus wave numbers.

2.3.3 X-ray Diffraction

Rigaku MiniFlex II Desktop X-ray Diffractometer (CuKa radiation =1.5406 A°, 30kV and 15mA with a scanned step size of 0.05° and scan speed is 4°/min) was applied to the study the crystal structures of PEOs and PEO/SPI membranes.

2.3.4 Scanning Electron Microscopy

The morphologies of fracture surfaces of PEO/SPI membranes were analyzed using SEM (FEI Quanta 200F). Cryofracture was conducted in liquid nitrogen after cooling the membranes in liquid nitrogen for 5 mins. Gold coating was sputtered onto the fracture surfaces before SEM observation. The compatibility between PEOs and SPI, as well as the fracture behaviors of the membranes were studied.

2.3.5 Current-Voltage Characteristics

By Current-Voltage test (I-V), the I-V curve was measured to figure out the electric field/voltage level where there is a very significant leaking. There are some parameters that should be set before the I-V measurement such as the frequency, sample thickness, sample and electrode areas, temperature, and maximum voltage. Therefore, it is of great importance to know the amount of these parameters. In this study, the sample and circular electrode areas were equal to $0.16cm^2$. The highest voltage applied to the membranes was 2000V. The frequency set as $100s^{-1}$ and the sample thickness was 55μm. The electrode was cleaned by ethanol after each test in order to prevent the effect of contaminants on the results.

2.3.6 Hysteresis Measurement

In this study, the monopolar hysteresis behaviors of the membranes were analyzed using a Precision LC II Ferroelectric Test System (Radiant Technology,Inc) equipped with a high voltage amplifier (Matsusada, AMJ-4B10). The polarization behavior and energy storage performances were calculated using monopolar hysteresis loops. The testing frequency was 10 Hz, and the maximum electric field was 80 kV/cm.

.

CHAPTER THREE

RESULTS AND DISCUSSION

3.1 Contact Angle Measurement

The contact angle of the solutions performs an integral role in the amount of shrinkage, final film thickness and surface quality. The relation between contact angle and the wetting of a droplet on a surface is shown in Figure 3.1.

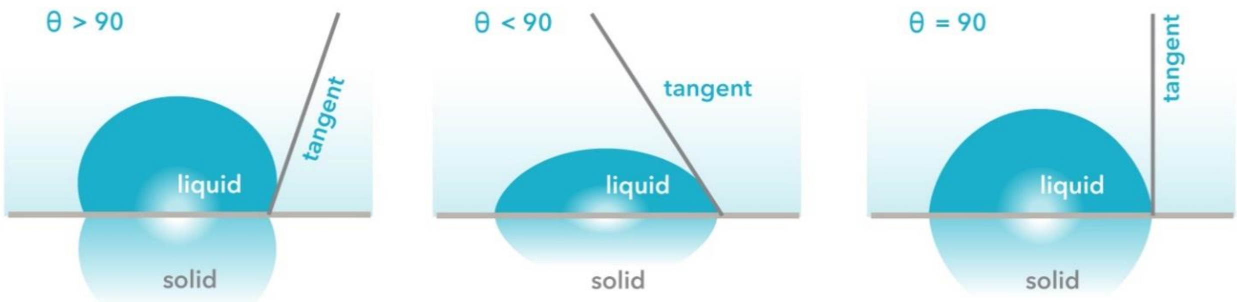

Figure 3.1. Effect of contact angle on hydrophobicity [113].

When a droplet on a surface has a smaller contact angle than 90°, there is a good contact between the solution and the surface that means good wettability of the solution. There are three thermodynamic equilibrium phases between these surfaces, which determine the contact angle value. Hence, there are three surface energies; solid-liquid, liquid-vapor, and solid-vapor denoted by γ_{sl}, γ_{lv}, and γ_{sv}, respectively [114]. The equation 3.1 known as Young's equation [114] illustrates the relation between surface energies and the contact angle:

$$\gamma_{sv} - \gamma_{sl} - \gamma_{lv} \cos\theta_C = 0 \tag{3.1}$$

Where θ_C is the contact angle.

Since the surface used in this contact angle study is a hydrophobic surface, the lower contact angle means the more compatibility between the solution and this surface. In other words, the solution would be more hydrophobic when it has smaller contact angle. That is to say, the higher the contact angle is, the more hydrophilic the solution will be. In order to make a good contact between the solution and the surface, the lower contact angle is desired. The contact angles of different solvent and solutions have been measured: deionized water, high molecular PEO in water, pure SPI in water, and the mixture of SPI/HPEO with different contents of SPI. Table 3.1 illustrates the results of the contact angle test:

TABLE 3.1. THE CONTACT ANGLE OF DIFFERENT SOLUTIONS ON A HYDROPHOBIC SURFACE.

Name	**Avg. Contact Angle (°)**	**Standard Deviation (°)**
Water	100.904	3.00
HPEO	87.59	1.75
HPEO/10wt% SPI	74.842	1.48
HPEO/30wt% SPI	80.052	0.74
HPEO/50wt% SPI	79.048	1.62
HPEO/70wt% SPI	77.176	1.54
SPI	77.188	0.65

Referred to Table 3.1, the water is the most hydrophilic compared to other solutions in this study. Adding HPEO to the water decreases the contact angle and results in a better wettability. The SPI solution has smaller contact angle in compare to PEO solution and deionized water. In addition, it suggests that adding SPI decreases the contact angle of the solutions. In other words, the difference in surface tension energy between the liquids and the non-polar/hydrophobic surface is smaller by adding SPI to the HPEO.

The SPI has both hydrophilic and hydrophobic groups in its structure. When the SPI is folded before the heat treatment in deionized water, the hydrophobic groups aggregated inside of the SPI, and the hydrophilic groups are the more available on the surface [115]. There is a possibility that by heat treatment of SPI, these hydrophobic structures are more available. Meanwhile, the hydrophilic-hydrophilic interactions between PEO and SPI might also contribute to the reduced exposure of hydrophilic groups in SPI. Consequently, the hydrophobicity of the solution increases when SPI is introduced to it. It should be noted here that the heat treatment in this study was only 60 ˚C, which could only denature some low molecular weight component in the SPI [95, 116]. However, even without high degree heat denaturation, the effects of SPI on the wettability of the solution is significant with the addition of only 10 wt% SPI.

The shrinkage of the solution during casting is dependent on the surface tension between the solution and solid surface. Since the pure PEO has a high contact angle, the shrinkage happened right after casting the solution on the non-polar polymeric surface. The addition of SPI helped the solution to spread out due to a good wettability. It proves that the differences between the surface tension of the hydrophobic non-polar polymeric surface and the solution is getting smaller.

3.2 Fourier Transform Infrared Spectrum

One of the first steps of analysis is to figure out the chemical structures of the materials at their pristine conditions. In this case, the structures of pure PEO and pure SPI before and after heat treatment have been studied via FTIR. Figure 3.2 illustrates the FTIR spectrum of the pure PEO, regardless of the molecular weight. The assignment of characteristic peaks of PEO is summarized in Table 3.2.

The strong absorption band at 2860 cm^{-1} is assigned to symmetric and asymmetric C-H stretching modes of the CH_2 group. Those bands appearing in the region 1335-1340 cm^{-1} correspond to the symmetric CH_2 wagging mode of PEO. Moreover, the bands observed at 1280 cm^{-1} suggest the symmetric and asymmetric CH_2 twisting mode [117]. The presence of the crystalline structure of PEO is suggested by two peaks of the C-O-C stretching vibration at 1095 and 1145 cm^{-1} [118]. Figure 3.3 showing the FTIR results for SPI powder. The important vibration modes are mentioned in Table 3.3.

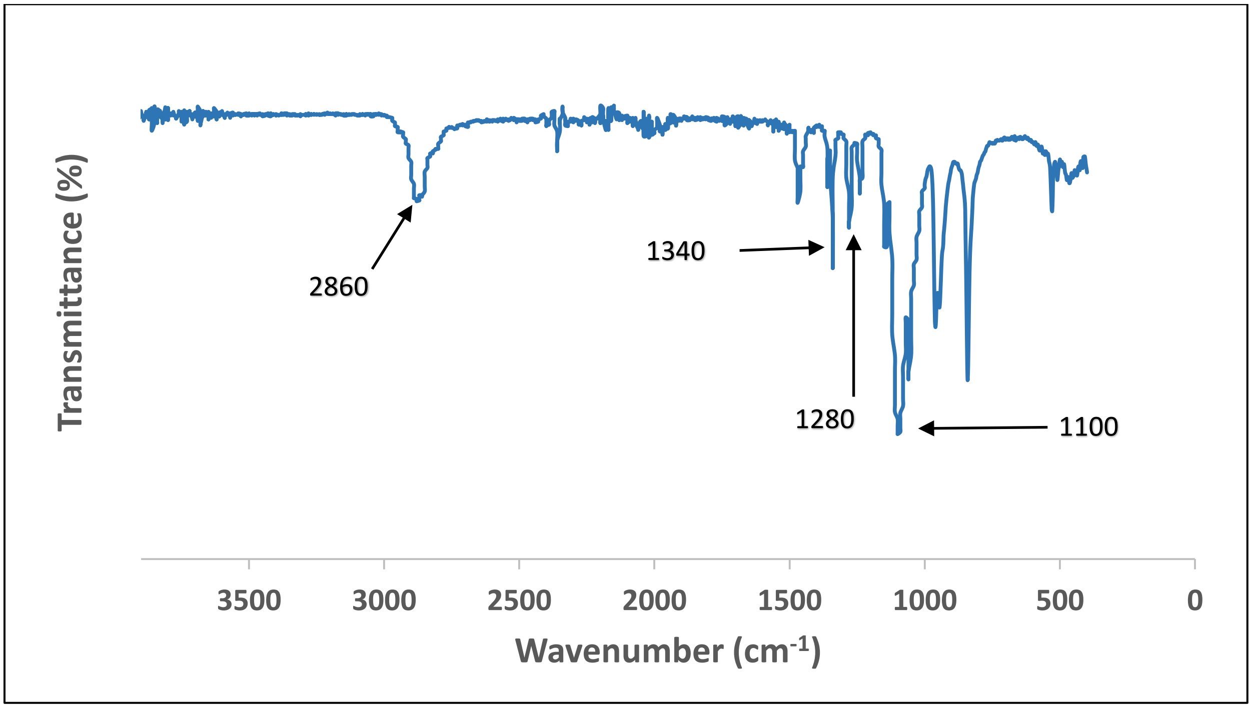

Figure 3.2. FTIR spectrum of of pure PEO.

TABLE 3.2. FTIR PEAK ASSIGNMENT OF PURE PEO.

Wave number (cm^{-1})	**Attributable**
945	C-O-C stretch [119]
1095	C-O-C vibration [118]
1144	C-O-C vibration (asymmetric strength mode) [117, 118]
1278	Asymmetric and symmetric CH_2 twisting mode [117]
1340	Asymmetric CH_2 wagging [117]
2860	Asymmetric and symmetric C-H stretching of CH_2 [117]

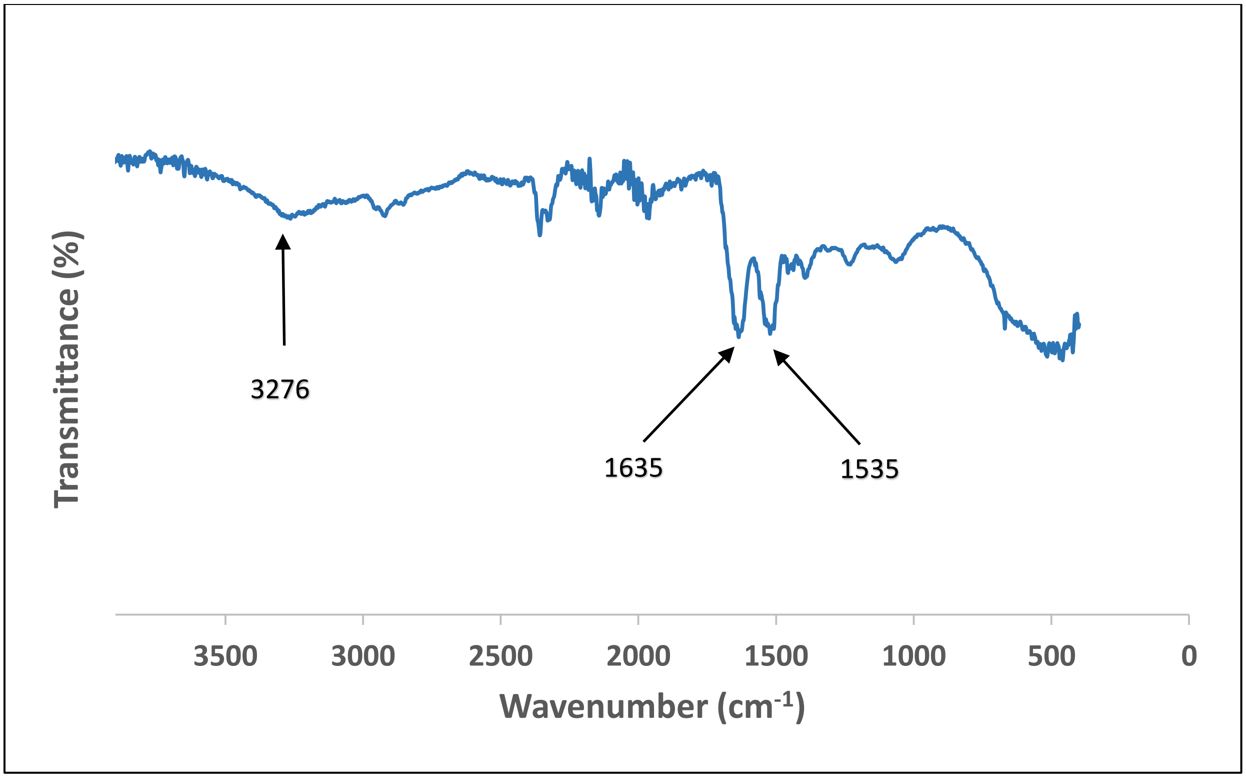

Figure 3.3. FTIR spectrum of as received SPI powder.

TABLE 3.3. FTIR PEAK ASSIGNMENT OF SPI POWDER.

Wave Number (cm^{-1})	**Attributable**
1535	Amide II (N-H)
1635	Amide I (C=O) [120]
3276	N-H stretching vibration

In order to find the effect of denaturation on bonds through the SPI, another FTIR test have been measured on the heat treated SPI sample and the results are provided in Figure 3.4. By comparing two FTIR figures for SPI powder and heat-treated SPI, it is clear that the only difference between two results are the intensity of the peaks. Table 3.4 illustrates the most important FTIR peaks of the heat treated SPI and their attributable.

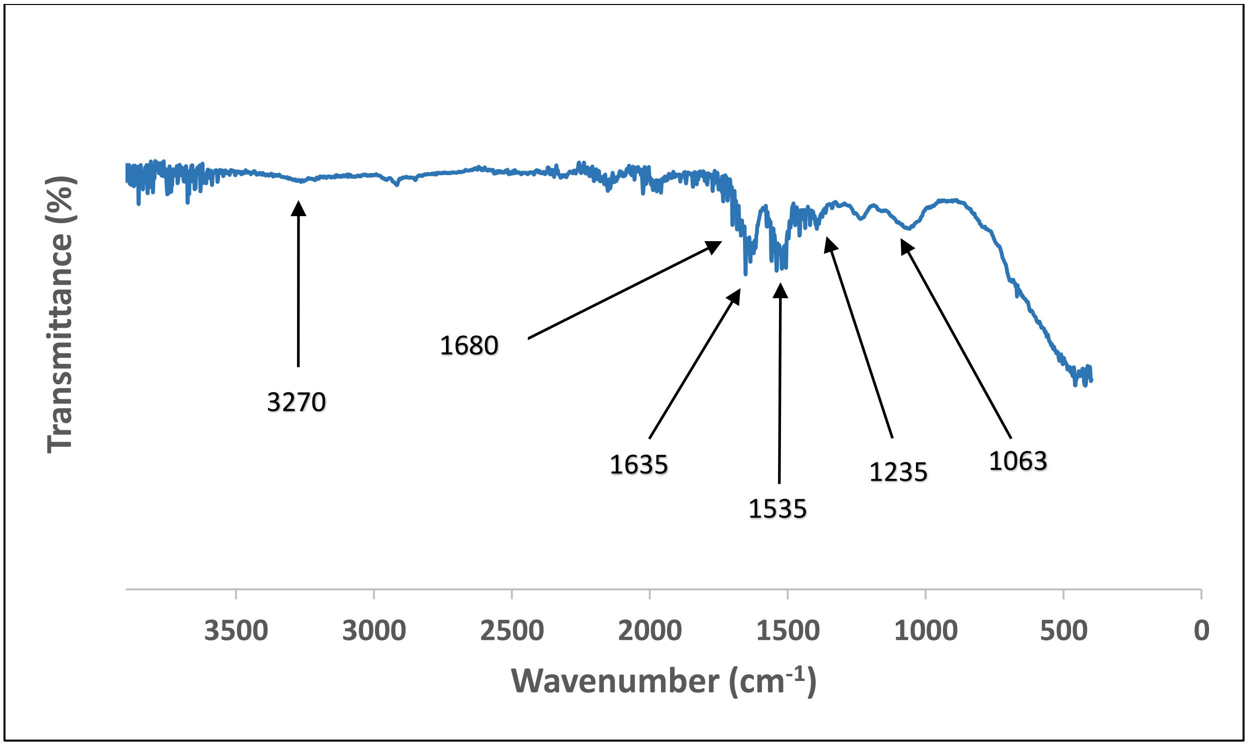

Figure 3.4. FTIR spectrum of heat treated SPI.

TABLE 3.4. FTIR PEAK ASSIGNMENT OF HEAT TREATED SPI.

Wave Number (cm^{-1})	**Attributable**
1063	Out of plane C-H bending [121]
1235	C-N Stretching and N-H bending (amide III) [121]
1535	N-H bending (amide II) [121]
1635	Peptide linkage (C=O stretching) (amide I) [121]
1680	The formation of β-sheet structure [122]
2918	CH_2 asymmetrical stretching [121],CH_2 and CH_3 and RCH_2 [123]
3000-3500	free and bound O-H and N-H groups [121]

Those bands observed in the region of 3500-3000 cm^{-1} are assigned to free and bound O-H and N-H groups, which are able to form hydrogen bonding with the carbonyl group of the peptide linkage in the protein. The absorption band at 2920 cm^{-1} is attributable to CH_2 asymmetrical stretching [121, 123]. The formation of β-sheet structure is assigned to the band at 1680 cm^{-1} [122]. Addition band observed at 1635 cm^{-1} is related to peptide linkage (C=O stretching) (amide I), while the band at 1535 cm^{-1} and 1235 cm^{-1} correspond to N-H bending (amide II), and C-N Stretching and N-H bending (amide III), respectively. The band at 1063 cm^{-1} is assigned to the out of plane C-H bending [121]. The structural analysis by FTIR has been done to track the effect of SPI content on HPEO as shown in Figure 3.5.

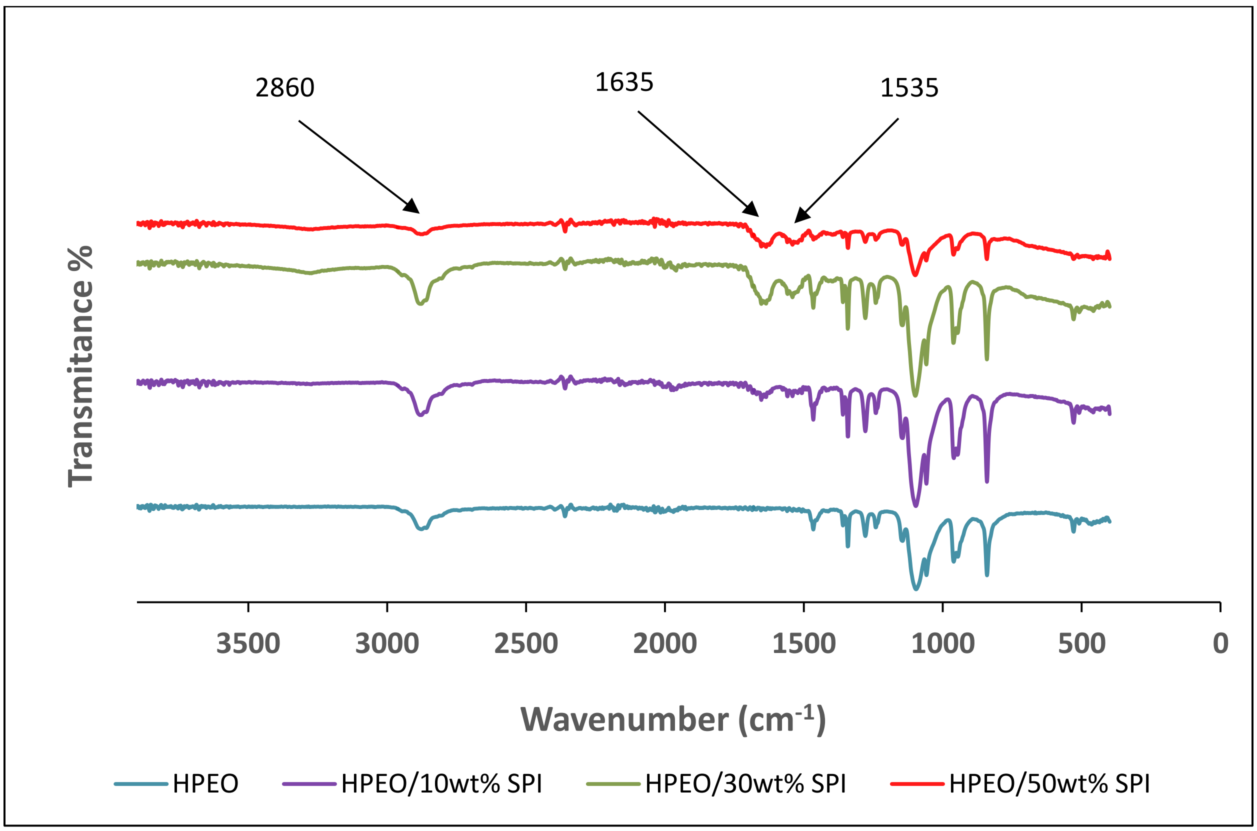

Figure 3.5. FTIR spectra of HPEO and HPEO/SPI membranes.

The most obvious changes can be seen at three wavenumbers. Increasing the content of SPI contributes to new N-H bending (amide II) and peptide linkage (C=O stretching) (amide I) at 1535

cm^{-1} and 1635 cm^{-1} wavenumbers, respectively. Moreover, the higher the SPI content is, the intensity of asymmetric and symmetric C-H stretching of CH_2 would be decreased at 2860 cm^{-1}. Figure 3.6 illustrates the effects of SPI content on the structure of LPEO.

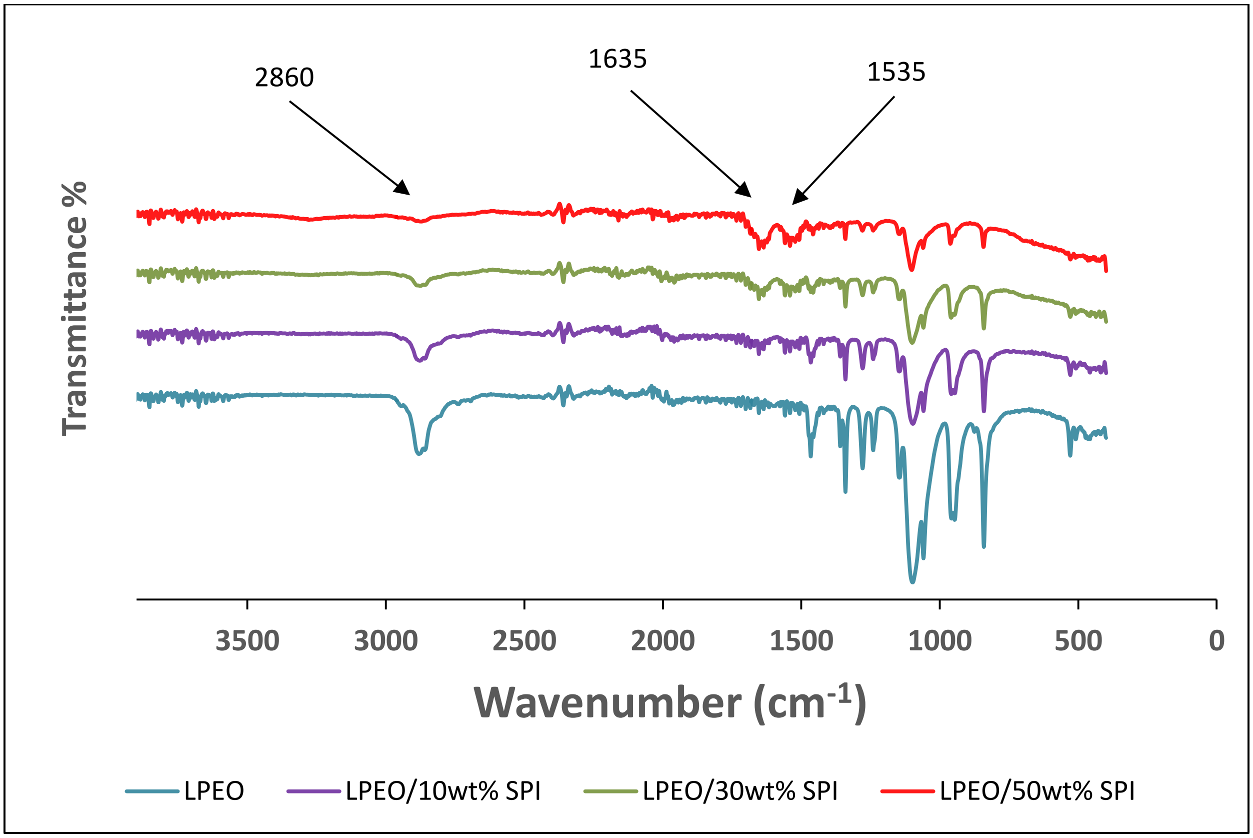

Figure 3.6. FTIR spectra of LPEO and LPEO/SPI membranes.

As expected and can be seen in Figure 3.6, the results for LPEO/SPI samples are the same as those of HPEO/SPI samples, since both LPEO and HPEO have the same chemical structures.

3.3 X-ray Diffraction

The XRD test has been done on the samples to find the amount of crystallinity of the structure in different SPI concentration. Figure 3.7 and Figure 3.8 show the XRD results for the HPEO and LPEO membranes, respectively.

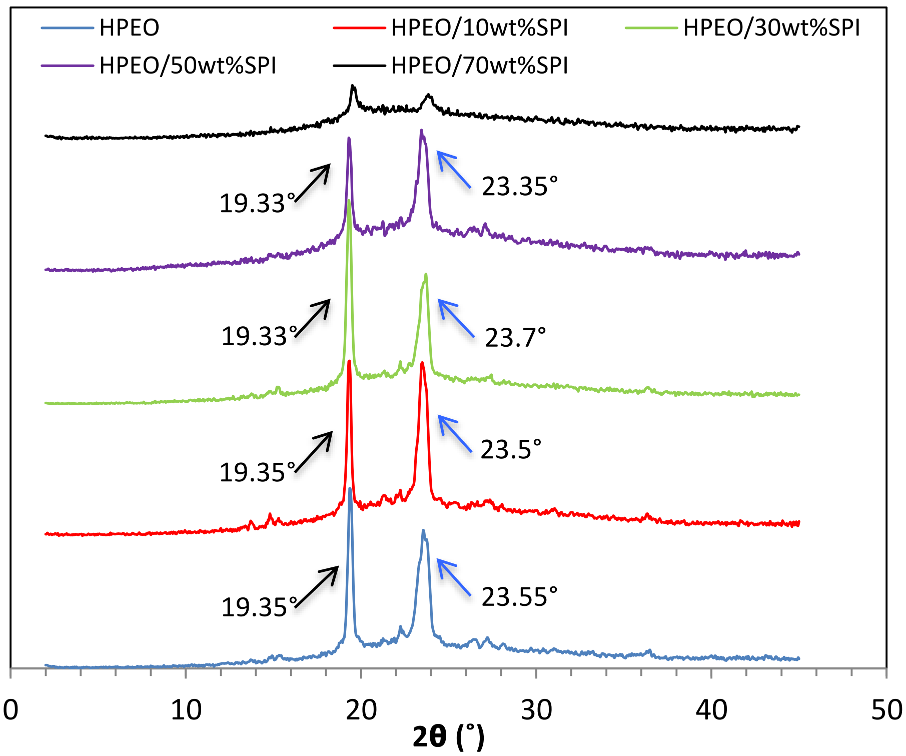

Figure 3.7. XRD spectra of HPEO and HPEO/SPI membranes.

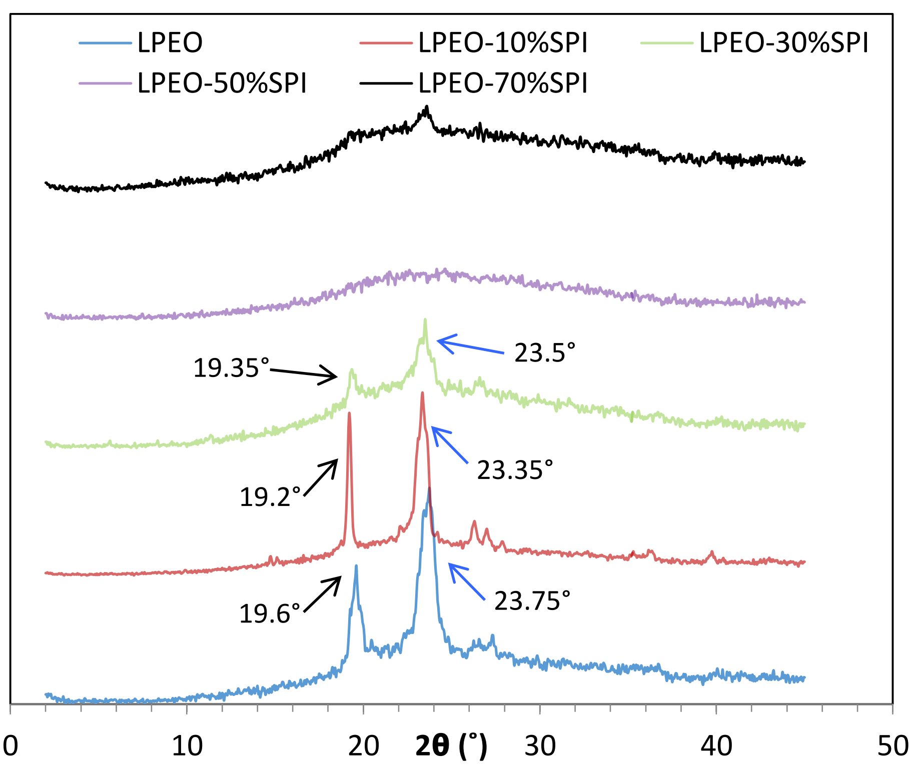

Figure 3.8. XRD spectra of LPEO and LPEO/SPI membranes.

The relative intensity between 19.3° and 23.3° peak changes. Ye and Woo [124] suggested that the strong intermolecular interaction between PEO and other incorporate substance would introduce changes in relative intensity of the (032) crystal plane to (120) crystal plane in the PEO crystallized. Moreover, there are two weak peaks at around 25° and 26.3° also represent PEO structures. Their intensity is low, so not much literatures mentioned them. Table 3.5 illustrates the assignment of each peak to different crystallographic planes in PEO. The XRD results shown in Table 3.6 suggest that by increasing the SPI content, the membranes crystallinity will decrease for both HPEO and LPEO. The strong interactions between protein and PEO were also reported as the main reason for the reduced crystallinity [106, 112].

TABLE 3.5. ASSIGNMENT OF XRD DIFFRACTION PEAKS IN PEO.

Peaks	**Crystal plane of PEO**
19.3°	(120)
23.5°	(112) / (032)
25°	(024)
26.3°	(131)

TABLE 3.6. CRYSTALLINITY OF PEO/SPI MEMBRANES.

	0% SPI	**10%SPI**	**30%SPI**	**50%SPI**	**70%SPI**
Crystallinity (%) of HPEO	37.32	26.26	26.39	16.97	5.0
Crystallinity (%) of LPEO	30.73	31.94	9.29	-	-

3.4 Scanning Electron Microscopy

In order to be able to analysis the structure of membranes and SPI effect on it, the SEM images have been gotten from the free surface and the fracture surface of membranes. Figure 3.9 and Figure 3.10 show the free and fracture surfaces of HPEO/10wt% SPI, respectively.

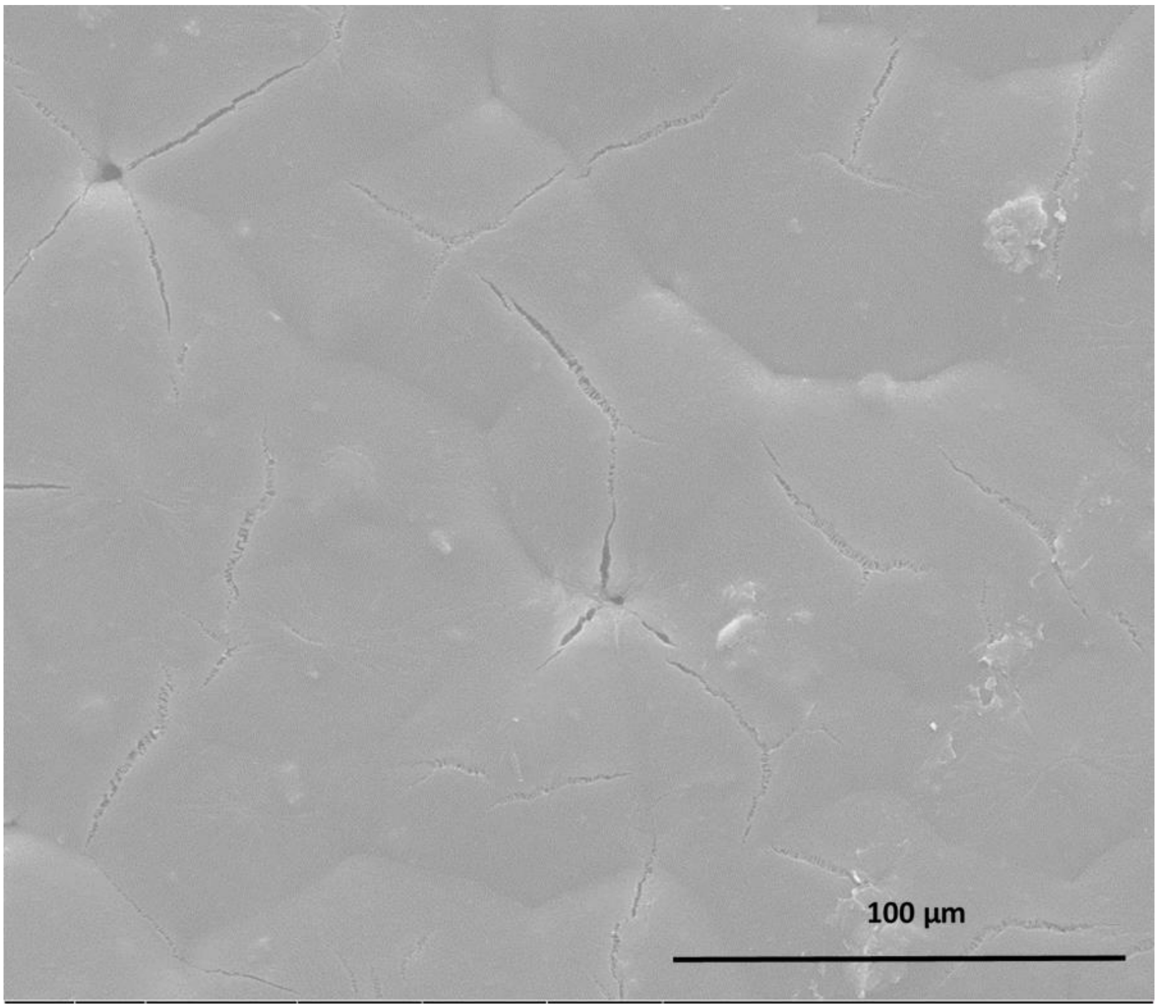

Figure 3.9. Free surface of HPEO/10wt% SPI membrane.

As can be seen, the free surface is uniform while it contains some cracks, which probably is caused during cryofracture. In the meanwhile, the fracture surface shows there are some fiber-like structures, which are believed to be elongated PEO crystal lamellae formed during cryofracture. This kind of "fibrillation" reflects excellent ductility of the PEO materials. The morphologies of both free surface and fracture surface suggest very good compatibility as a result of PEO-SPI interactions. Meanwhile, some particulate phases are found in fracture surface. These particulate phases should be formed by the aggregated hydrophobic structures in SPI.

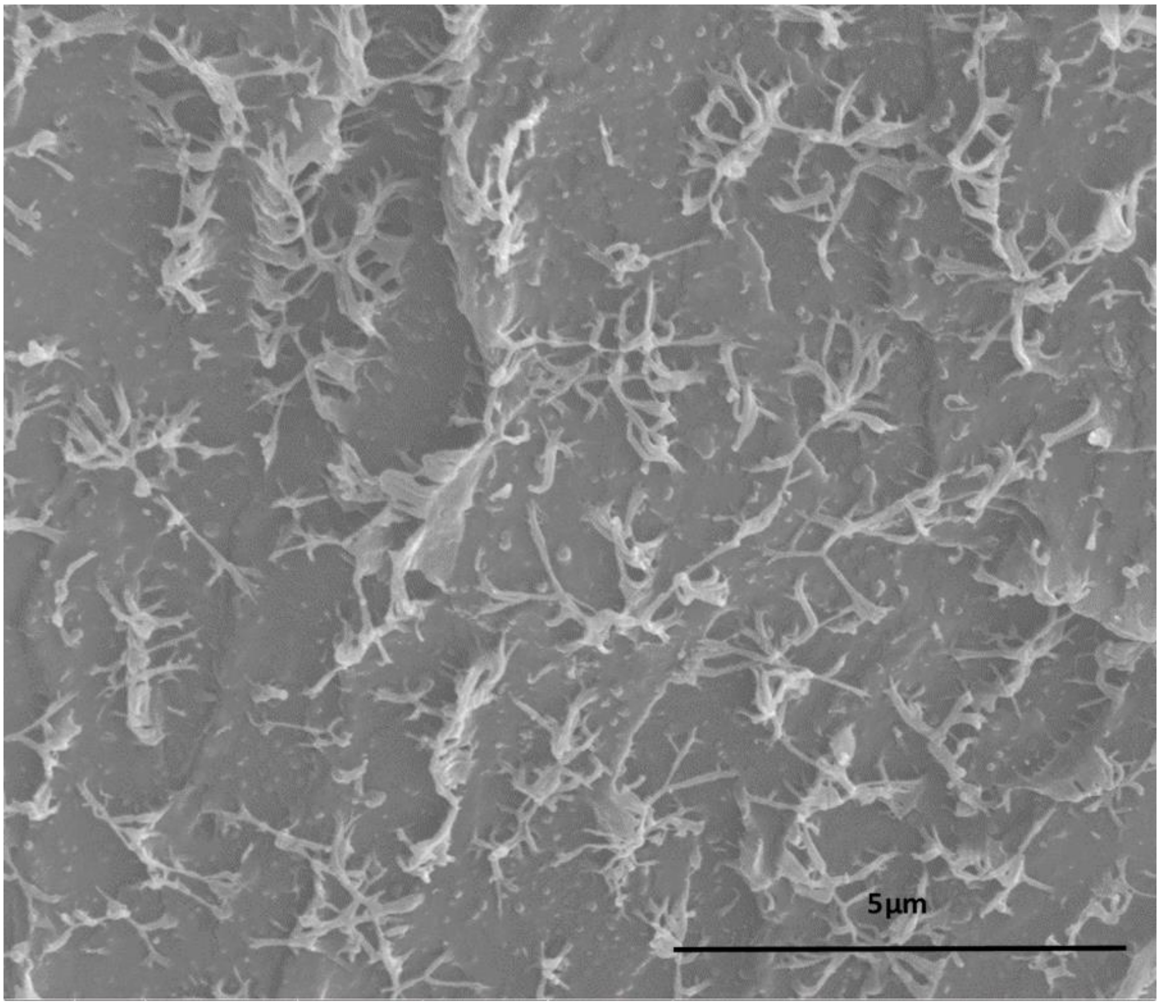

Figure 3.10. Fracture surface of HPEO/10wt% SPI membrane.

Figure 3.11 and Figure 3.12 are shown to study the free and fracture surfaces of HPEO.SPI 30%wt, respectively. The surface is still uniform compare to membrane with 10wt% SPI, however, the crack is propagated and there are some bridges formed during cryofracture. The fracture surface shows more particulate phase. At the same time, only very few fibrous structures are observed in Figure 3.12, suggesting reduced ductility compared with HPEO.10wt% SPI membrane.

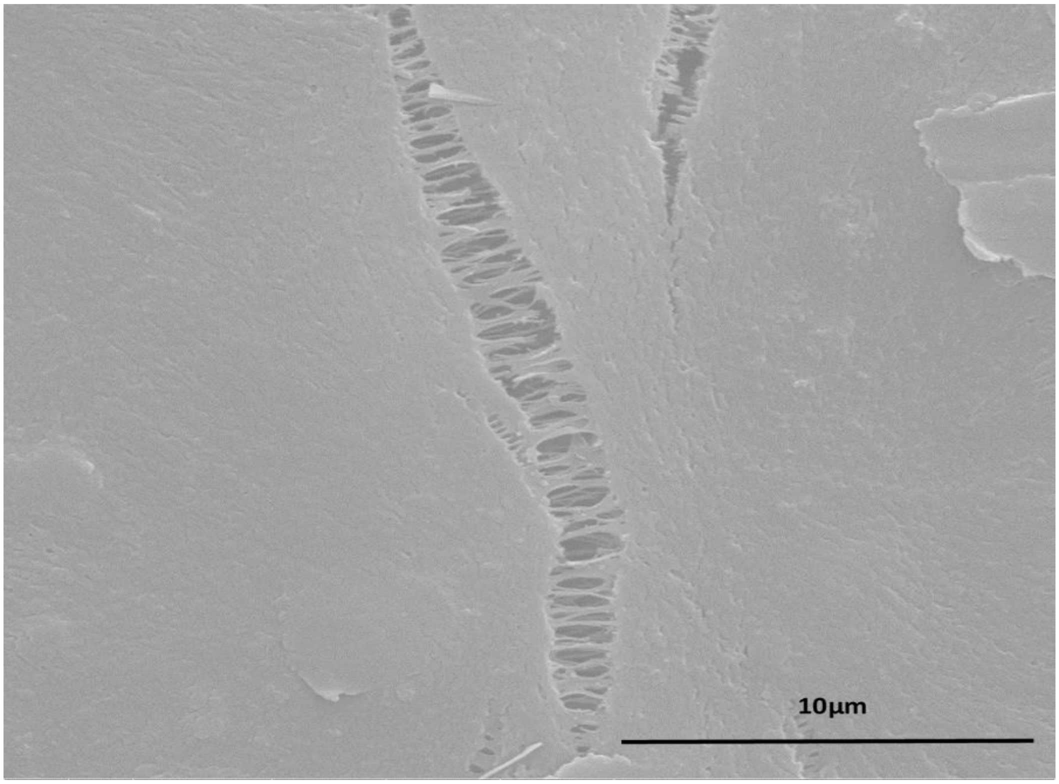

Figure 3.11. Free surface of HPEO/30wt% SPI membrane.

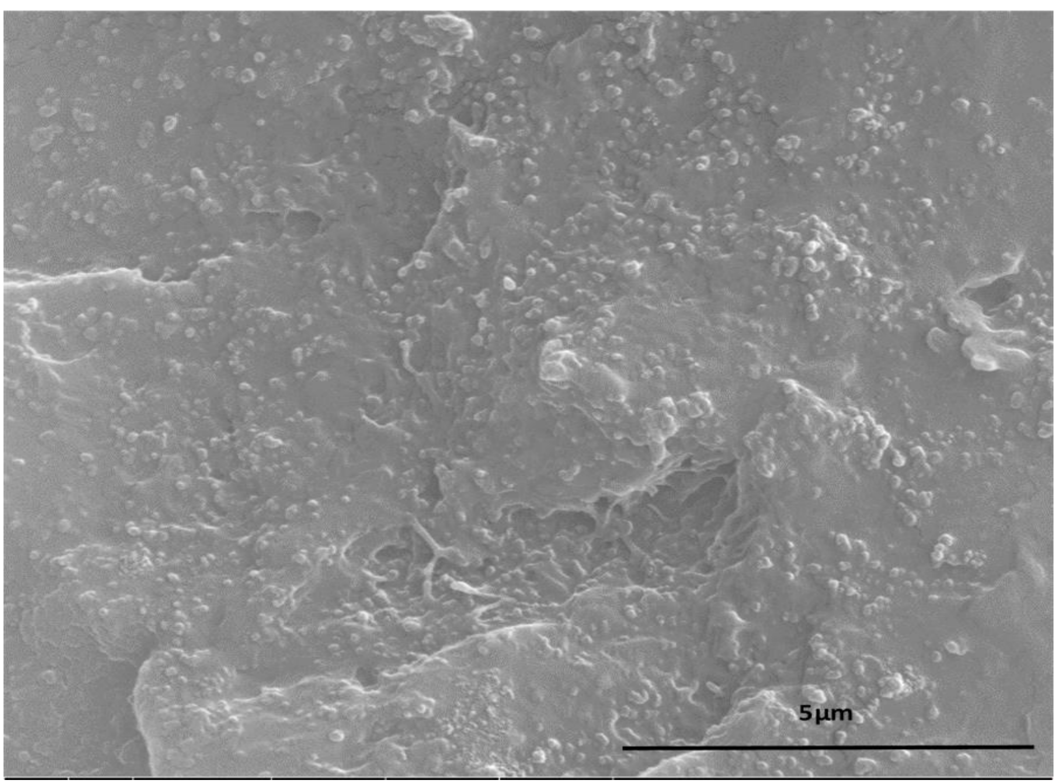

Figure 3.12. Fracture surface of HPEO/30wt% SPI membrane.

Figure 3.13 represents free surface of HPEO/50wt% SPI, while Figure 3.14 shows the fracture surface of the membrane. It is interesting to notice that the free surface of HPEO/50wt% SPI has a very unique surface morphology. Instead of rather smooth free surfaces in HPEO/10wt% SPI and HPEO/30wt% SPI, at 50wt% SPI loading, the membrane surface is rough. It is not uniform and contains a large number of branch shaped structures. In the meantime, the fracture surface has s similar morphology to that of HPEO/30wt% SPI membrane. While a great number of SPI particles are observed, the PEO and SPI show very good compatibility. However, the fibrous structures completely disappear.

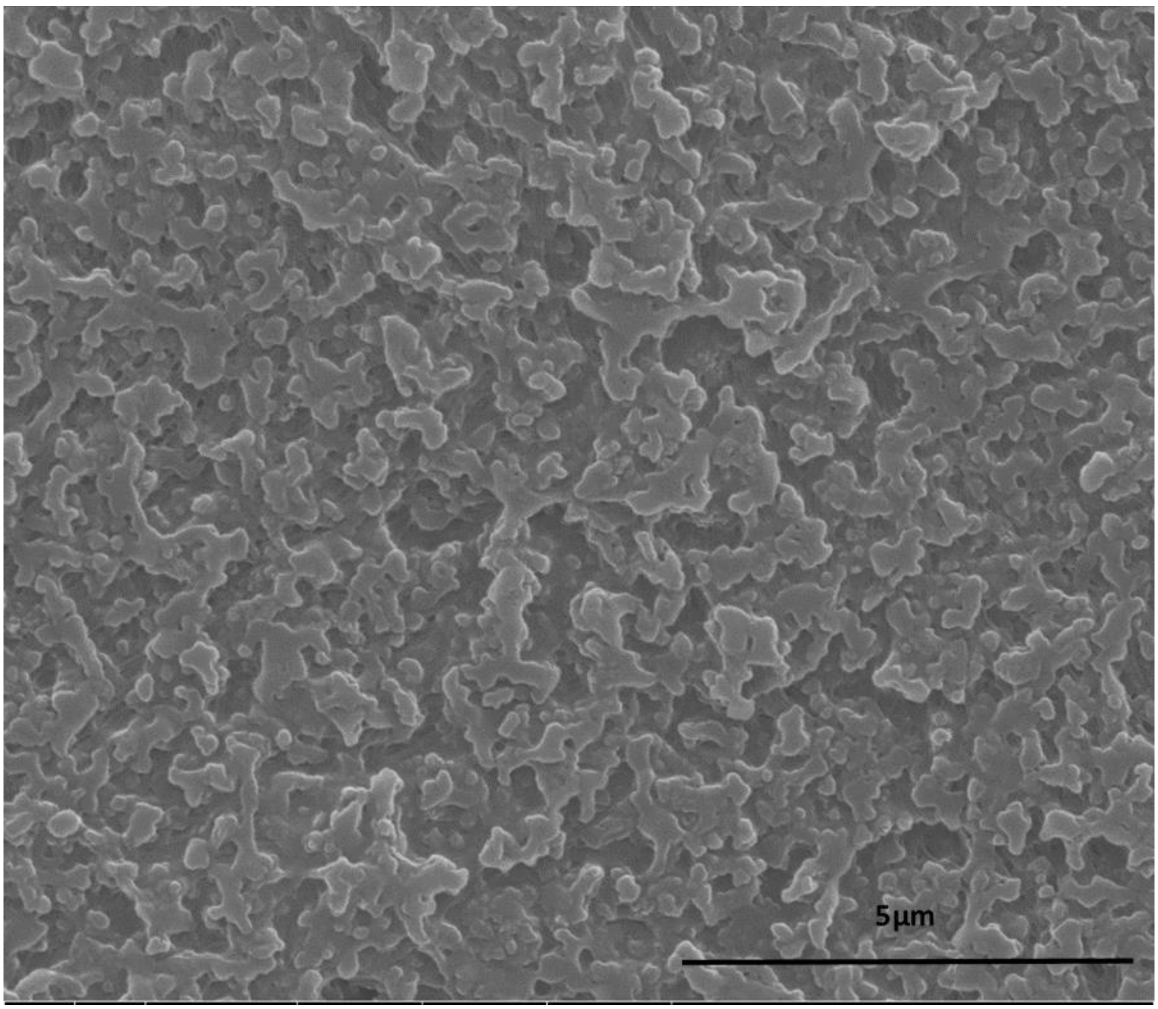

Figure 3.13. Free surface of HPEO/50wt% SPI membrane.

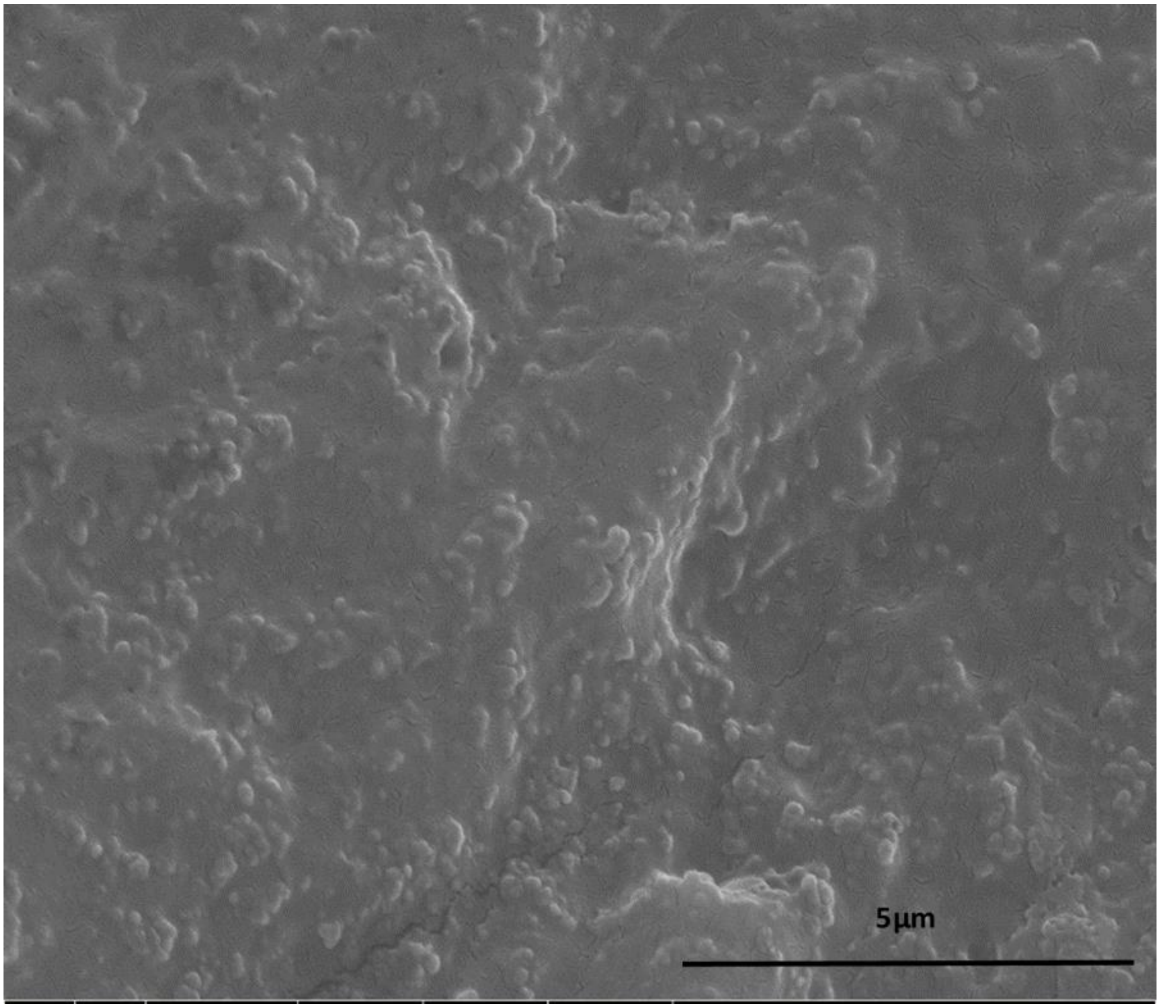

Figure 3.14. Fracture surface of HPEO/50wt% SPI membrane.

Figure 3.15 and Figure 3.16 illustrate the free and fracture surfaces of LPEO/10wt% SPI, respectively. The free surface is so uniform and smooth. Similar to HPEO/10wt% SPI membrane in Figure 3.9, it is hard to observe the SPI phase on the free surface. Although there is no ”fibrillation” observed on the fracture surface in Figure 3.16, the fracture surface has some propagated cracks with a few number of bridges. This structural feature suggests that during cryofracture, the PEO crystal lamellae in membrane elongated. However, due to the low molecular weight and the resulting weak chain entanglement, the strain hardening phenomenon is limited in LPEO membranes, therefore, the “fibrillation” phenomenon is not significant.

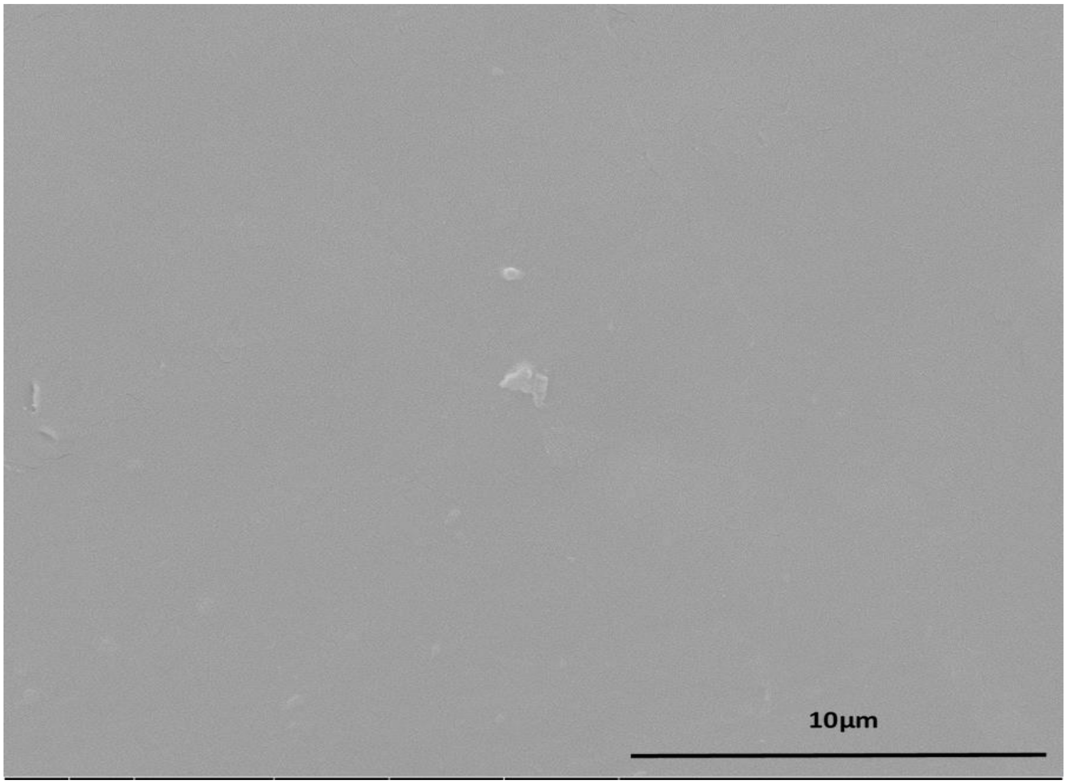

Figure 3.15. Free surface of LPEO/10wt% SPI membrane.

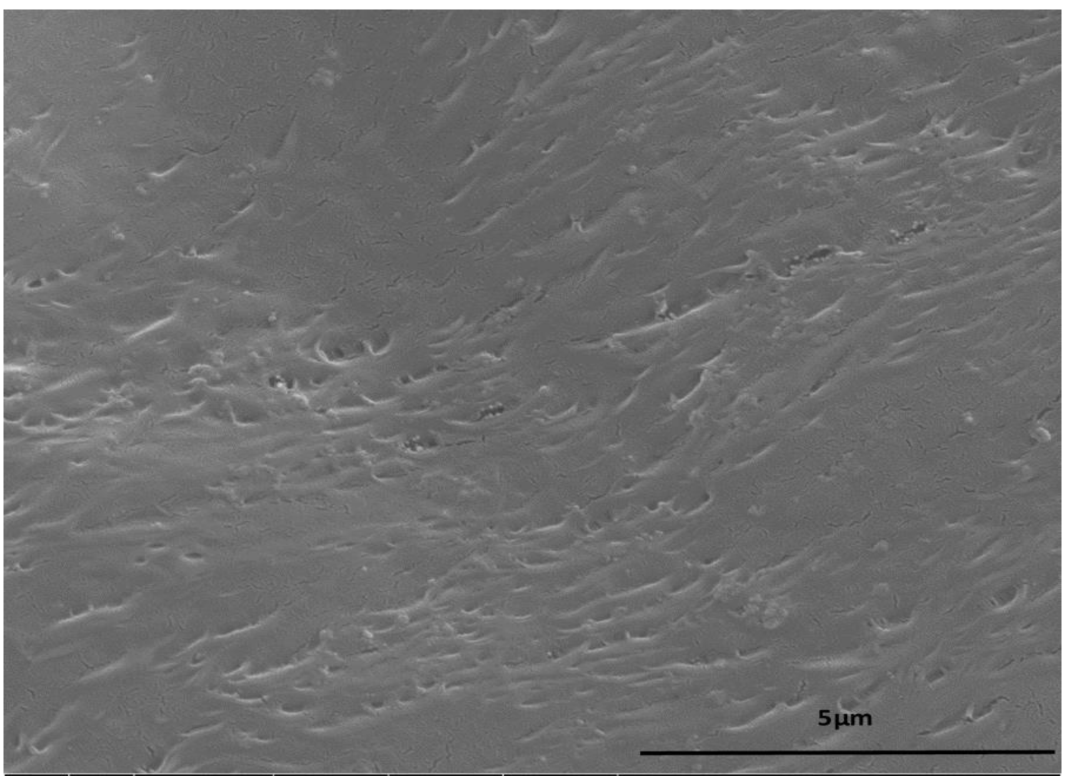

Figure 3.16. Fracture surface of LPEO/10wt% SPI membrane.

Figure 3.17 and Figure 3.18 prove the free and fracture surfaces of LPEO/30wt% SPI, respectively. Obviously, the free surface is rougher with clear phase separation observation. Moreover, compared with HPEO/30wt% SPI, a lot of voices and cracks are found on the free surface of LEPO/30wt% SPI membranes. This might suggest that high molecular weight in HPEO might form stronger interactions (entanglement) with SPI. Regarding the fracture surface, although it primarily shows a typical brittle failure, few fibers are found on the surface, corresponding to the stretched and elongated PEO crystal lamellae.

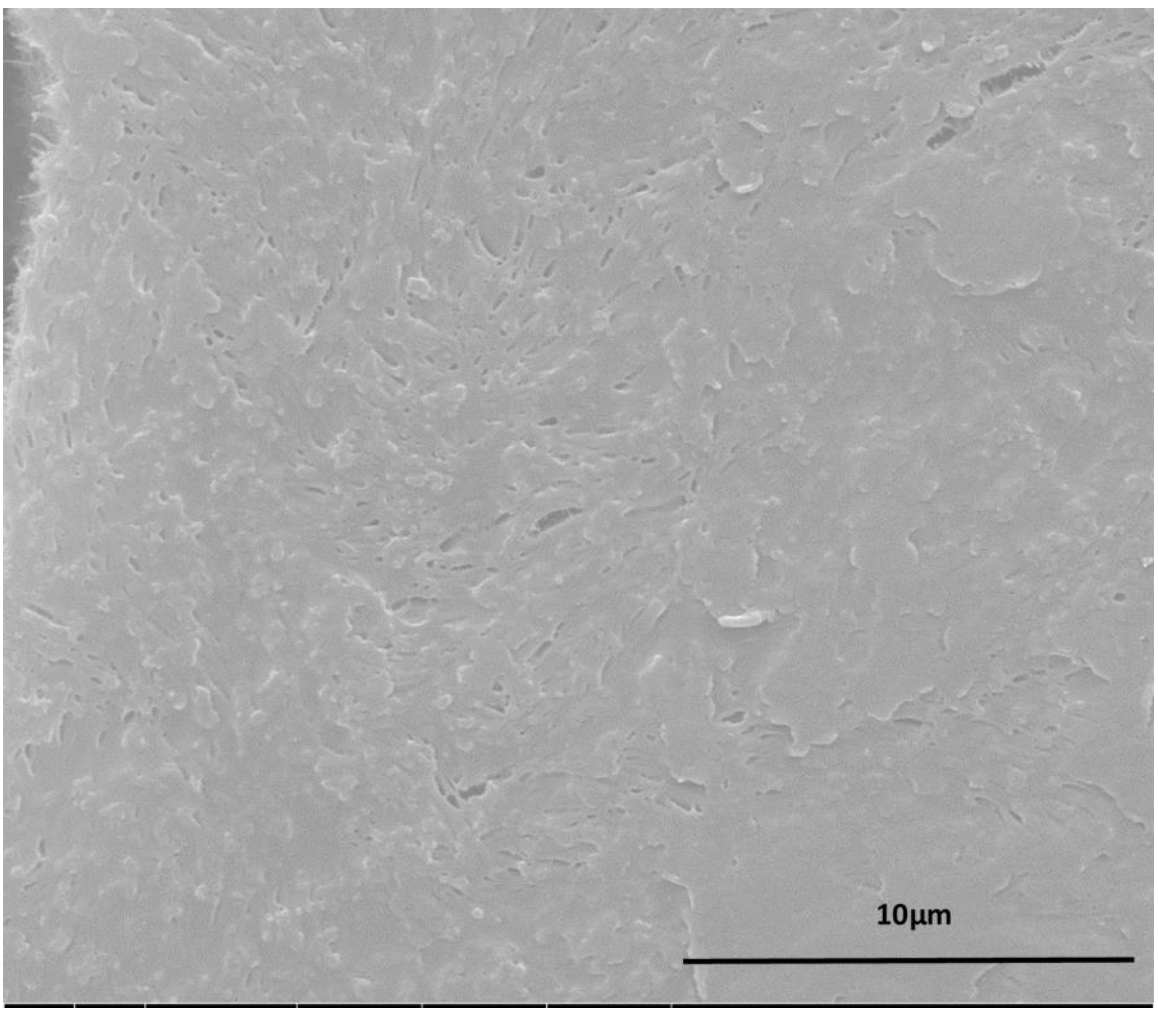

Figure 3.17. Free surface of LPEO/30wt% SPI membrane.

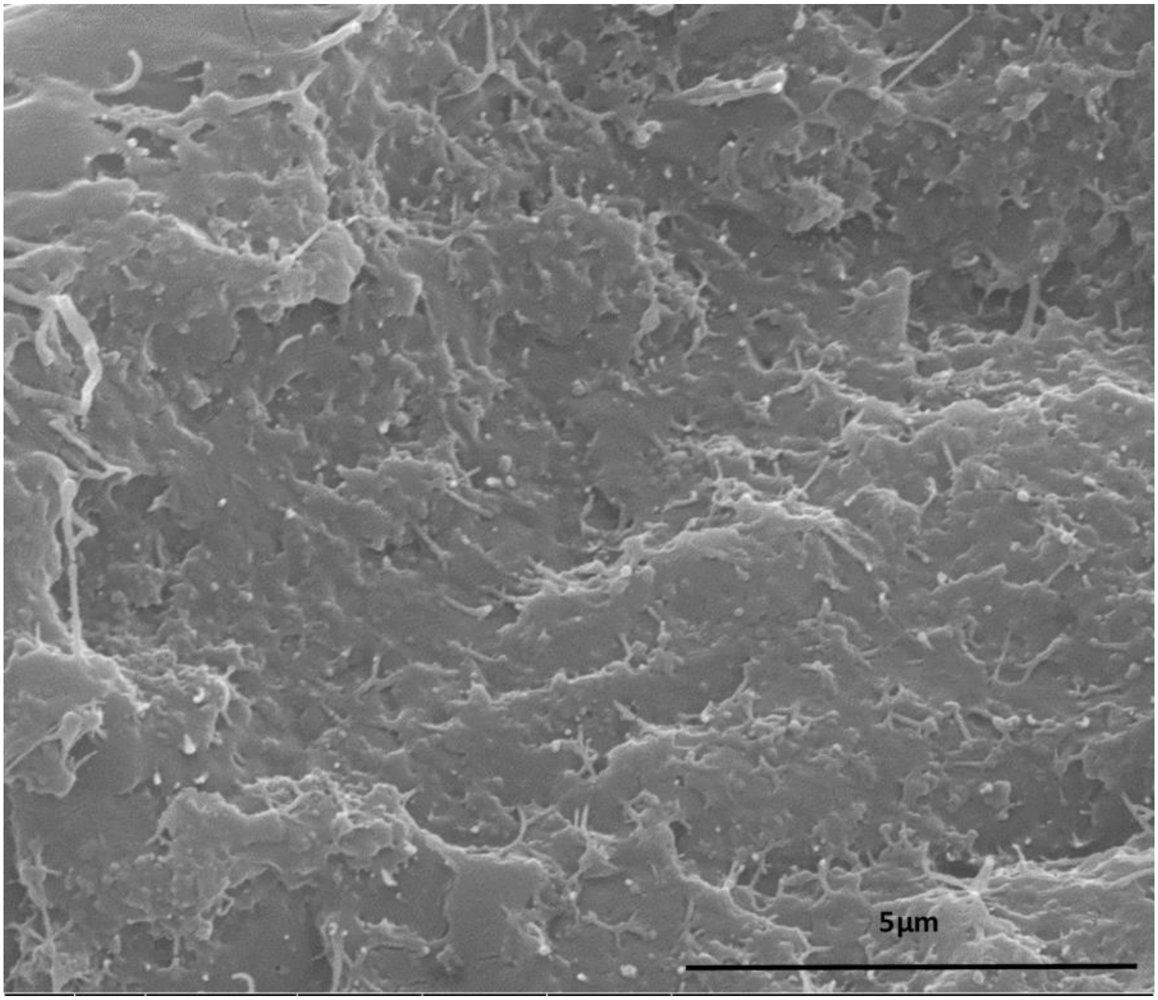

Figure 3.18. Fracture surface of LPEO/30wt% SPI membrane.

The free and fracture surfaces of the LPEO/50wt% SPI membranes shown in Figure 3.19 and Figure 3.20, respectively. As expected, a rough free surface is found in LPEO/50wt% SPI membranes. Meanwhile, the surface is full of porous structures with most of the pores in the nanoscale. The porous structures were not found in HPEO/50wt% SPI. This might suggest the week entanglement in LPEO and interactions with SPI. In Figure 3.20, surprisingly, there are only few porous structures found, suggesting that the porous structures are only near the surface layer of the membranes, which might also relate to the drying process during sample preparation. At last, the SPI also has very good compatibility with LPEO with many nanoscale particulate SPI phases found in LPEO.

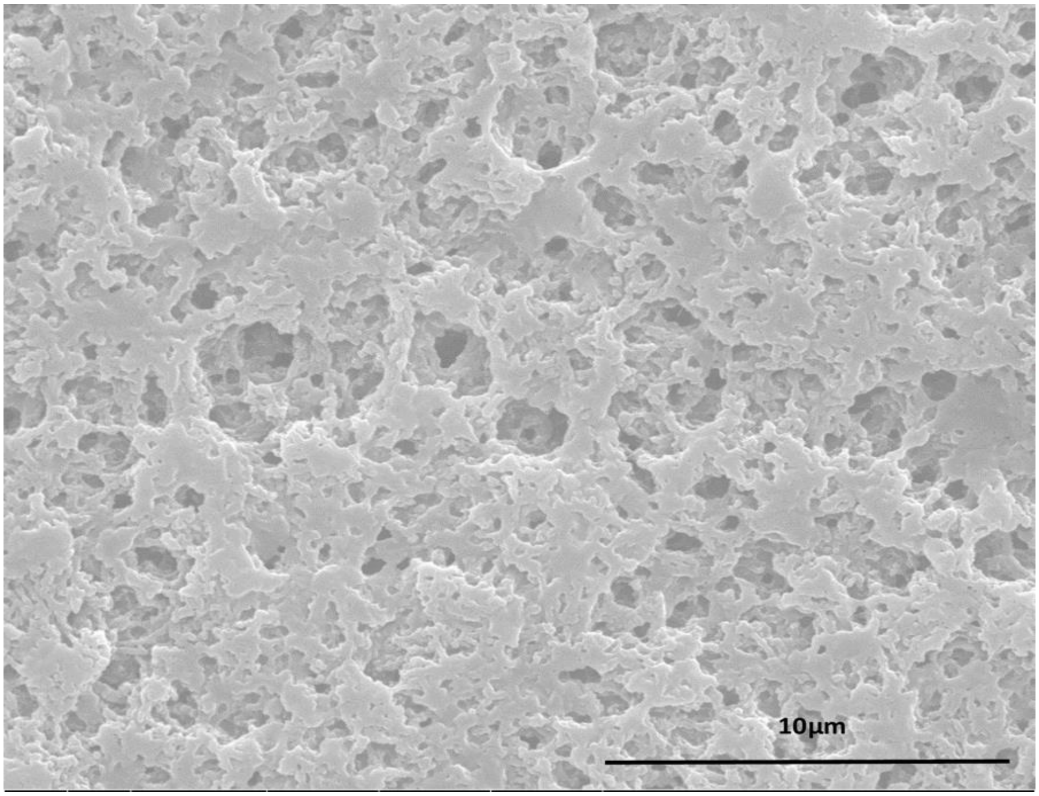

Figure 3.19. Free surface of LPEO/50wt% SPI membrane.

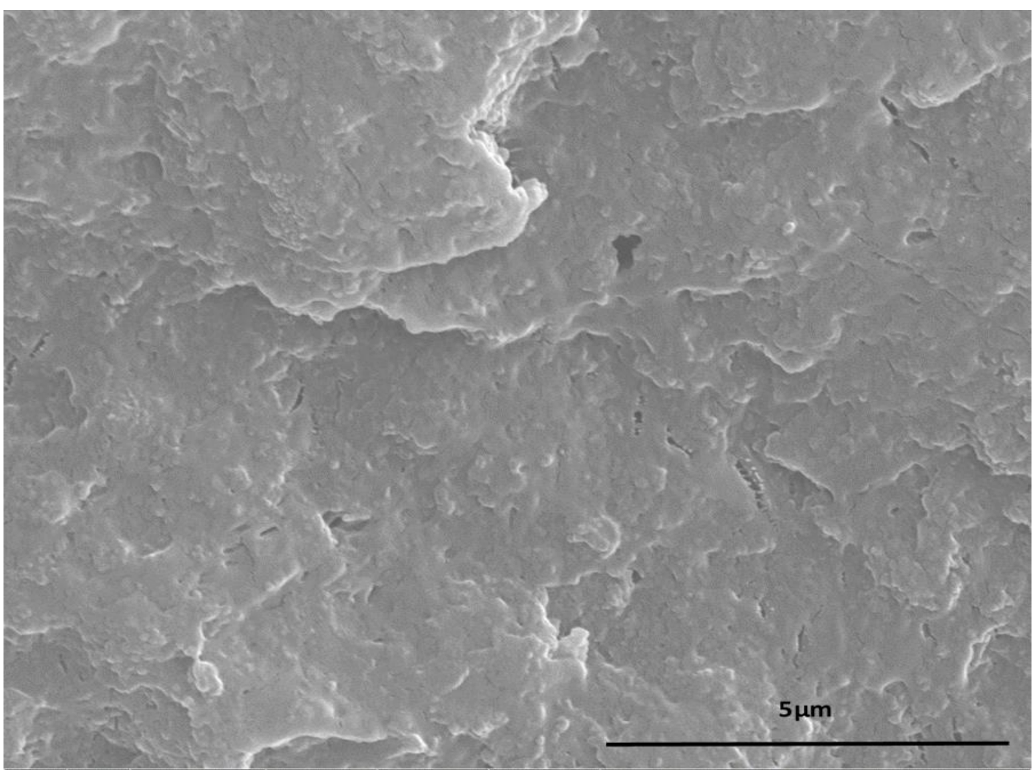

Figure 3.20. Fracture surface of LPEO/50wt% SPI membrane.

3.5 Current-Voltage Characteristics

When the leaking is too much, the membranes are not able to successfully store energy. In other words, the leaking means to convey the electric charges through the membrane (from one side of capacitor to another side) and in this situation the electric charges will not be stored as electric energy. This information assesses the limitation of maximum voltage for the hysteresis measurement. Moreover, another important characterization can be studied by the I-V curve where there is a relationship between current, voltage, and resistance as equation 3.2 shows:

$$R = \frac{V}{I} \tag{3.2}$$

Where R is resistance (Ω), V is voltage (V) and I is current (A).

In order to plot the I-V curve, the current axis is logarithmic. As shown in Figure 3.21, the lower the slope is, the smaller the resistance would be. In other words, the lines near to the voltage axis are shown higher resistivity than the lines near to the current axis.

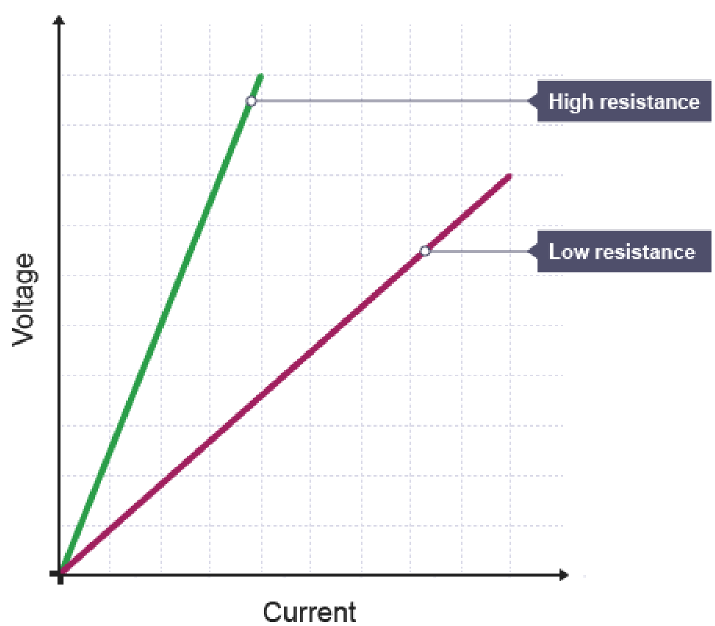

Figure 3.21. Different electrical properties determined by current-voltage curve [125].

Once the resistance of the membranes has calculated by equation 3.2, the resistivity could be found by equation 3.3:

$$\rho = \frac{A}{L} R \qquad (3.3)$$

Where ρ is the resistivity in Ωm, A is the sample area in m^2, L is the thickness of the membrane in m, and R is in Ω.

The leakage current is one of the important characteristics that could be obtained from the I-V curve measurements. Ideally for an insulator, the current should not do a flow while a voltage is applied. However, in real case there is a current flow known as leakage current. The lower the leakage current, the better dielectric material would be. The current voltage curve measurement for different samples are plotted and shown in Figure 3.22 and Figure 3.23 for HPEO and LPEO samples, respectively.

In order to make a comparison between the electrical properties of the membranes, the resistivity of the membranes at linear part of the graph ($0 < V < 170V$) have been calculated by equations 3.3 and the results are mentioned in Table 3.7. The lower slope in I-V curve means the higher electrical resistivity. In other words the higher the resistivity is, the better insulator the material would be.

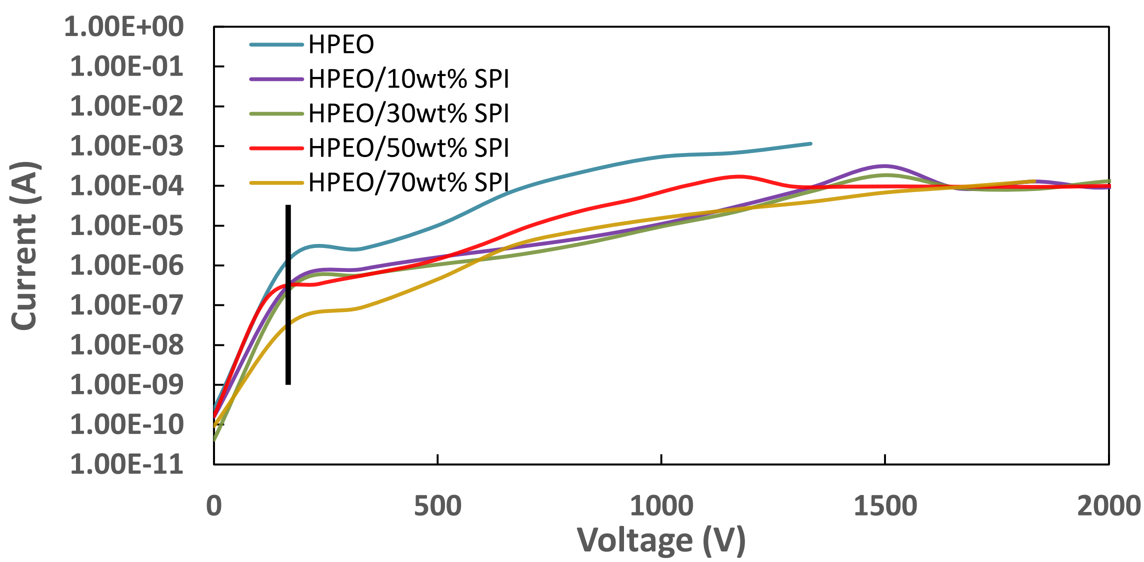

Figure 3.22. Effects of SPI content on I-V characteristics of HPEO/SPI membranes.

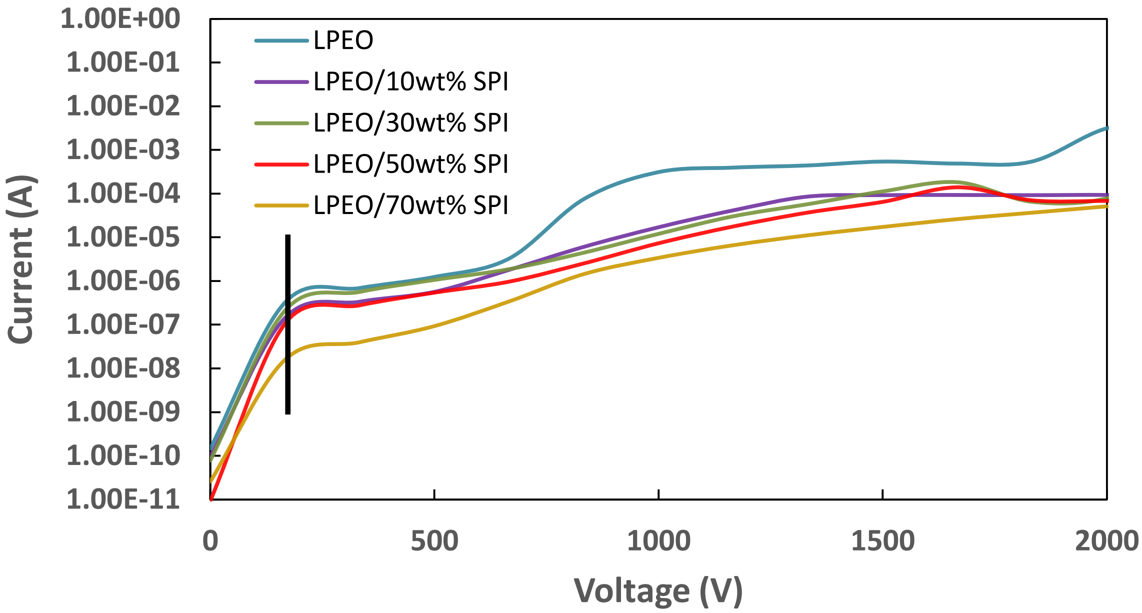

Figure 3.23. Effects of SPI content on I-V characteristics of LPEO/SPI membranes.

TABLE 3.7. ELECTRICAL RESISTIVITY OF THE MEMBRANES.

Sample	Resistivity (Ω.m ×10^7)	Standard Deviation (Ω.m ×10^7)
HPEO	3.02	0.53
HPEO/10wt% SPI	14.41	3.93
HPEO/30wt% SPI	21.53	1.22
HPEO/50wt% SPI	75.46	70.34
HPEO/70wt% SPI	231.52	115.49
LPEO	13.00	6.63
LPEO/10wt% SPI	30.49	3.02
LPEO/30wt% SPI	31.94	13.40
LPEO/50wt% SPI	61.93	22.68
LPEO/70wt% SPI	540.19	518.56

As shown in Table 3.7, the resistance of the PEO membranes increases when a content of the SPI is added. That means SPI makes the PEO membrane a better insulator. Since the thickness of all samples were equal, SPI has the same effect on the resistivity of the membranes as well.

3.6 Hysteresis Behaviors of PEO/SPI Membranes

Hysteresis test being used to investigate the polarization and some of the electrical energy properties such as the energy efficiency, energy storage, and energy lost. As Figure 3.24 shows a hysteresis loop, at the small electric fields the polarization increases linearly by enhancing the electric field. This contributes from the fact that at lower field amplitudes there is not enough energy to switch unfavorable direction of domains polarization. By increasing the electric field, the energy exceeds the minimum amount to change the direction of domains polarization and as a result, a dramatic increase in polarization can be seen. At the end of the charging process, there is a small number of domains with unfavorable directions which leads a smooth change in polarization by increasing the electric field [126].

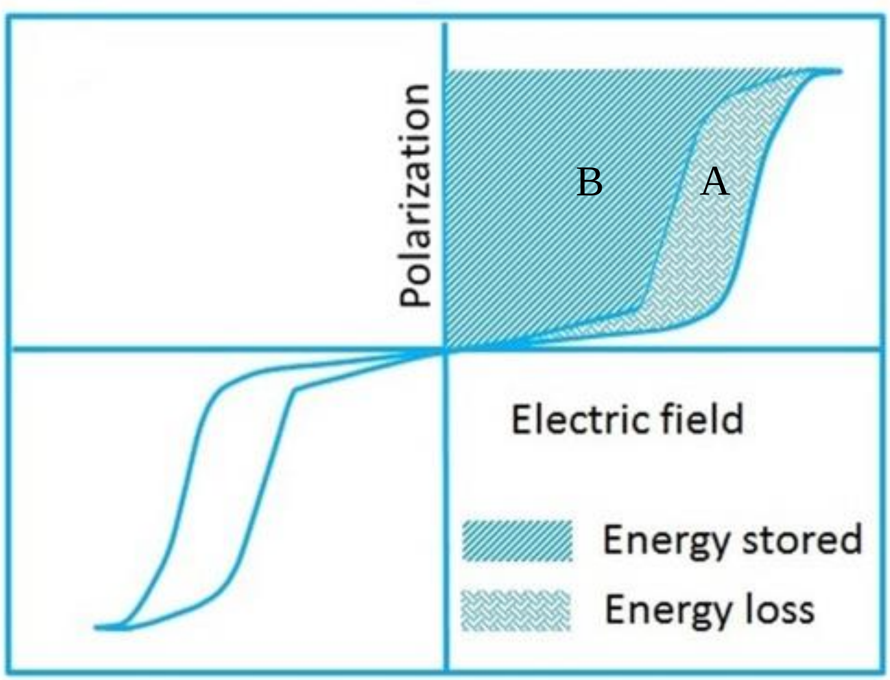

Figure 3.24. Example of a bipolar hysteresis loop [127].

During the discharging process, some of the domains will back-switch but other domains cannot. This behavior during charge and discharge process contains some electrical information about the material. There are some important parameters can be excluded from this hysteresis loop; the area “A+B” represents the amount of energy that can be stored during the charging process. The area “B” illustrates the amount of energy can be released during the discharge process, which means the actual energy we can utilized during discharge process. As a result, the area “A” represent the consumed energy which is a type of energy lost, since after we stored the energy in charging process, we cannot release this energy when we need to use it. These three different areas represent three different information to evaluate the efficiency by using the ratio between them. Energy efficiency can be calculated by a simple equation shown below:

$$Efficiency = \frac{B}{(A+B)} \tag{3.4}$$

Basically, the total area (A+B) should be as high as possible to have maximum energy stored (during the charging process) and at the same time, in order to have a higher efficiency the all energy should be released (during discharge process). As a result, these are two main goals to have a good dielectric material in case of efficiency.

As discussed before, ferroelectric hysteresis loop contains a number of important characteristics of materials. Figure 3.25 shown to illustrate the effect of SPI content on HPEO. The maximum polarization of the membranes is mentioned in Table 3.8.

Figure 3.25 proves introducing SPI to the HPEO leads to a better hysteresis behavior. In order to make a better conclusion about the effect of SPI content, Figure 3.26 is provided. As shown in Figure 3.26, the loop area decreased by introducing higher content of SPI to the solution. Moreover, Table 3.8 and Figure 3.26 prove that increasing the SPI content leads to a lower maximum polarization through the HPEO membranes.

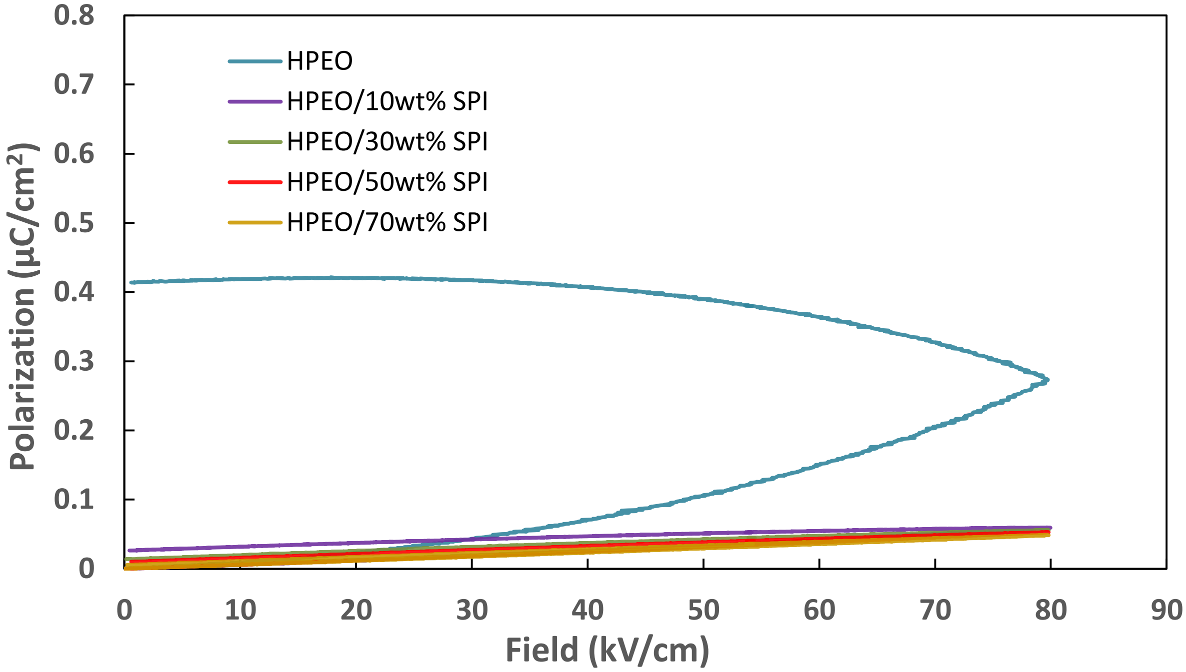

Figure 3.25. Monopolar hysteresis loops of HPEO and HPEO/SPI membranes.

TABLE 3.8. MAXIMUM POLARIZATION OF HPEO MEMBRANES.

Sample	**Maximum Polarization (μC/cm^2)**
HPEO	0.271
HPEO.SPI 10%	0.059
HPEO.SPI 30%	0.056
HPEO.SPI 50%	0.052
HPEO.SPI 70%	0.048

The dielectric behavior of the LPEO in presence of SPI has been studied and the hysteresis measurements mentioned in Figure 3.27. As can be seen, the figure illustrates that having SPI through the LPEO membranes contributes to a lower loop area. As discussed in section 2.3.6, the smaller loop area means the lower energy loss. The maximum polarization of the membranes is mentioned in Table 3.9.

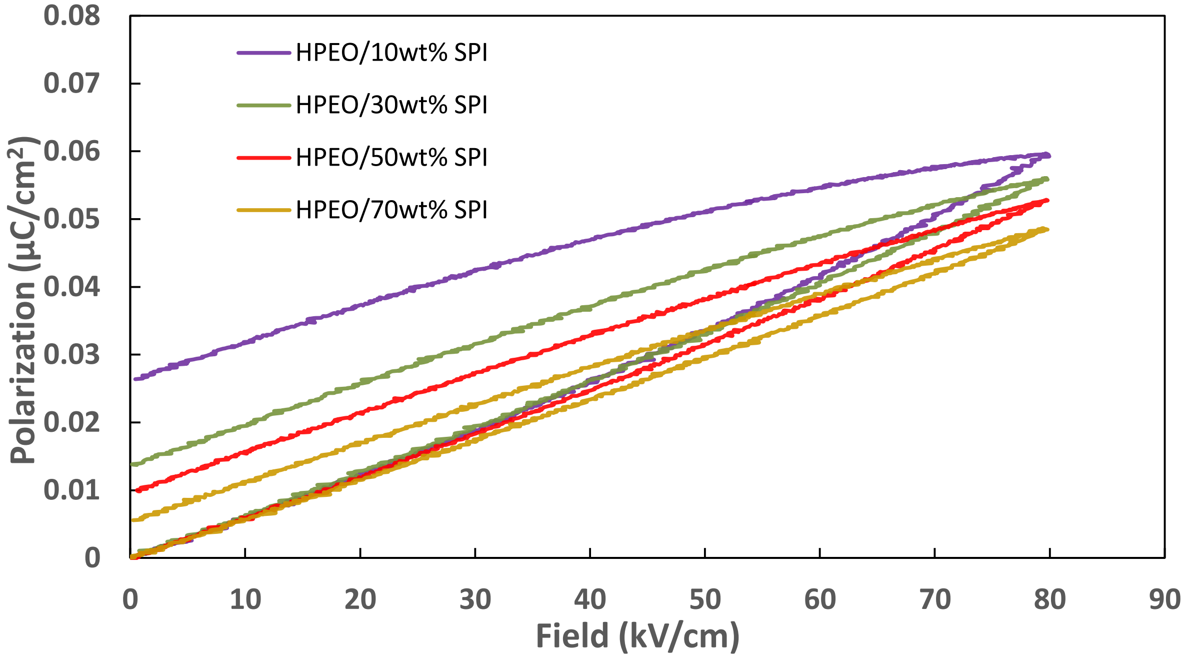

Figure 3.26. Effects of SPI content on hysteresis behaviors of HPEO/SPI membranes.

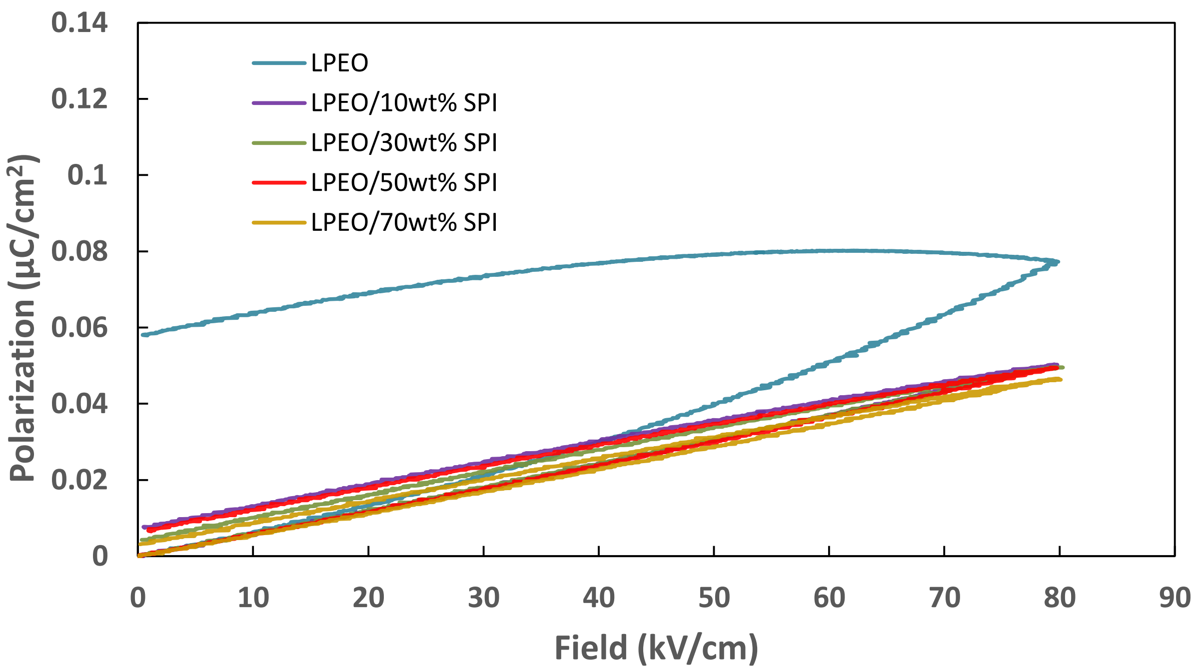

Figure 3.27. Effects of SPI content on hysteresis behaviors of LPEO and LPEO/SPI membranes.

TABLE 3.9. MAXIMUM POLARIZATION OF LPEO MEMBRANES.

Sample	**Maximum Polarization (μC/cm^2)**
LPEO	0.0770
LPEO.SPI 10%	0.0503
LPEO.SPI 30%	0.0496
LPEO.SPI 50%	0.0494
LPEO.SPI 70%	0.0465

Same as the HPEO membranes, higher content of SPI contributes to a decrease in maximum polarization of LPEO membranes. Since the loops for LPEO/SPI membranes are very close to each other, they are shown in Figure 3.28.

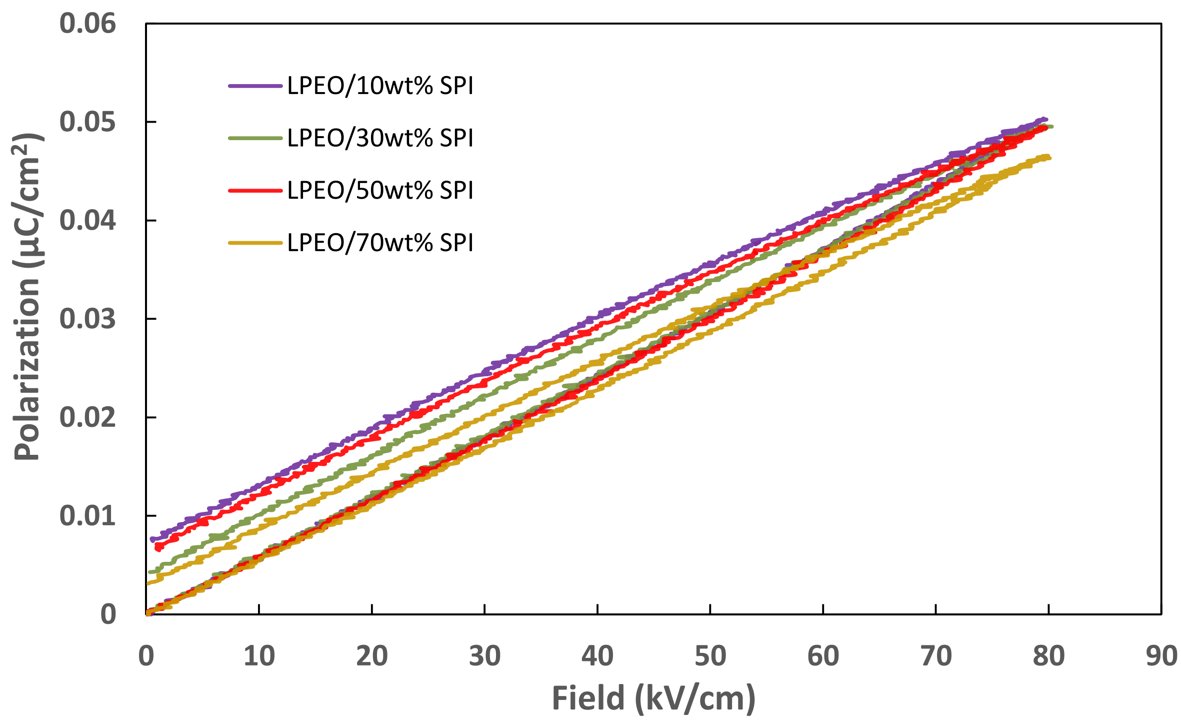

Figure 3.28. Effects of SPI content on hysteresis behaviors of LPEO and LPEO/SPI membranes.

It could be excluded from Figure 3.25 and Figure 3.27 that adding SPI to the PEO membranes decreases the polarizability of the membranes. Moreover, comparing the HPEO/SPI membranes with LPEO/SPI membranes prove that the maximum polarization of those samples contain HPEO is higher than that of the samples contain LPEO.

3.6.1 Effects of SPI Content on Energy Performances of HPEO/SPI Membranes

The effect of SPI on the electrical energy performance of the HPEO/SPI membranes can be tracked by studying the consumed energy, stored energy, released energy, or generally the energy efficiency. As shown in Figure 3.29 (a), the presence of SPI makes a dramatic decrease in case of consumed energy.

In addition, increasing the amount of SPI from 0 %wt to 70 %wt decreases the consumed energy of the membranes. In the meanwhile, the capacity of energy storage shows the same behavior as consumed energy, as shown in Figure 3.29 (b). As a result, we need to study the released energy and efficiency to achieve a better understand of the SPI content effect on the HPEO membranes. Figure 3.30 (a) proves that increasing the SPI content to the HPEO leads to a more energy released by the membrane. At the same time, Figure 3.30 (b) illustrates the enhancement of the membrane’s energy storage efficiency by increasing the SPI content. In other words, presenting SPI to the HPEO not only decreases the energy lost, but also increases the energy efficiency. Since the HPEO had a negative amount of released energy, it is not shown in Figure 3.30.

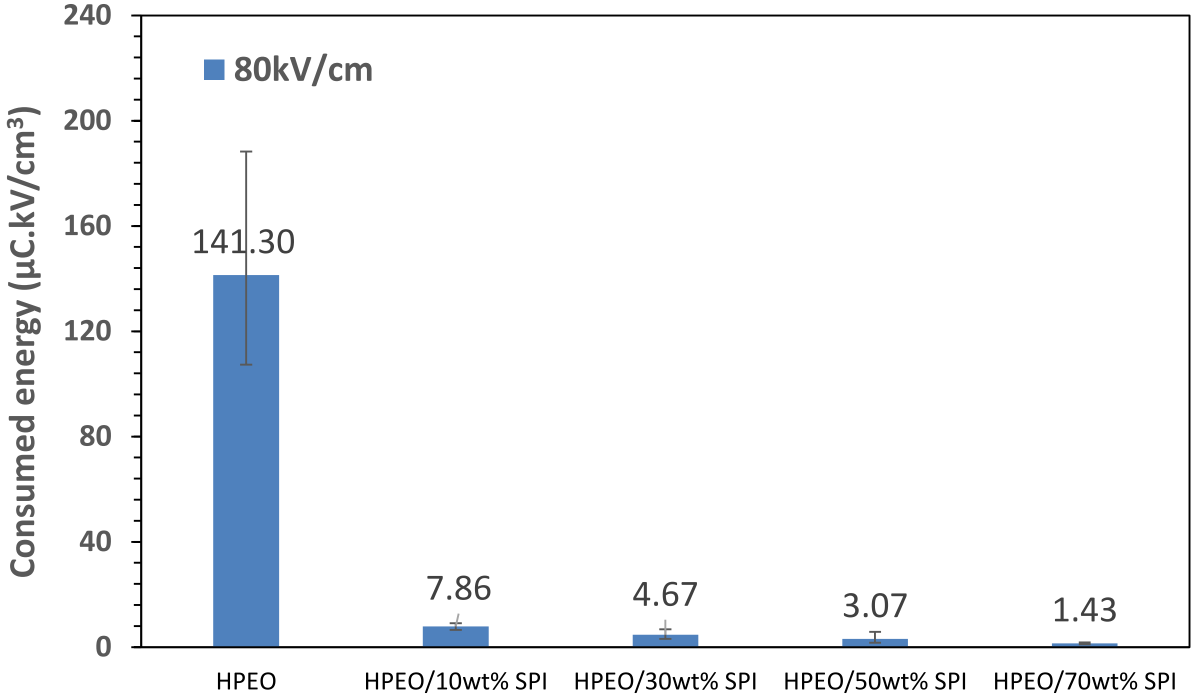

(a)

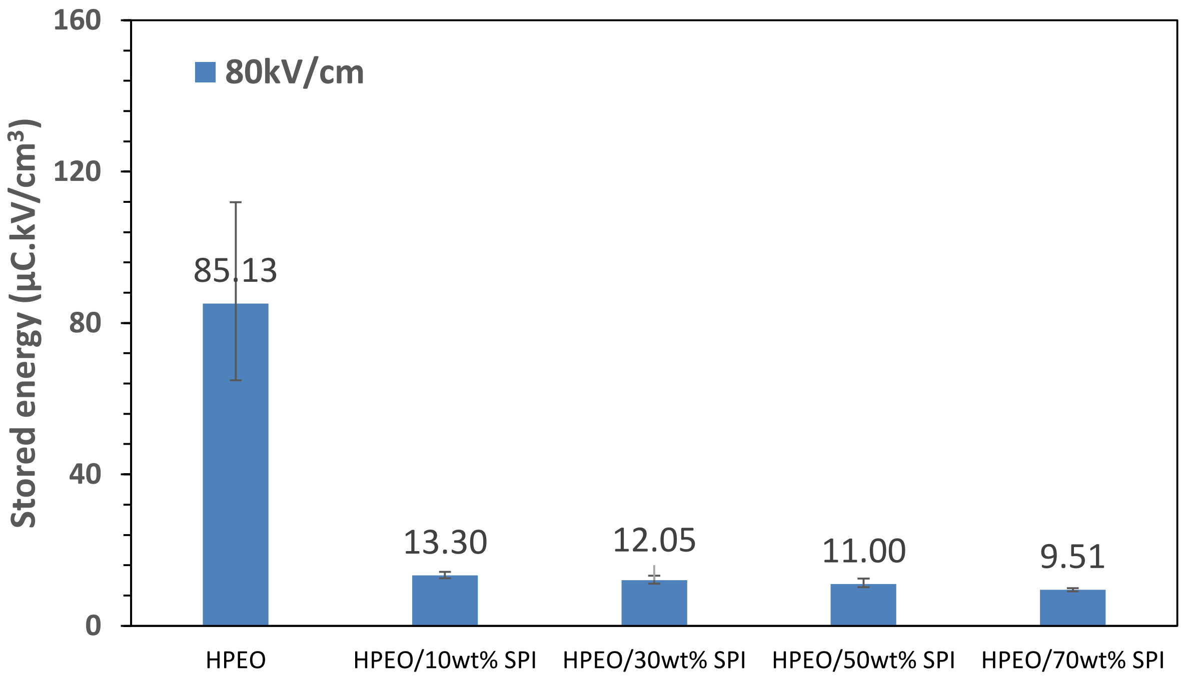

(b)

Figure 3.29. Effects of SPI on HPEO/SPI membranes: (a) Consumed energy, and (b) Stored energy.

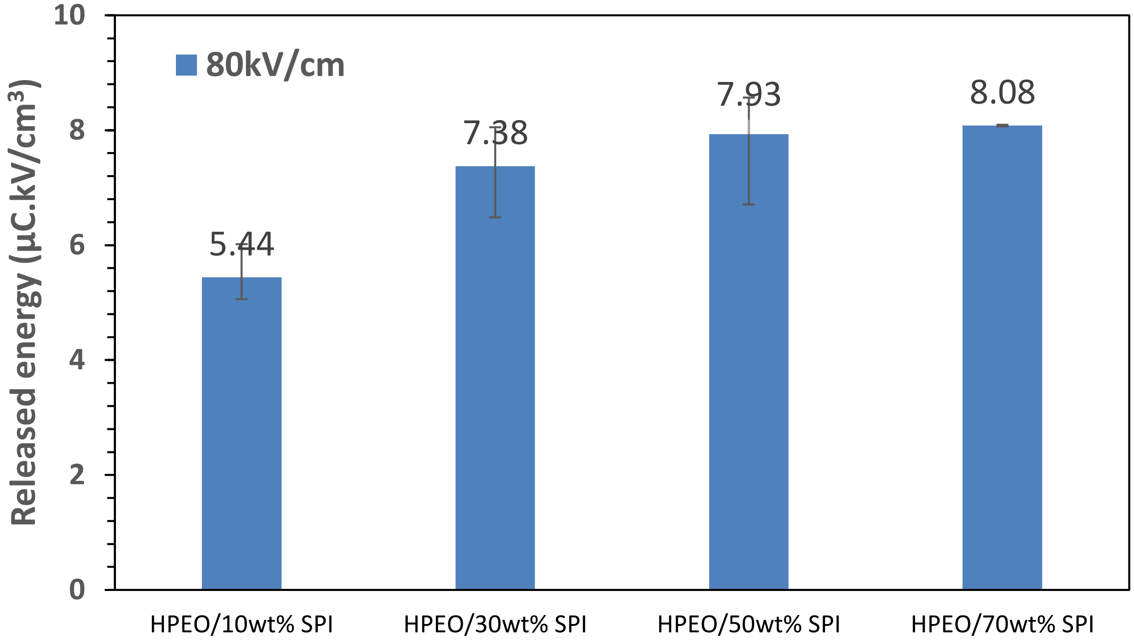

(a)

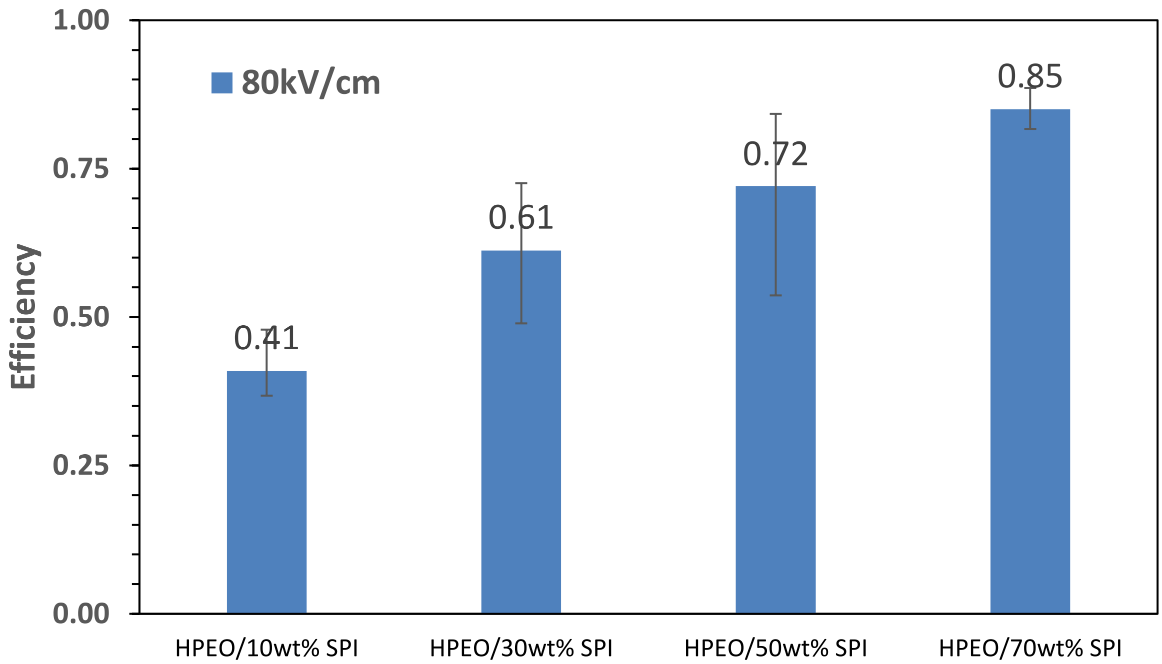

(b)

Figure 3.30. Effects of SPI on HPEO/SPI membranes: (a) Released energy, and (b) Efficiency.

3.6.2 Effects of SPI Content on Energy Performances of LPEO/SPI Membranes

Figure 3.31 (a) shows that pure LPEO has a huge lost energy in compare with the samples contain SPI, and this energy lost will even be decreased by more SPI content. At the same time, the energy stored by membranes prove that having more SPI content through the LPEO membranes make a smaller stored energy, as shown in Figure 3.31 (b).

The study proves that the SPI has an effect on the energy storage of LPEO and it gets more importance while having more SPI content leads to a dramatic increase in case of released energy, found in Figure 3.32 (a). That is to say, although the sample made by 30%wt SPI has not highest stored energy, it releases much more energy than other samples. This phenomenon comes from the good ability of the SPI in compare to LPEO to release the energy. It should be noted that having more content of SPI on the membrane contributes to the brittleness of membranes which is not desirable. As a result, it is of great importance to make a balance between the mechanical properties and the dielectric behavior of the membranes based on the required application.

Figure 3.32 (b) proves the energy efficiency places at highest amount where 30%wt of SPI is used. However, there is no big difference in case of efficiency between those LPEO/SPI membranes contain at least 30%wt SPI. In addition, there is not a dramatic difference between LPEO/SPI membranes which contain 10%wt and 30%wt SPI in case of electrical energy storage efficiency, while the LPEO efficiency is almost zero!

3.6.3 Effects of Polymer Molecular Weight on Energy Performances

Obviously, the molecular weight has remarkable effects on the hysteresis behaviors and energy performances of the membranes. In order to study the effect of polymer molecular weight on membrane dielectric properties, the HPEO and LPEO membranes should be compared at the same SPI content. As a result, the comparison will be discussed at different content of SPI.

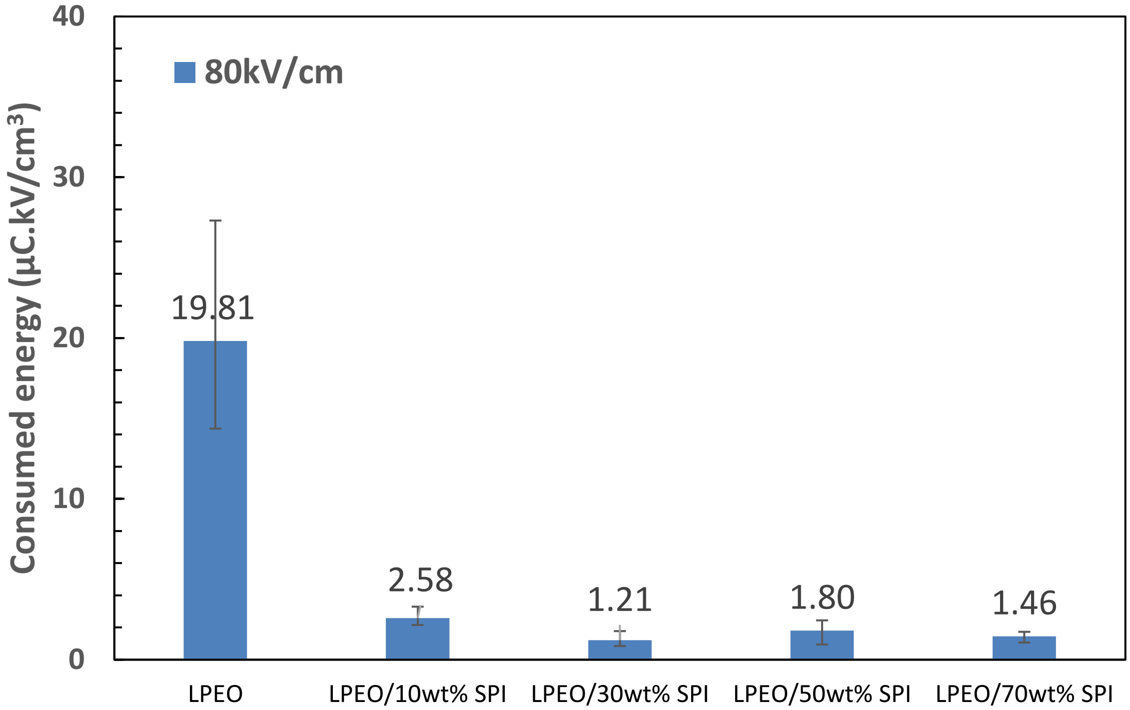

(a)

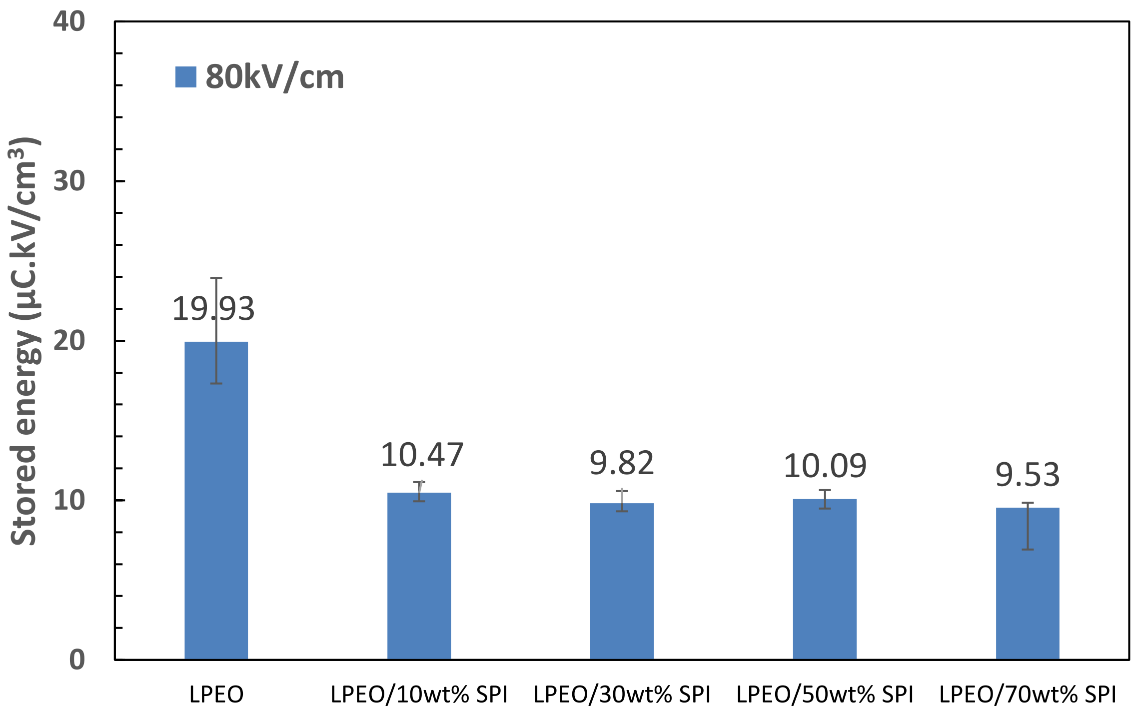

(b)

Figure 3.31. Effects of SPI on LPEO/SPI membranes: (a) Consumed energy, and (b) Stored energy.

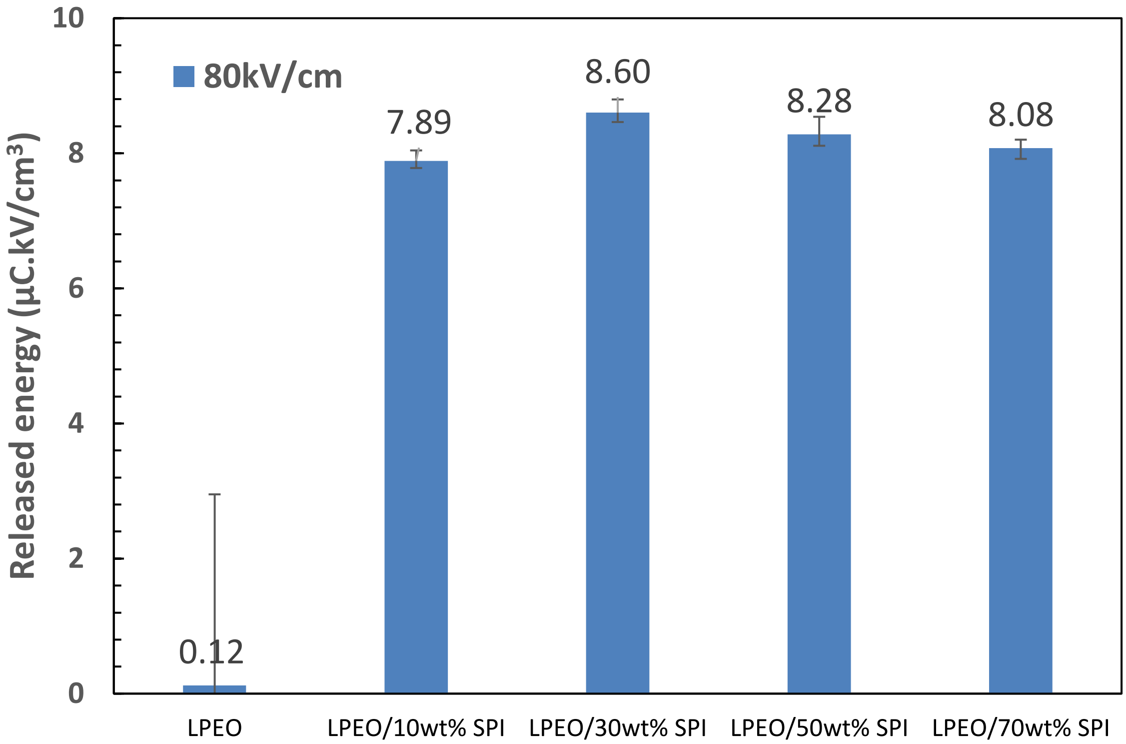

(a)

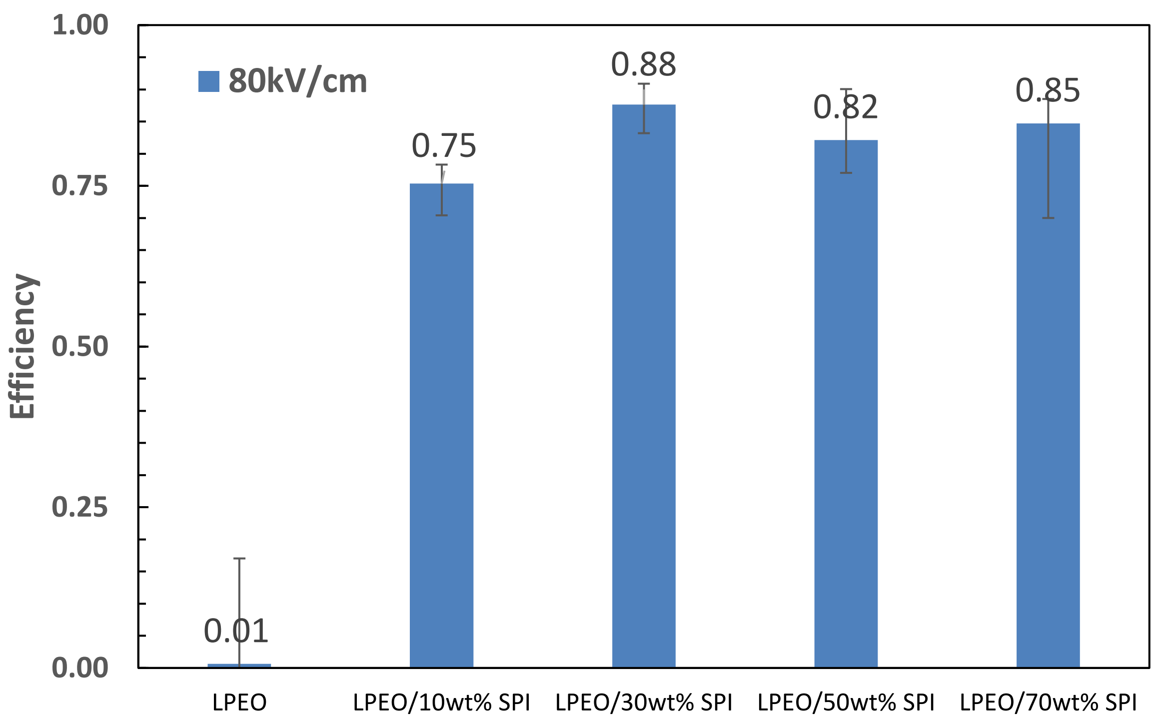

(b)

Figure 3.32. Effects of SPI on LPEO/SPI membranes: (a) Released energy, and (b) Efficiency.

Pure PEO: although the amount of energy can be saved in HPEO is much higher than that of LPEO, since the HPEO has higher amount of consumed energy than LPEO, the released energy plays an integral role to determine the efficiency. However, the energy recovered area of the HPEO is negative. As a result, the efficiency of the HPEO is negative (-0.659), while the efficiency of the LPEO is positive near to zero (0.0062).

PEO/SPI 10%: Same as the pure PEO, when 10% SPI is introduced to the PEO, the consumed and stored energy of HPEO/10wt% SPI is still greater than that of LPEO/10wt% SPI. However, the difference is not as high as before. The released energy of the LPEO/10wt% SPI is higher than that of the HPEO/10wt% SPI and as a result, the efficiency of the LPEO/10wt% SPI is greater.

PEO/SPI 30% and PEO/SPI 50%: by increasing the SPI content to 30wt% and 50wt%, no dramatic change was observed in case of energies. However, the efficiency difference is getting smaller between HPEO and LPEO membranes.

PEO/SPI 70%: Since the differences between the energies for HPEO and LPEO are getting smaller by increasing the content of SPI, both membranes show the same amount of efficiency where 70 percentage of the membrane is made by SPI.

In general, it is obvious that although introducing SPI to the PEO membranes contributes to reduce the amount of consumed and stored energy, it enhances the efficiency. This effect is more evident for the HPEO membranes rather than LPEO membranes.

CHAPTER FOUR

CONCLUSION

In this study, the electric and dielectric properties of the PEO/SPI membranes were investigated. The enhancement of the dielectric constant, resistivity and energy efficiency was observed in the membranes contained SPI. The enhancement effect was mainly from the presence of the SPI-PEO interactions. Although the heat treatment did not affect the chemical bonding through the SPI which was verified by the experimental results of FTIR, it induces the changes in soy protein polar structures. Moreover, the structural changes happened through the protein structure contributes to enlargement of the membrane's wettability due to a better accessibility to the hydrophilic regions of the SPI after denaturation.

Pure PEOs used in this study are very typical ductile polymers, even the cryofracture process could not completely suppress the ductile failure in the PEOs. The interactions between PEOs and SPI tends to make the PEO more brittle. Specifically, "fibrillation" is a very representative feature of ductile failure in polymer materials, which have been found in a variety of ductile polymers and is usually related to the elongation of crystal lamellae [128]. In HPEO/10wt% SPI membrane, we can easily observe the fibrillation of HPEO, However, this fibrillation phenomenon disappeared in the HPEO/50wt% SPI membrane, suggesting a more brittle failure mode as the concentration of SPI increased. Meanwhile, the nano-scale particulate second phase was also observed. These particles are believed to be caused by aggregated non-polar protein structures in SPI, which repel the polar PEO structures.

In LPEO/10wt% SPI, although the fibrillation of LPEO was not as distinct as that of HPEO, the elongation of LPEO crystal lamellae was still observed. The more brittle behavior of LPEO membranes compared with HPEO membranes should be related to the molecular weight. In spite of the differences between HPEO and LPEO, the effects of increasing loading of SPI was the same, that is, the LPEO/50wt%SPI membrane shows the very similar brittle fracture morphology as the HPEO/50wt%SPI membrane. The increasing brittleness of PEO/SPI membranes is likely caused by two reasons. Firstly, the strong polar interactions between PEO and SPI limited the chain mobility of PEO, and secondly, the concentration of brittle phase (SPI) increased.

The hysteresis behavior in this study is related to the switch of dipoles in the materials by high electric field). The reduced polarization suggests that it was getting more difficult to switch the dipoles, in particular, the dipoles in PEO phase, after the SPI was introduced to PEOs. This is somewhat consistent with the microstructure change of the fracture surfaces of PEO/SPIs, which revealed that the strong interactions between SPI and PEOs led to reduced mobility PEO chains and increased brittleness. In other words, the strong interactions between SPI and PEO created large resistance to the switch of dipoles. Although it is unclear now how the molecular weight affects the polarization behaviors of PEO materials, both PEOs showed high polarizability. Meanwhile, SPI has highly polarizable structures as well. However, with the addition of only 10wt% SPI, the unexpected reduction in polarization and distinctive hysteresis behavior were found in PEO/SPI membranes. Such dramatic changes at low SPI content cannot simply be explained by the effective medium theories [129], and they suggest the importance of PEO-SPI interactions to the polarization of PEO/SPI membranes. Future work will be needed to explore their interaction mechanisms.

In semi-crystalline polymers, crystal structures have complicated effects on the polarization of polymers. With the increasing of polymer crystallinity, both reduced and increased polarization have been reported [130-133]. Meanwhile, the changes in crystallinity were often accompanied with the changes in thickness of crystal lamellae and phase transformation and so on. It is possible that the dramatic reduction in polarization is related to the changes in crystal structures of PEOs by the addition of SPI. But XRD results are not very supportive of this assumption in this study. The addition of SPI affected the crystal structures of PEOs in two aspects, regardless of molecular weight: (1) crystallinity and (2) relative intensity of peaks. An obvious declining trend of crystallinity of PEO in the membranes was found with the increasing loading of SPI. In particular, when the concentration of SPI exceeded 50wt%, amorphous structures were dominant in the LPEO/SPI membranes, without observable diffraction peaks. A similar suppression of PEO crystallization was reported in an early study [110]. This decline in both HPEO and LPEO might contribute to the reduced polarization. However, it is interesting to notice that with 10wt% SPI loading, the crystallinity of LPEO barely changed, which is inconsistent with the greatly reduced polarization at 80kV/cm. Moreover, as the crystallinity decreased, the polarization of both groups of PEO/SPI membranes did not change much. Based on this observation, the changes in crystallinity could not be the primary reason for the different hysteresis behaviors of PEO/SPI membranes. In addition to the reduced crystallinity, the changes in the relative intensity of both diffraction peaks were observed as well. In this study, it is believed that this was because of the strong interactions between PEOs and SPI, although the variation of the relative peak intensity was not monotonic with the increasing SPI loading. The same interactions should also be responsible for the brittle behaviors, as well as the reduced polarization Moreover, the strong interactions between protein and PEO were also reported as the main reason for the reduced crystallinity [106, 112].

Experimental results of the current-voltage measurement show that introducing SPI to the both HPEO and LPEO membranes will increase the resistivity of the membranes. In other words, the presence of the SPI decreases the leakage current which means the membrane would be a better insulator. SPI has the same effects on the polarization behaviors of PEO films, regardless the molecular weight of PEO matrix. Pure PEOs (inserted plots) show a typical high-loss polarization behavior with high polarization as measured by P_{max} (Polarization at the maximum electric field, which is 80kV/cm in this study). Meanwhile, the hysteresis loops of both PEOs show large loop areas. This suggests that a great number of dipoles switched during charging process were not switched back during discharging process. In terms of energy storage performances, the large loop areas are equivalent to high energy loss, due to a large amount of unrecovered energy stored during charging. This type of hysteresis behavior means that the current still passes through the sample after the polarization has quit switching. This kind of leakage phenomenon is not significant in LPEO sample.

The addition of SPI has remarkably changed the polarization behaviors of both PEO materials. First of all, both the P_{max} and loop areas (energy loss) were largely reduced with the addition of only 10wt% SPI; secondly, the increasing amount of SPI in the membranes only led to slight changes in the hysteresis behaviors of PEO/SPI membranes. All the PEO/SPI membranes have greatly reduced stored energy density, compared with ~ 85.13mJ/cm^3 for HPEO and ~ 19.93mJ/cm^3 for LPEO. This is in consistence with the reduced polarization. However, the lower amount of electric energy stored during charging process does not necessarily lead to deteriorated energy storage performances of the resulting PEO/SPI membranes. This is because besides the amount of stored energy during charging, the amount of discharged energy is also critical to the energy applications. The decrease of consumed energy density because of the addition of SPI, led to enhanced discharged energy density in PEO/SPI membranes. For pure HPEO, because of the leakage, it was found that the consumed energy density (~141.30mJ/cm^3) was even higher than the stored energy density (~85.13mJ/cm^3), leading to a negative discharged energy density. In other words, the stored electric energy cannot be released for use during discharging process. Therefore, in PEO/SPI membranes, although the stored energy density was much lower in comparison with pure PEOs, the enhanced discharged energy density and higher energy efficiency have been achieved.

The aforementioned effects are significant at only 10wt% SPI loading. The increasing content of SPI only weakly changed these energy performances. Specifically, the stored energy density slightly decreased, and the discharged energy density continued increasing in HPEO/SPI membranes, while the variation of both properties was less obvious in LPEO/SPI membranes. As the concentration of SPI increases, the differences of HPEO/SPI and LPEO/SPI membranes are getting smaller, due to the increasing dominance of SPI. The enhanced discharged energy density and low energy loss suggest that the resulting PEO/SPI membranes have good potential in energy storage applications and transient electronic materials.

CHAPTER FIVE

FUTURE RESEARCH

The exploration of the polymer-protein dielectric materials will be continued in order to improve energy density. As shown in this study, the presence of the SPI enhances the energy efficiency of the PEO membranes.

Although both HPEO and LPEO shown very good dielectric properties with the presence of the SPI, they still do not show signs of polarization saturation. Therefore, new materials design will be applied to improve the polarization without increasing the consumed energy density. To achieve this goal, the first step is to conduct in-depth study on the PEO-SPI interactions. According to the completed research, it has been found the PEO-SPI interactions played a significant role in the polarization behaviors. Therefore, a profound understanding of the interaction mechanisms will be necessary. It is possible that different methods of protein denaturation could change the dielectric properties of the PEO/SPI membranes via altering the interaction mechanisms. Dielectric spectroscopy within broad frequency and temperature ranges is being used to study the interaction mechanisms between PEOs and SPI. Equivalent circuits models will be proposed to provide insights in the dielectric polarization of PEO, SPI and their blends. Various denaturation and modification methods have been being applied to SPI to achieve different protein structures. The effects of protein structures together with compositions on the polarization and energy performances will be studied.

One long term goal of this research is to explore the potential of the PEO/SPI, and similar materials systems in the applications of transient electronic materials and devices. Related transient properties will be analyzed including solubility analysis, electrical fatigue properties, as well as time dependent dielectric properties and so on.

REFERENCES

REFERENCES

[1] Farakoh Incorporation, 2012, "Power Capacitors," Tehran, Iran, http://www.farakoh.ir.

[2] Brusso, B., and Chaparala, S., 2014, "The Evolution of Capacitors [History]," *Institute of Electrical and Electronics Engineers-Industry Applications Magazine*, Vol. 20(6), pp. 8-12.

[3] Yin, Y., 2010, "An Experimental Study on PEO Polymer Electrolyte Based All-Solid-State Supercapacitor," Ph.D. Thesis, University of Miami, Florida, United States.

[4] Kaiser, C. J., 2012, *The Capacitor Handbook*, Springer Science & Business Media, Berlin, Germany.

[5] Mullin, W. F., 1971, *ABC's of Capacitors*, Sams Publishing, Indiana, United States.

[6] Blair, D., 1978, *Electrical Breakdown of Gases*, John Wiley and Sons, Chichester, United Kingdom.

[7] Scherz, P., 2006, *Practical Electronics for Inventors*, McGraw-Hill Education, New York, United States.

[8] Chen, H., Cong, T. N., Yang, W., Tan, C., Li, Y., and Ding, Y., 2009, "Progress in Electrical Energy Storage System: A Critical Review," *Progress in Natural Science*, Vol. 19(3), pp. 291-312.

[9] El-Habrouk, M., Darwish, M., and Mehta, P., 2000, "Active Power Filters: A Review," *Institution of Electrical Engineers-Electric Power Applications*, Vol. 147(5), pp. 403-413.

[10] Joffe, E. B., and Lock, K.-S., 2011, *Grounds for Grounding: A Circuit to System Handbook*, John Wiley and Sons, New Jersey, United States.

[11] Singh, B., Singh, B. N., Chandra, A., Al-Haddad, K., Pandey, A., and Kothari, D. P., 2003, "A Review of Single-Phase Improved Power Quality AC-DC Converters," *Institute of Electrical and Electronics Engineers-Transactions on Industrial Electronics*, Vol. 50(5), pp. 962-981.

[12] Space Technology, 2007, "Types of Power Supply," California, United States, http://www.rcptv.com/spacetec-be/power_supplies_more_info.htm.

[13] Brooks, D. G., UltraCAD Design, 2000, "ESR and Bypass Capacitor Self Resonant Behavior How to Select Bypass Caps," Washington, United States, http://electronica.ugr.es/~amroldan/cursos/2014/pcb/modulos/temas/esr-and-bypass-caps.pdf.

[14] Gupta, K., and Gupta, N., 2015, "Passive Components (Capacitors)," Advanced Electrical and Electronics Materials: Processes and Applications, John Wiley and Sons, New Jersey, United States.

[15] Guinta, S., Analoge Devices, 1996, "Capacitance and Capacitors," Massachusetts, United States, http://www.analog.com/en/analog-dialogue/articles/capacitance-and-capacitors.html.

[16] Engineering Edge, 2016, "Ceramic Capacitors Review," Georgia, United States, http://www.engineersedge.com/instrumentation/ceramic_capacitors.htm.

[17] Embedded Design, 2013, "Types of Capacitors and Their Application," California, United States, http://kuldeep-great.blogspot.com/2013/10/types-of-capacitors-and-their.html.

[18] Vijatović, M. M., Bobić, J. D., and Stojanović, B. D., 2008, "History and Challenges of Barium Titanate: Part II," *Science of Sintering*, Vol. 40(3), pp. 235-244.

[19] Vijatović, M. M., Bobić, J. D., and Stojanović, B. D., 2008, "History and Challenges of Barium Titanate: Part I," *Science of Sintering*, Vol. 40(2), pp. 155-165.

[20] Chemistry Structures and 3D Molecules, 2016, "Cubic Perovskite Structure", Three Dimensional Chemistry, http://www.3dchem.com/index.html.

[21] Guo, L., Luo, H., Gao, J., Guo, L., and Yang, J., 2006, "Microwave Hydrothermal Synthesis of Barium Titanate Powders," *Materials Letters*, Vol. 60(24), pp. 3011-3014.

[22] Boulos, M., Guillemet-Fritsch, S., Mathieu, F., Durand, B., Lebey, T., and Bley, V., 2005, "Hydrothermal Synthesis of Nanosized $BaTiO_3$ Powders and Dielectric Properties of Corresponding Ceramics," *Solid State Ionics*, Vol. 176(13), pp. 1301-1309.

[23] Seveyrat, L. S., Hajjaji, A., Emziane, Y., Guiffard, B., and Guyomar, D., 2007, "Re-Investigation of Synthesis of $BaTiO_3$ by Conventional Solid-State Reaction and Oxalate Coprecipitation Route for Piezoelectric Applications," *Ceramics international*, Vol. 33(1), pp. 35-40.

[24] Xu, H., and Gao, L., 2003, "Tetragonal Nanocrystalline Barium Titanate Powder: Preparation, Characterization, and Dielectric Properties," *Journal of the American Ceramic Society*, Vol. 86(1), pp. 203-205.

[25] Hippel, A. V., Breckenridge, R. G., Chesley, F. G., and Tisza, L., 1946, "High Dielectric Constant Ceramics," *Industrial and Engineering Chemistry*, Vol. 38(11), pp. 1097-1109.

[26] Kotlan, J., Ctibor, P., Pala, Z., Homola, P., and Nehasil, V., 2014, "Improving Dielectric Properties of Plasma Sprayed Calcium Titanate ($CaTiO_3$) Coatings by Thermal Annealing," *Ceramics international*, Vol. 40(8), pp. 13049-13055.

[27] Gupta, K., and Gupta, N., 2015, "Dielectric Materials: Types and Applications," Advanced Electrical and Electronics Materials: Processes and Applications, John Wiley and Sons, New Jersey, United States.

[28] Radio Electronics, 2010, "Glass Capacitors," London, United Kingdom, http://www.radio-electronics.com/info/data/capacitor/glass-dielectric-capacitors.php.

[29] AVX Corporation/Kyocera, 2012, "Glass Dielectric Caps," South Carolina, United States, http://dtsheet.com/doc/1472528/glass-dielectric-capacitors.

[30] Capacitance, 2012, "Leyden Jar", Emad Sedky, http://emadrlc.blogspot.com/2012/12/chapter-9-capacitance.html.

[31] Online Electrical Engineering Study, 2016, "Capacitor and Capacitance," New York, United States, http://www.electrical4u.com/what-is-capacitor-and-what-is-dielectric/.

[32] Tancap Technology, 2010, "Application of Capacitors," Shenzhen, China, http://www.china-capacitors.com/en/zhishiview.asp?id=48.

[33] Sedha, R. S., 2008, *Applied Electronics*, Chand Publishing, Delhi, India.

[34] Zhu, L., and Wang, Q., 2012, "Novel Ferroelectric Polymers for High Energy Density and Low Loss Dielectrics," *Macromolecules*, Vol. 45(7), pp. 2937-2954.

[35] Sarjeant, W. J., Zirnheld, J., and MacDougall, F. W., 1998, "Capacitors," *Institute of Electrical and Electronics Engineers-Transactions on Plasma Science*, Vol. 26(5), pp. 1368-1392.

[36] Sarjeant, W., Clelland, I. W., and Price, R. A., 2001, "Capacitive Components for power Electronics," *Institute of Electrical and Electronics Engineers*, Vol. 89(6), pp. 846-855.

[37] Ho, J., Ramprasad, R., and Boggs, S., 2007, "Effect of Alteration of Antioxidant by UV Treatment on the Dielectric Strength of BOPP Capacitor Film," *Institute of Electrical and Electronics Engineers-Transactions on Dielectrics and Electrical Insulation*, Vol. 14(5), pp. 1295-1301.

[38] Rabuffi, M., and Picci, G., 2002, "Status Quo and Future Prospects for Metallized Polypropylene Energy Storage Capacitors," *Institute of Electrical and Electronics Engineers-Transactions on Plasma Science*, Vol. 30(5), pp. 1939-1942.

[39] Reed, C., and Cichanowskil, S., 1994, "The Fundamentals of Aging in HV Polymer-Film Capacitors," *Institute of Electrical and Electronics Engineers-Transactions on Dielectrics and Electrical Insulation*, Vol. 1(5), pp. 904-922.

[40] Holman, J. S., and Stone, P., 2001, *Chemistry*, Nelson Thornes, Chentelham, United Kingdom.

[41] Jones, D. R., and Ashby, M. F., 2005, *Engineering Materials 2: An Introduction to Microstructures, Processing and Design*, Butterworth-Heinemann, Oxford, United Kingdom.

[42] Wang, C., Pilania, G., Boggs, S., Kumar, S., Breneman, C., and Ramprasad, R., 2014, "Computational Strategies for Polymer Dielectrics Design," *Polymer*, Vol. 55(4), pp. 979-988.

[43] Zulkifli, A., 2012, "Polymeric Dielectric Materials," Dielectric Material, Creative Commons, California, United States.

[44] Blythe, A. R., and Bloor, D., 2005, *Electrical properties of polymers*, Cambridge University Press, Cambridge, England.

[45] Simpson, J., and Clair, A. S., 1997, "Fundamental Insight on Developing Low Dielectric Constant Polyimides," *Thin Solid Films*, Vol. 308, pp. 480-485.

[46] Xie, S.-H., Zhu, B.-K., Li, J.-B., Wei, X.-Z., and Xu, Z.-K., 2004, "Preparation and Properties of Polyimide/Aluminum Nitride Composites," *Polymer testing*, Vol. 23(7), pp. 797-801.

[47] Liu, L., Liang, B., Wang, W., and Lei, Q., 2006, "Preparation of Polyimide/Inorganic Nanoparticle Hybrid Films by Sol–Gel Method," *Journal of composite materials*, Vol. 40(23), pp. 2175-2183.

[48] Li, H., Liu, G., Liu, B., Chen, W., and Chen, S., 2007, "Dielectric Properties of Polyimide/Al_2O_3 Hybrids Synthesized by In-Situ Polymerization," *Materials Letters*, Vol. 61(7), pp. 1507-1511.

[49] Calberg, C., Blacher, S., Gubbels, F., Brouers, F., Deltour, R., and Jérôme, R., 1999, "Electrical and Dielectric Properties of Carbon Black Filled Co-Continuous Two-Phase Polymer Blends," *Journal of Physics D: Applied Physics*, Vol. 32(13), pp. 1517-1525.

[50] Katsunami, K., Ishii, K., Tanaka, Y., and Ohki, Y., 1991, "Dielectric Properties of Polymer Blend of Polypropylene and Polyethylene," *Proceedings of Third International Conference on Properties and Applications of Dielectric Materials*, The Institute of Electrical and Electronics Engineers, Tokyo, Japan, Vol. 2, pp. 999-1002.

[51] Yada, R., 2004, *Proteins in Food Processing*, Elsevier, Amsterdam, Netherland.

[52] Liu, K., 2000, "Expanding Soybean Food Utilization," *Food Technology*, Vol. 54(7), pp. 46-58.

[53] Shurtleff, W., and Aoyagi, A., Soyfoods Center, 2004, "History of Soybeans and Soyfoods," California, United States, http://www.soyinfocenter.com/HSS/glidden.php.

[54] Cargill, 2016, "Soy Proteins," Minnesota, United States, http://www.cargillfoods.com/emea/en/products/proteins/soy-proteins/index.jsp.

[55] National Soybean Research Laboratory, 2015, "All About Soy," Illinois, United States, http://nsrl.illinois.edu/content/all-about-soy.

[56] Barać, M. B., Stanojević, S. P., Jovanović, S. T., and Pešić, M. B., 2004, "Soy Protein Modification—A Review," *Acta Periodica Technologica*, Vol. 35(35), pp. 3-16.

[57] Roy, A., Kucukural, A., and Zhang, Y., 2010, "I-TASSER: A Unified Platform for Automated Protein Structure and Function Prediction," *Nature protocols*, Vol. 5(4), pp. 725-738.

[58] Koga, N., Tatsumi-Koga, R., Liu, G., Xiao, R., Acton, T. B., Montelione, G. T., and Baker, D., 2012, "Principles for Designing Ideal Protein Structures," *Nature*, Vol. 491(7423), pp. 222-227.

[59] Ball, D. W., Hill, J. W., and Scott, R. J., 2011, *Introduction to Chemistry: General, Organic, and Biological*, Creative Commons, California, United States.

[60] Gelabert, N. P., 2015, "Monte Carlo Simulations for Protein Denaturation," Master's Thesis, University of Barcelona, Barcelona, Spain.

[61] German, B., Damodaran, S., and Kinsella, J. E., 1982, "Thermal Dissociation and Association Behavior of Soy Proteins," *Journal of Agricultural and Food Chemistry*, Vol. 30(5), pp. 807-811.

[62] Damodaran, S., and Kinsella, J. E., 1982, "Effect of Conglycinin on the Thermal Aggregation of Glycinin," *Journal of Agricultural and Food Chemistry*, Vol. 30(5), pp. 812-817.

[63] Hermansson, A., 1986, "Soy Protein Gelation," *Journal of the American Oil Chemists Society*, Vol. 63(5), pp. 658-666.

[64] Sorgentini, D. A., Wagner, J. R., and Anon, M. C., 1995, "Effects of Thermal Treatment of Soy Protein Isolate on the Characteristics and Structure-Function Relationship of Soluble and Insoluble Fractions," *Journal of Agricultural and Food Chemistry*, Vol. 43(9), pp. 2471-2479.

[65] Petruccelli, S., and Anon, M., 1994, "Relationship Between the Method of Obtention and the Structural and Functional Properties of Soy Proteins Isolates. 1. Structural and Hydration Properties," *Journal of Agricultural and Food Chemistry*, Vol. 42(10), pp. 2161-2169.

[66] Petruccelli, S., and Anon, M., 1994, "Relationship Between the Method of Obtention and the Structural and Functional Properties of Soy Protein Isolates. 2. Surface Properties," *Journal of Agricultural and Food Chemistry*, Vol. 42(10), pp. 2170-2176.

[67] Rhee, K. C., 1994, "Functionality of Soy Proteins," Protein functionality in food systems, Marcel Dekker, New York, United States.

[68] Arrese, E. L., Sorgentini, D. A., Wagner, J. R., and Anon, M. C., 1991, "Electrophoretic, Solubility and Functional Properties of Commercial Soy Protein Isolates," *Journal of Agricultural and Food Chemistry*, Vol. 39(6), pp. 1029-1032.

[69] Velickovic, D., Radovic, B. V., Barac, M., and Simic, D., 1992, *The Change of Trypsin-Inhibitor Activity as a Function of Pressure and the Duration of Thermal Treatment of Soybean Flour*, University of Belgrade, Belgrade, Serbia.

[70] Velickovic, D., Radovic, B. V., Barac, M., and Simic, D., 1997, "Effect of Soybean Thermal Inactivation on Trypsin Inhibitor Activity of Protein Isolate," Review of Research, Faculty of Agriculture, Zemun, Serbia.

[71] Velickovic, D., Radovic, B. V., Barac, M., and Simic, D., 2000, "Change of Soybean Polypeptide Composition During Thermal Inactivation of Trypsin Inhibitors," *Acta Periodica Technologica*, Vol. 31, pp. 193-199.

[72] Ker, Y., and Toledo, R., 1992, "Influence of Shear Treatments on Consistency and Gelling Properties of Whey Protein Isolate Suspensions," *Journal of Food Science*, Vol. 57(1), pp. 82-85.

[73] Subirade, M., Loupil, F., Allain, A.-F., and Paquin, P., 1998, "Effect of Dynamic High Pressure on the Secondary Structure of β-Lactoglobulin and on Its Conformational Properties as Determined by Fourier Transform Infrared Spectroscopy," *International Dairy Journal*, Vol. 8(2), pp. 135-140.

[74] Meyer, E. W., and Williams, L., 1977, *Chemical Modification of Soy Proteins*, American Chemical Society, District of Columbia, United States.

[75] Liu, Y., 2005, "Formaldehyde-Free Wood Adhesives from Soybean Protein and Lignin: Development and Characterization," Ph.D. Thesis, Oregon State University, Oregon, United States.

[76] Wolf, W. J., 1970, "Soybean Proteins. Their Functional, Chemical, and Physical Properties," *Journal of Agricultural and Food Chemistry*, Vol. 18(6), pp. 969-976.

[77] Walstra, P., 1989, "Principles of Foam Formation and Stability," Foams: Physics, Chemistry and Structure, Springer, Heidelberg, Germany.

[78] Barać, M., 2002, *Chemical and Enzymatic Modification of Soy Protein Concentrate*, University of Belgrade, Belgrade, Serbia.

[79] Wei, M., Fan, L. H., Huang, J., and Chen, Y., 2006, "Role of star-like hydroxylpropyl lignin in soy-protein plastics," *Macromolecular Materials and Engineering*, Vol. 291(5), pp. 524-530.

[80] Sun, X. Z. S., Kim, H. R., and Mo, X. Q., 1999, "Plastic performance of soybean protein components," *Journal of the American Oil Chemists Society*, Vol. 76(1), pp. 117-123.

[81] Mekonnen, T., Misra, M., and Mohanty, A. K., 2016, "Fermented Soymeals and Their Reactive Blends with Poly(butylene adipate-co-terephthalate) in Engineering Biodegradable Cast Films for Sustainable Packaging," *Journal of the American Chemical Society-Sustainable Chemistry & Engineering*, Vol. 4(3), pp. 782-793.

[82] Tian, K., Shao, Z. Z., and Chen, X., 2010, "Natural Electroactive Hydrogel from Soy Protein Isolation," *Biomacromolecules*, Vol. 11(12), pp. 3638-3643.

[83] Snyders, R., Shingel, K. I., Zabeida, O., Roberge, C., Faure, M. P., Martinu, L., and Klemberg-Sapieha, J. E., 2007, "Mechanical and microstructural properties of hybrid poly(ethylene glycol)-soy protein hydrogels for wound dressing applications," *Journal of Biomedical Materials Research Part A*, Vol. 83a(1), pp. 88-97.

[84] Wyman, J., 1931, "Studies on the dielectric constant of protein solutions I. Zein," *Journal of Biological Chemistry*, Vol. 90(2), pp. 443-476.

[85] Ferry, J. D., and Oncley, J. L., 1938, "Studies of the dielectric properties of protein solutions II The water-soluble proteins of normal horse serum," *Journal of the American Chemical Society*, Vol. 60, pp. 1123-1132.

[86] Kukic, P., Farrell, D., McIntosh, L. P., Garcia-Moreno, E. B., Jensen, K. S., Toleikis, Z., Teilum, K., and Nielsen, J. E., 2013, "Protein Dielectric Constants Determined from NMR Chemical Shift Perturbations," *Journal of the American Chemical Society*, Vol. 135(45), pp. 16968-16976.

[87] Wolf, M., Gulich, R., Lunkenheimer, P., and Loidl, A., 2012, "Relaxation dynamics of a protein solution investigated by dielectric spectroscopy," *Biochimica Et Biophysica Acta-Proteins and Proteomics*, Vol. 1824(5), pp. 723-730.

[88] Rosen, D., 1963, "Dielectric Properties of Protein Powders with Adsorbed Water," *Transactions of the Faraday Society*, Vol. 59(489), pp. 2178-&.

[89] Nakanishi, M., and Sokolov, A. P., 2015, "Protein dynamics in a broad frequency range: Dielectric spectroscopy studies," *Journal of Non-Crystalline Solids*, Vol. 407, pp. 478-485.

[90] Ermolina, I., and Feldman, Y., 2015, "Amino Acids and Peptides," *Dielectric Relaxation in Biological Systems: Physical Principles, Methods, and Applications*, pp. 228-247.

[91] Bywater, R. P., and Veryazov, V., 2013, "The preferred conformation of dipeptides in the context of biosynthesis," *Naturwissenschaften*, Vol. 100(9), pp. 853-859.

[92] Park, M. H., Kim, J., Lee, S. C., Cho, S. Y., Kim, N. R., Kang, B., Song, E., Cho, K., Jin, H. J., and Lee, W. H., 2016, "Critical role of silk fibroin secondary structure on the dielectric performances of organic thin-film transistors," *Rsc Advances*, Vol. 6(7), pp. 5907-5914.

[93] Mao, L. K., Hwang, J. C., and Chueh, Y. L., 2014, "Materials and interfaces issues in pentacene/PTCDI-C-8 ambipolar organic field-effect transistors with solution-based gelatin dielectric," *Organic Electronics*, Vol. 15(10), pp. 2400-2407.

[94] He, X. L., Zhang, J., Wang, W. B., Xuan, W. P., Wang, X. Z., Zhang, Q. L., Smith, C. G., and Luo, J. K., 2016, "Transient Resistive Switching Devices Made from Egg Albumen Dielectrics and Dissolvable Electrodes," *Acs Applied Materials & Interfaces*, Vol. 8(17), pp. 10954-10960.

[95] Kumar, R., Liu, D., and Zhang, L., 2008, "Advances in proteinous biomaterials," *Journal of Biobased Materials and Bioenergy*, Vol. 2(1), pp. 1-24.

[96] Thakur, V. K., Thunga, M., Madbouly, S. A., and Kessler, M. R., 2014, "PMMA-g-SOY as a sustainable novel dielectric material," *Journal of Royal Society of Chemistry Advances*, Vol. 4(35), pp. 18240-18249.

[97] Ji, J. Y., Lively, B., and Zhong, W. H., 2012, "Soy Protein-Assisted Dispersion of Carbon Nanotubes in a Polymer Matrix," *Materials Express*, Vol. 2(1), pp. 76-82.

[98] Zhu, M., Tan, C., Fang, Q., Gao, L., Sui, G., and Yang, X., 2016, "High Performance and Biodegradable Skeleton Material Based on Soy Protein Isolate for Gel Polymer Electrolyte," *American Chemical Society-Sustainable Chemistry and Engineering*, Vol. 4(9), pp. 4498-4505.

[99] Bazinet, L., Lamarche, F., Labrecque, R., and Ippersiel, D., 1997, "Effect of KCl and Soy Protein Concentrations on the Performance of BipolarMembrane Electroacidification," *Journal of Agricultural and Food Chemistry*, Vol. 45(7), pp. 2419-2425.

[100] Liu, Y. Y., Zeng, X. A., Deng, Z., Yu, S. J., and Yamasaki, S., 2011, "Effect of Pulsed Electric Field on the Secondary Structure and Thermal Properties of Soy Protein Isolate," *European Food Research and Technology*, Vol. 233(5), pp. 841-850.

[101] Wagner, A., and Kliem, H., 1998, "Ionic space charge relaxation and high dielectric permittivity in poly(ethylene oxide)," *Proceedings of Materials Research Society*, Solid State Ionics, Cambridge University Press, Warrendale, Vol. 548.

[102] Kliem, H., Schroder, K., and Bauhofer, W., 1996, "High dielectric permittivity of poly(ethylene oxide) in humid atmospheres," *Proceedings of Conference on Electrical Insulation and Dielectric Phenomena,* Inistitue of Electical and Electronics Engineers, Vols I & II, pp. 12-15.

[103] Khanbareh, H., van der Zwaag, S., and Groen, W. A., 2015, "Piezoelectric and pyroelectric properties of conductive poly(ethylene oxide)-lead titanate composites," *Smart Materials and Structures*, Vol. 24(4).

[104] Ghorpade, V. M., Gennadios, A., Hanna, M. A., and Weller, C. L., 1995, "Protein Isolate Poly(Ethylene Oxide) Films," *Cereal Chemistry*, Vol. 72(6), pp. 559-563.

[105] Vega-Lugo, A. C., and Lim, L. T., 2008, "Electrospinning of Soy Protein Isolate Nanofibers," *Journal of Biobased Materials and Bioenergy*, Vol. 2(3), pp. 223-230.

[106] Xu, X. Z., Jiang, L., Zhou, Z. P., Wu, X. F., and Wang, Y. C., 2012, "Preparation and Properties of Electrospun Soy Protein Isolate/Poly(ethylene oxide) Nanofiber Membranes," *American Chemical Society Applied Materials & Interfaces*, Vol. 4(8), pp. 4331-4337.

[107] Thirugnanaselvam, M., Gobi, N., and Karthick, S. A., 2013, "SPI/PEO Blended Electrospun Martrix for Wound Healing," *Fibers and Polymers*, Vol. 14(6), pp. 965-969.

[108] Lubasova, D., Netravali, A., Parker, J., and Ingel, B., 2014, "Bacterial Filtration Efficiency of Green Soy Protein Based Nanofiber Air Filter," *Journal of Nanoscience and Nanotechnology*, Vol. 14(7), pp. 4891-4898.

[109] Souzandeh, H., Johnson, K. S., Wang, Y., Bhamidipaty, K., and Zhong, W. H., 2016, "Soy-Protein-Based Nanofabrics for Highly Efficient and Multifunctional Air Filtration," *American Chemical Society Applied Materials & Interfaces*, Vol. 8(31), pp. 20023-20031.

[110] Ji, J. Y., Li, B., and Zhong, W. H., 2012, "An Ultraelastic Poly(ethylene oxide)/Soy Protein Film with Fully Amorphous Structure," *Macromolecules*, Vol. 45(1), pp. 602-606.

[111] Acar, H., Cinar, S., Thunga, M., Kessler, M. R., Hashemi, N., and Montazami, R., 2014, "Study of Physically Transient Insulating Materials as a Potential Platform for Transient Electronics and Bioelectronics," *Advanced Functional Materials*, Vol. 24(26), pp. 4135-4143.

[112] Colin-Orozco, J., Zapata-Torres, M., Rodriguez-Gattorno, G., and Pedroza-Islas, R., 2015, "Properties of Poly (ethylene oxide)/whey Protein Isolate Nanofibers Prepared by Electrospinning," *Food Biophysics*, Vol. 10(2), pp. 134-144.

[113] Precision Tensiometers, 2016, "Contact Angle Measurement", Biolin Scientific, http://www.biolinscientific.com/attension/applications/?card=AA7.

[114] Yuan, Y., and Lee, T. R., 2013, "Contact Angle and Wetting Properties," Surface science techniques, Springer, Berlin, Germany.

[115] Damodaran, S., Parkin, K. L., and Fennema, O. R., 2007, *Fennema's food chemistry*, Chemical Rubber Company Press, New York, United states.

[116] Du, Y. C., Li, S. Z., Zhang, Y. C., Rempel, C., and Liu, Q., 2016, "Treatments of protein for biopolymer production in view of processability and physical properties: A review," *Journal of Applied Polymer Science*, Vol. 133(17), p. 13.

[117] Suthanthiraraj, S. A., and Sheeba, D. J., 2007, "Structural Investigation on PEO-Based Polymer Electrolytes Dispersed with Al_2O_3 Nanoparticles," *Journal of Ionics*, Vol. 13(6), pp. 447-450.

[118] Tonin, C., Aluigi, A., Vineis, C., Varesano, A., Montarsolo, A., and Ferrero, F., 2006, "Thermal and Structural Characterization of Poly (Ethylene-Oxide)/Keratin Blend Films," *Journal of thermal analysis and calorimetry*, Vol. 89(2), pp. 601-608.

[119] Su, Y.-l., Wang, J., and Liu, H.-z., 2002, "FTIR Spectroscopic Study on Effects of Temperature and Polymer Composition on the Structural Properties of PEO-PPO-PEO Block Copolymer Micelles," *Journal of Langmuir*, Vol. 18(14), pp. 5370-5374.

[120] Hammann, F., and Schmid, M., 2014, "Determination and Quantification of Molecular Interactions in Protein Films: A Review," *Materials*, Vol. 7(12), pp. 7975-7996.

[121] Guerrero, P. M., 2013, "Processing and Characterization of Soy Protein-Based Materials," Ph.D. Thesis, Universidad del Pais Vasco, Donosita-San Sebastian, Spain.

[122] Nishinari, K., Fang, Y., Guo, S., and Phillips, G., 2014, "Soy Proteins: A Review on Composition, Aggregation and Emulsification," *Food Hydrocolloids*, Vol. 39, pp. 301-318.

[123] Sun, Q., Wang, P., Lei, H., Han, D.-q., Feng, P., Wu, H., and CHENG, M., 2009, "Characteristics of Soy Protein Isolate Films Modified by Glycerol and Oleic Acid," *Food Science*, Vol. 30(15), pp. 52-58.

[124] Yen, K. C., and Woo, E. M., 2009, "Formation of Dendrite Crystals in Poly (Ethylene Oxide) Interacting with Bioresourceful Tannin," *Polymer bulletin*, Vol. 62(2), pp. 225-235.

[125] British Broadcasting Corporation, 2014, "Resisting," London, United Kingdom, http://www.bbc.co.uk/schools/gcsebitesize/science/triple_ocr_gateway/electricity_for_gadgets/resisting/revision/2/.

[126] Damjanovic, D., 2006, "Hysteresis in Piezoelectric and Ferroelectric Materials," The science of hysteresis, Elsevier, Amsterdam, Netherland.

[127] Chauhan, A., Patel, S., Vaish, R., and Bowen, C. R., 2015, "Anti-Ferroelectric Ceramics for High Energy Density Capacitors," *Journal of Materials*, Vol. 8(12), pp. 8009-8031.

[128] Li, B., Gong, G., Xie, B. H., Yang, W., and Yang, M. B., 2008, "Influence of molecular weight on impact fracture behavior of injection molded high density polyethylene: Scanning electron micrograph observations," *Journal of Applied Polymer Science*, Vol. 109(2), pp. 1161-1167.

[129] Li, J. Y., Zhang, L., and Ducharme, S., 2007, "Electric energy density of dielectric nanocomposites," *Applied Physics Letters*, Vol. 90(13).

[130] Urayama, K., Tsuji, M., and Neher, D., 2000, "Layer-thinning effects on ferroelectricity and the ferroelectric-to-paraelectric phase transition of vinylidene fluoride-trifluoroethylene copolymer layers," *Macromolecules*, Vol. 33(22), pp. 8269-8279.

[131] Xu, H. S., Ni, S. L., and Yang, C. Z., 2003, "High polarization levels in poly(vinylidene fluoride-trifluoroethylene) ferroelectric thin films doped with diethyl phthalate," *Journal of Applied Polymer Science*, Vol. 88(6), pp. 1416-1419.

[132] Zeng, Z. G., Zhu, G. D., Zhang, L., and Yan, X. J., 2009, "EFFECT OF CRYSTALLINITY ON POLARIZATION FATIGUE OF FERROELECTRIC P(VDF-TrFE) COPOLYMER FILMS," *Chinese Journal of Polymer Science*, Vol. 27(4), pp. 479-485.

[133] Xia, W. M., Zhang, Q. P., Wang, X., and Zhang, Z. C., 2014, "Electrical Energy Discharging Performance of Poly(vinylidene fluoride-co-trifluoroethylene) by Tuning Its Ferroelectric Relaxation with Polymethyl Methacrylate," *Journal of Applied Polymer Science*, Vol. 131(7), pp. 1-9 (40114).